CT-726-SSI
Don-2013

xx (208587 1)

Centro de Investigación y de Estudios Avanzados

del Instituto Politécnico Nacional

Unidad Guadalajara

Métodos Avanzados para el Análisis de Voltaje y Flujo de Potencia Reactiva Modal

Tesis que presenta:
Diego Mijangos Pulido

para obtener el grado de:
Maestro en Ciencias

en la especialidad de:
Ingeniería Eléctrica

Director de tesis:
Dr. Arturo Román Messina

Centro de Investigación y de Estudios Avanzados

del Instituto Politécnico Nacional

Unidad Guadalajara

Advanced Methods for the Analysis of Modal Voltage and Reactive Power Flow

A thesis presented by:
Diego Mijangos Pulido

to obtain the degree of:
Master in Science

in the subject of:
Electrical Engineering

Thesis Advisor:
Dr. Arturo Román Messina

Métodos Avanzados para el Análisis de Voltaje y Flujo de Potencia Reactiva Modal

Tesis de Maestría en Ciencias
Ingeniería Eléctrica

Por:
Diego Mijangos Pulido
Ingeniero Mecatrónico
Universidad de Panamericana 2002-2007

Becario de CONACYT. expediente No. 243164

Director de Tesis:
Dr. Arturo Román Messina

Advanced Methods for the Analysis of Modal Voltage and Reactive Power Flow

Master of Science Thesis
In Electrical Engineering

By:
Diego Mijangos Pulido
Mechatronic Engineer
Universidad de Panamericana 2002-2007

Thesis Advisor:
Dr. Arturo Román Messina

Agradecimientos

Agradezco a mi familia, novia y amigos por el fuerte apoyo ofrecido durante todo este tiempo.

De manera muy especial al Dr. Arturo Román Messina por sus consejos, sugerencias y recomendaciones otorgadas para la realización de este trabajo de investigación.

A los profesores del CINVESTAV Unidad Guadalajara por su valiosa contribución a mi desarrollo académico.

A todos los compañeros del área de Sistemas Eléctricos de Potencia, por su amistad, consejos y ayuda.

Y finalmente al CONACyT por el apoyo económico brindado durante el transcurso de este proyecto.

Resumen

El análisis de flujo de potencia modal proporciona una técnica de análisis muy general para investigar la influencia de generadores, dispositivos de control, cargas y la red de transmisión en la estabilidad de pequeña señal de sistemas de potencia a gran escala.

Esta tesis propone un marco sistemático para el análisis de flujo de potencia oscilatoria en grandes sistemas de potencia. Se hace hincapié en el estudio de voltaje modal y las contribuciones de potencia reactiva. Un enfoque que conserva la estructura del sistema para el cómputo de potencia oscilatoria es presentado y probado. Métodos para la interpretación de la estructura modal son dados y herramientas especiales para el estudio de la distribución de flujo de potencia modal son desarrollados.

Basado en esta representación, un marco unificado para estudios de flujo de potencia oscilatoria modal es desarrollado para analizar el comportamiento modal de acciones de control de FACTS y el comportamiento de las cargas. El método puede ser utilizado para el estudio de redes con varias estructuras y tamaño arbitrario y puede también ser aplicado a datos medidos.

La metodología de análisis es demostrada en dos sistemas prácticos de prueba. Los resultados muestran que la técnica propuesta es aplicable a modelos de sistemas grandes y complejos.

Abstract

Modal power flow analysis provides a very general analysis technique to investigate the influence of generators, control devices, loads and transmission network on the small-signal stability of large-scale power systems.

This thesis proposes a systematic framework for the analysis of power swing flow of large-scale power systems. Emphasis is placed on the study of modal voltage and reactive power contributions. A structure-preserving approach to power swing computation flow is presented and tested. Methods for interpreting modal structure are then given and special tools for studying power flow distribution are developed.

Based on this representation, a unified framework for modal power oscillation flow studies is then developed to analyze the sensitivity of modal behavior to FACTS control action and load behavior. The method can be used to study networks with various structures and arbitrary size and can be applied to measured data.

The analysis methodology is demonstrated on two practical test systems. Results show that the proposed technique is applicable to large, complex power system models.

Index

Chapter3

Modal Power Oscillation Flow 27

Chapter4

Advanced Power Flow Methodologies 58

Chapter5

Application 78

Chapter6

Conclusions 104

Index of Figures and Tables

Chapter1
Introduction.

This introductory chapter presents a brief description of the research work in this thesis and serves as a general introduction to the problem of small-signal system modeling. The background and motivation, along with the problem statement, the objectives and the contributions of this research are also presented in this chapter.

A brief review of previous works is also summarized. The chapter closes with the structure of the thesis and a summary of the work done.

1.1 Background and Motivation

Power systems exhibit a number of unique dynamical processes that provoke intense system interactions.

Interarea oscillations in the low frequency range (0.1-2 Hz) have been evidenced in many power systems often associated with the interconnection of power systems through weak transmission lines. Electromechanical oscillations can develop between groups of machines of an interconnected system and can propagate through tie lines to neighboring systems. Physically, the frequency and damping of the oscillations depends on various factors such as the electrical distances between machines, the equivalent inertia and load and transmission characteristics [1]-[3].

Small perturbations in particular, may trigger electromechanical oscillations involving groups of generators swinging against each other. For such situations, power system dynamic behavior can be described as the superposition of oscillation modes called electromechanical modes of oscillations. With today's practical power systems becoming more and more stressed, complex phenomena involving interaction between the fundamental modes of oscillation may occur.

Oscillations related to the interconnection of systems are of particular interest. Due to its relatively large number of degrees-of-freedom, power systems exhibit highly complex phenomena including modal interactions and complex transient motions characterized by the emergence and subsequent mode decay.

As discussed in [1], critical interface are often limited by insufficient damping torque and are often highly dependent on network and control actions. Quantification of spatial and temporal patterns of dominant modes is an important step toward developing regional control systems and protective and control actions.

Traditional approaches to the study of electromechanical oscillations have focused on the analysis of modal properties of linear state space representations which require complete or partial specification of system modes of oscillations [2],[3]. These models have proven very valuable. However, they can provide only partial characterization of system behavior.

Recent developments in the application of linear analysis techniques have provided mechanisms to analyze oscillatory phenomena in power systems. As discussed later in this research, large-scale power system models derived from physical concepts are represented by nonlinear differential-algebraic equation (DAE)

2

systems. Even with simplifications and approximations, the resulting models may be overwhelmingly large too expensive for direct small signal analysis reflecting the complexity of modern interconnected systems.

The models presented in this thesis are motivated by an attempt to assess the effect of network influence on system behavior. New algorithms to compute the power oscillation flow associated with a mode or given modes of concerns are proposed and evaluated. In this approach, the magnitudes and phases of the power flow associated with a mode of concern can be determined and the specific contribution of system elements to the oscillatory process can be singled out.

Modal power flow algorithms provide a rapid quantitative technique for visualization of complex intersystem oscillations. The results may also be relevant to the interpretation of structural properties and to the design of system controllers to direct the time-varying power flows across the network.

1.2 Problem Statement

Power systems networks are composed of a large number of subsystems interacting in structured ways. Understanding the behavior of such complex systems, including their response characteristics continues to be a significant quest.

Sustained or poorly damped intersystem oscillations are a growing cause for concern in many weakly interconnected power systems. Wide-area phenomena involve a complicated interaction between machine dynamics and transmission system dynamics especially if the power systems are extensively interconnected.

In an interconnected system, the location of major critical paths may be complicated by the facts that there are multiple modes of oscillation and multiple loads. In addition, proper identification of loads having a significant influence on system behavior may result in enhanced load modulation techniques.

Oscillations can be aggravated or stimulated by a number of factors. Loads in particular can provide damping by varying the load voltage in phase with local frequency variations [14]. Ties having a large participation in the modal power are also good candidates for wide area monitoring and control.

Intersystem oscillations are essentially manifested by a periodic interchange of mechanical energy caused by the relative rotor acceleration of the system

generators or interconnected systems. A challenge is to develop a model which accurately captures the relevant dynamics of both generators and controllers and load characteristics. Consideration of network effects is vital to understand the nature of modal and to identify critical transmission paths. Furthermore, load characteristics often play a role in the physical mechanism underlying oscillations.

The advent of transmission system controls, on the other hand, offers a direct means for controlling oscillations. Recent studies show that loads can contribute significantly to interarea oscillations [15, 16]. Other devices such as FACTS controllers may also contribute to the oscillations.

As power systems become more and more complex, the onset of interarea oscillations is manifesting in rather more complex manners, often as complex oscillations involving the interaction of various system modes. For large-scale power systems, however, the exchange of oscillating energy through transmission lines may be difficult to determine.

By identifying the impact of machines and the transmission characteristics on the oscillation pattern, the predominant cause can be determined and remedial actions can be developed.

The work in this thesis is focused on the analysis of modal oscillation flow associated with major interarea modes. Major challenges being addressed include:

a) The generalization of existing approaches to the study of large power system DAE models.

b) The analysis of the effect of voltage and reactive power contributions to the power oscillation flow.

c) The identification of voltage control areas and dominant loads related to the power oscillation flow.

1.3 Relations with Previous Literature

A great deal of work has been reported in the literature on determination of modal properties from large DAE models. These include the analysis of modal properties such as eigenvalue information, the computation of modal controllability and observability and sensitivity information. Recent research reports summarize the experience in the application of these techniques [9] and [17]-[19]. Other

advances can be traced back to the study of modal controllability and observability in large DAE models.

The concept of power swing flow was introduced by Zhou at [7] as a means to identify the distribution and strength of power flow associated with critical interarea modes. Nayebzdeh and Messina et al. [15] extended this idea to allow the study of large power system models described by state space realizations.

With this method, the transmission corridors and system parameters having a large contribution to critical system oscillations modes are determined. The method is particularly well suited for investigating inter-system oscillations in large-scale power systems with embedded FACTS controllers.

Nayebzdeh and Messina [15], Ochoa [8] and also Segundo et al. [16] advocated the use of modal power swing flow to compute voltage and power-oscillation flow for each mode of concern in power systems with embedded FACTS controllers.

Much of the previous research in modal power flow analysis has been concerned with the computation of system oscillation modes. What is missing, even after extensive small signal studies is an understanding of the essential aspects of the network contribution to the power oscillation flow. Thus, for instance, the effects of loads on system behavior can lead to the concept of load modulations.

Several authors have recently outlined that the method could be used to identify voltage control areas.

The idea of a voltage control areas has been presented in works as [10, 11], where the power system is separated in smaller areas in order to ensure the effectiveness of reactive support. The concept of electrical distance was used in these works.

Also in [10] after portioning the power network, it is necessary to identify the mix of sources of reactive support that would be effective, it is done by determining the sensitivity of load bus voltages to reactive injections of sources as exposed in [12]. This identification is based on analysis techniques of the static representation of the power system through a complex power balance equations. This and another methodologies for the study and analyses of voltage stability are presented and discussed in references [5, 12], where the electric power systems is modeled by its power balance equations, a static representation.

Bolden [14], discusses the use of this concept to design and locate voltage control devices.

1.4 Thesis Objectives

The primary objective of this research is the development of new techniques for the analysis of power swing flows in large-scale interconnected power systems. Other related objectives include:

- The assessment of voltage and reactive power contribution to the power swing flow.

- The identification of critical loads and voltage control areas.

- The generalization of modal power flow algorithms to extract modal information from measured data.

1.5 Contributions of this Thesis

This research provides an attempt to extend modal power flow analysis to address modal power flow analysis for power systems modeled as DAEs. Major contributions in this work include new techniques for modeling and analysis of large-scale DAE models, and for the identification of transmission elements having a large contribution to the oscillations flow.

Other contributions include:

1. The development of a new methodology for the analysis of voltage control areas in the small signal stability problem. In this sense, modal reactive contributions are determined.

2. The study of the importance of an active load model in the damping of the system. The development of alternative methodologies to identify dominant loads in the system.

3. An alternative strategy to compute modal power flow based on modal analysis of large differential-algebraic systems.

4. The extension of existing approaches to compute power swing flow from measured data.

1.6 Organization of the Thesis

The organization of the thesis is as follows:

In **Chapter 2** the underlying model of the system is presented. The chapter offers an overview of ongoing research in small-signal power flow analysis of large interconnected power systems. A procedure to determine modal voltage control areas as well as the procedure to find the dominant loads for any swing mode/modes in the power system is introduced. Examples are used throughout to illustrate various points.

Chapter 3 gives a description of the proposed algorithm used to compute modal power oscillation flow of electric power systems and describes characteristics of the oscillation problem in detail. A detailed review of the method including mathematical properties is presented, along with a brief description of the effects of FACTS controllers and load characteristics on the oscillation flow. Several options for computing the power oscillation flow are presented. Algorithms to compute the contribution of machines, loads and control systems to the swing energy are developed. Emphasis is placed on the contribution of reactive power to the power oscillation flow.

In **Chapter 4**, a novel framework for dynamic characterization of modal behavior is presented based on the analysis of the modal properties differential-algebraic equation systems. The theoretical basis of the proposed technique is established. The general numerical scheme used in the computation of power oscillation flow is finally described. Further, the chapter addresses various aspects of modal power flow computation. The incorporation of PMU measurements to modal estimation is discussed and hybrid estimators incorporating network information and observational data are proposed. The proposed technique when combined with a wide-area monitoring system would be an effective tool for detecting and identifying the source of transient disturbances in the power system.

Chapter 5 discusses the application of the developed methodology to the study of practical power systems.

Finally, in **Chapter 6** some concluding remarks and suggestions for future research are presented. Possible improvements are considered.

1.7 References

[1] Analysis and control of power system oscillations, CIGRE Task Force 07 of Advisory Group 01 of Study Committee 38, Final Report, Paris, France, Dec.1996.

[2] M. J. Gibbard, N. Martins, J. J. Sanchez-Gasca, N. Uchida, V. Vittal and L. Wang, "Recent Applications of Linear Analysis Techniques", IEEE Trans. on Power Systems, vol. 16, no. 1, pp. 154-162. Feb. 2001.

[3] G. J. Rogers, "Demystifying Power Systems Oscillations" IEEE Computer Aplications in Power Systems, July 1996, 30-35.

[4] R. Graham, "Cap Tutorial Power System Structure and Oscillations. IEEE Computer Applications in Power Systems". April 1999. Pages 14-21.

[5] P. Kundur, "Power System Stability and Control", McGraw-Hill, Inc. Ney York, 1994.

[6] P. W. Sauer and M. A. Pai, "Power System Dynamics and Stability", Prentice Hall, 1998.

[7] E. Z. Zhou, "Power Oscillation Study of Electric Power Systems", Electrical Power and Energy Systems. Vol. 12. No. 2, pp 143-150, 1995.

[8] M. Ochoa, "Aplicación de Métodos de Potencia y Energía Modal al Análisis de Oscilaciones Interárea". Centro de Investigación y Estudios Avanzados del I.P.N. (CINVESTAV), Unidad Guadalajara. Guadalajara Jalisco. June 2001.

[9] T. Smed, "Feasible Eigenvalue Sensitivity for Large Power Systems", IEEE Trans. Power Systems, Vol. 8 No. 2 May 1993.

[10] G. Radman, and J. Powell, "Dynamic Voltage Stability Improvement Using Coordinated Control of Dynamic VAR-Sources". Bulk Power System Dynamics and Control VII. Revitalizing Operational Reliability, 2007 iREP Symposium. August 19-24, 2007-Charleston, SC, USA.

[11]   J. Zhong, E. Nobile, and K. Bhattacahrya, "Localized Reactive Power Markets Using the Concept of Voltage Control Areas" IEEE Trans. Power Systems. Vol. 15 No. 3, pp 1536-1561. Aug. 2004.

[12]   Y. Moon, H. Ryu, and J. Lee, "Uniqueness of Static Voltage Stability Analysis in Power Systems". IEEE Power Engineering Society Summer Meeting. 2001 Vol. 3 pp. 1536-1541. Jul 2001.

[13]   L. Vanfretti, J. H. Chow, "Computation and Analysis of Power System Voltage Oscillations from Interarea Modes" IEEE Power & Energy Society General Meeting, 2009. 26-30 July 2009, pp 1-8.

[14]   R. L. Bolden, "Use of stabilizing signals in static VAR compensators to enhance the damping of power systems" Symposium on Static VAR Systems, Capricornia Institute, Australia, November 1985.

[15]   M. Nayebzadeh and A. R. Messina, "Advanced Concepts of Analyzing Static VAR Compensators to Damp Inter-Area Oscillation Modes" European Transactions on Electric Power. ETEP Vol. 9, No. 3, May/June 1999.

[16]   F. R. Segundo, and A. R. Messina, "Modeling and Simulation of Interline Power Flow Controllers: Application to Enhance System Damping" North American Power Symposium (NAPS), Oct 4-6, 2009, pp 1-6.

[17]   L.T.G. Lima, "Challenges on Small-Signal Analysis of Large Inteconnected Power Systems", Power Engineering Society General Meeting, 2007. IEEE, pp. 1 – 7.

[18]   Zhengchun Du, Wei Liu, and Wanliang Fang.Calculation of Rightmost Eigenvalues in Power Systems Using the Jacobi–Davidson Method" IEEE TRANSACTIONS ON POWER SYSTEMS, VOL. 21, NO. 1, 234-239,FEBRUARY 2006.

[19]   K. Wang F. Liu, D. Zhang, S. Yang, S. Mei and G. He. "Calculation of the Eigenvalues with Least Damping Ratios Based on the DAE Model in the Power System Small- Signal Stability Analysis" Power and Energy Society General Meeting, 2011 IEEE, pp. 1-7 July 2011.

Chapter2
Modal Voltage Control Areas and Dominant Loads

Over the past few years there has been considerable interest in studying oscillatory processes in power systems with forced load variations. In this chapter, a physically motivated procedure for identifying voltage control areas associated with critical interarea modes is proposed.

A single-machine infinite-bus (SMIB) system is analyzed as illustrative example. The physical and mathematical connection between system oscillations and voltage fluctuations is discussed.

Following a brief overview of small signal analysis in Section 2.1, a mechanical analogy is introduced. A framework is then outlined for a unified approach to assessing the impact of load characteristic variation for the active power in the system damping. The framework involves two steps: a) identification of mechanisms underlying oscillatory behavior, and b) assessment of the feasibility of using load modulation to enhance damping.

2.1 Motivational Example: Single Machine-Infinite Bus System

Much insight into the behavior of complex power systems can be found by examining the physics of simple power systems. In this section, we exploit an exact analogy between the temporal dynamics of a pendulum with the corresponding dynamics of a single-machine infinite bus system. We begin with a review of the equations for the SMIB system.

Consider the single-machine infinite bus test system shown in Fig. 2.1. For simplicity, the test system is partially represented by its classical model; transmission losses are neglected and the generator is represented by a constant voltage source E' behind transient reactance X'_d. Account is taken in this model of the effect of nonlinear voltage-dependent load characteristics.

The internal angle δ is defined as the angle by which E' leads the infinite bus voltage $|V_\infty|$ and θ the angle by which $|V|$ leads the infinite bus voltage.
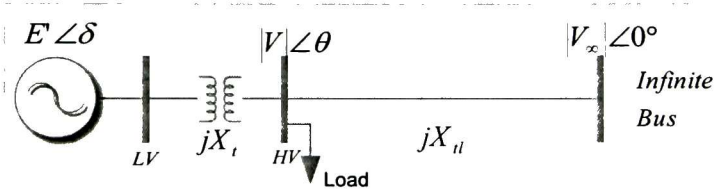
Figure 2.1: A single machine infinite bus system.

In the classical system representation, the differential-algebraic equations of motion of the system can be written as

$$\frac{d}{dt}\Delta\delta = \omega_0 \Delta\omega_r \tag{2.1}$$

$$2H\frac{d}{dt}\Delta\omega_r = [\Delta P_m - \Delta P_e - K_D\Delta\omega_r] \tag{2.2}$$

where $\Delta\delta$ is the angular position of the rotor in electrical radians with respect to the infinite system, ω is the angular position of the rotor in electrical rad/s, P_m is the mechanical input power in pu K_D is the generator damping coefficient in pu torque/pu speed, and H is the inertia constant in MWs/MVA.

In the case when $P_{load}=Q_{load}=0$, the solutions are well known. In the more general, and interesting case, the mismatch equations become

$$P_{Load} = P_e + P_{tl} \tag{2.3}$$

$$0 = Q_e + Q_{tl} \tag{2.4}$$

where

$$P_e = \frac{E'V}{X'_d + X_t} Sin(\delta - \theta)$$

$$Q_e = \frac{E'V Cos(\delta - \theta) - V^2}{X'_d + X_t}$$

$$P_{tl} = -\frac{V V_x}{X_{tl}} Sin(\theta)$$

$$Q_{tl} = \frac{V V_x Cos(\theta) - V^2}{X_{tl}}$$

and P_e, P_{tl}, Q_e and Q_{tl} are the active and reactive power flowing from the transformer and transmission line, respectively.

These equations have the same structure as those for the multi-machine power system model as described in Chapter 3.

Let now the state variables of the system be $\mathbf{x} = [\Delta\omega_r\ \Delta\delta\ \Delta\theta\ \Delta V/V]^T$ Expanding the nonlinear model (2.1)-(2.4) around some equilibrium point, the equation of motion can be described by the four-dimensional linear system,

$$
\begin{bmatrix} 2H & 0 & 0 & 0 \\ 0 & 1 & 0 & 0 \\ 0 & 0 & 0 & 0 \\ 0 & 0 & 0 & 0 \end{bmatrix} \frac{d}{dt} \begin{bmatrix} \Delta\omega_r \\ \Delta\delta \\ \Delta\theta \\ \Delta V/V \end{bmatrix} = \begin{bmatrix} -K_D & -K_1 & K_1 & -K_2 \\ \omega_0 & 0 & 0 & 0 \\ 0 & K_1 & -K_{13} & K_2 - K_6 \\ 0 & -K_2 & K_2 - K_6 & K_{78} \end{bmatrix} \begin{bmatrix} \Delta\omega_r \\ \Delta\delta \\ \Delta\theta \\ \Delta V/V \end{bmatrix} + \begin{bmatrix} 0 \\ 0 \\ -1 \\ 0 \end{bmatrix} \Delta P_{Load}
$$

$$\tag{2.5}$$

where,

$$K_1 = \frac{E'V}{X'_d + X_t} \cos(\delta - \theta); \quad K_2 = \frac{E'V}{X'_d + X_t} \sin(\delta - \theta); \quad K_3 = \frac{V V_x}{X_{tl}} \cos(\theta)$$

$$K_6 = \frac{|V||V_\infty|}{X_{tl}}\sin(\theta); \quad K_7 = \frac{E'|V|\cos(\delta-\theta)-2|V|^2}{X'_d+X_t}; \quad K_8 = \frac{|V||V_\infty|\cos(\delta-\theta)-2|V|^2}{X_{tl}}$$

$$K_{13} = K_1 + K_3; \qquad\qquad K_{78} = K_7 + K_8$$

Next, a mechanical analogy for the SMIB system is proposed and the effect of voltage variations on system behavior is investigated.

2.2 Voltage Oscillations from Swing Oscillation Modes

Voltage oscillations often accompany the rotor oscillations signaling the importance of various physical processes. Thus, for instance, it is known that voltage oscillations can be reduced when FACTs controllers are in operation near the electrical centers of the systems exchanging energy (the physical point where the voltage swings are greatest for the dominant swing mode) [8].

More formally, the dependence of voltage fluctuations with respect to the variation in electromechanical modes can be expressed as

$$\Delta V = f_V(\lambda_1, \lambda_2, ..., \lambda_{nmc}) \tag{2.6}$$

where *nmc* indicates the number of modes of concern. And separating in magnitude and phase angle, one has

$$\Delta V = \begin{cases} \Delta|V| = f_{\Delta|V|}(\lambda_1, \lambda_2, ..., \lambda_{nmc}) \\ \\ \Delta\theta_V = f_{\Delta\theta_V}(\lambda_1, \lambda_2, ..., \lambda_{nmc}) \end{cases} \tag{2.7}$$

where

$\Delta|V|$ denotes the magnitude of the modal bus voltage deviation.

$\Delta\theta_V$ denotes the phase of the modal bus voltage deviation.

Depending on the nature of the selected mode, the values for the voltage magnitude and phase angle deviations will be real or complex quantities and can be analyzed by calculating the argument and phase of the bus voltage deviations. The remainder of this section outlines the procedure.

2.2.1 *Magnitude of the Modal Bus Voltage Deviations*

Physically, the magnitude of the bus voltage deviation allows the identification of those buses where the swing oscillation has a stronger influence in the bus voltage magnitude. It can be defined as the variation of the voltage magnitude at each bus within the system with respect to an excited mode or modes of interest. It reflects the buses in the system where variations in voltage magnitude are greater. This information can be used to locate dynamic voltage support or monitoring system behavior [6].

2.2.2 *Pendulum Analogy*

A more insightful analysis into the nature of system oscillations can be attained from the analysis of a mechanical analogy. Following Samuelson, consider a single machine infinite bus system shown in Fig 2.2 [3, 4].
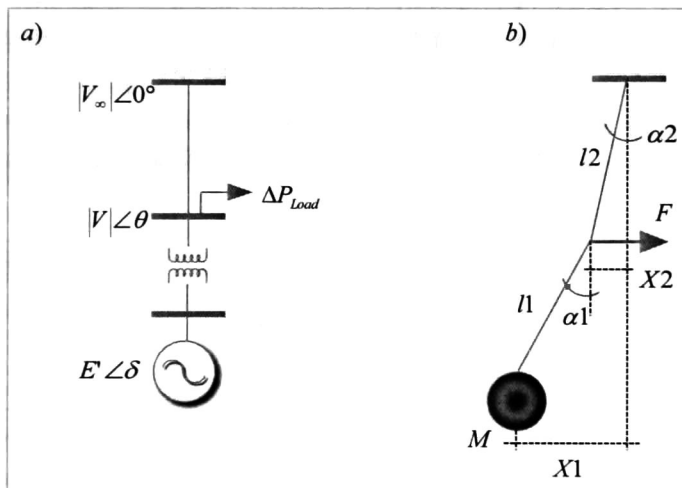
Figure 2.2: a) Single machine power system, b) Pendulum analogy.

The equations of motion of a single machine infinite bus system (Figure 2.2.a) have their exact analogy in a simple pendulum (Figure 2.2.b) for the case of a classical machine representation. As suggested in figure 2.2, the variation in active load power (ΔP_{Load}) can be represented as a force F acting on the flexible string. The deviations from a steady state point $X1$ and $X2$ correspond to the phase angles δ and θ.

It is intuitively obvious that as F approaches the mass the influence over the swinging mass will be greater. An effective way to damp the pendulum is to apply viscous damping i.e. let a force proportional to the mass velocity act on the mass.

Based on the DAE model (2.5), and assuming negligible variations in voltage magnitude and $K_D = 0$ the equation of motion of the SMIB can be written as

$$
\begin{bmatrix} 2H & 0 & 0 \\ 0 & 1/\omega_0 & 0 \\ 0 & 0 & 0 \end{bmatrix} \frac{d}{dt} \begin{bmatrix} \Delta\omega_r \\ \Delta\delta \\ \Delta\theta \end{bmatrix} = \begin{bmatrix} 0 & -K_1 & K_1 \\ 1 & 0 & 0 \\ 0 & K_1 & -K_{13} \end{bmatrix} \begin{bmatrix} \Delta\omega_r \\ \Delta\delta \\ \Delta\theta \end{bmatrix} + \begin{bmatrix} 0 \\ 0 \\ -1 \end{bmatrix} \Delta P_{Load} \qquad (2.8)
$$

For the case of small displacements, the state space equations associated with the mechanical system are

$$
\begin{bmatrix} 1 & 0 & 0 \\ 0 & 1 & 0 \\ 0 & 0 & 0 \end{bmatrix} \frac{d}{dt} \begin{bmatrix} V1 \\ X1 \\ X2 \end{bmatrix} = \begin{bmatrix} 0 & -C_1 & C_1 \\ 1 & 0 & 0 \\ 0 & C_1 & -C_2 \end{bmatrix} \begin{bmatrix} V1 \\ X1 \\ X2 \end{bmatrix} + \begin{bmatrix} 0 \\ 0 \\ -1/M \end{bmatrix} F \qquad (2.9)
$$

where $X1$ and $X2$ are the mass displacement $V1$ as the mass velocity, g represents the gravity force acting on the ball, and M is the mass of the pendulum.

and

$$
C_1 = \frac{-g}{l1}
$$

$$
C_2 = g(\frac{1}{l1} + \frac{1}{l2})
$$

$$
X1 = (l1)(\alpha1) + X2
$$

$$
X2 = (l2)(\alpha2)
$$

The following conclusions can be drawn from this analogy:

1. The phase angle of the bus voltage deviations indicates the relative oscillation pattern experienced by the buses inside the SMIB system, and allows the identification of buses with coherent oscillation behavior.

2. An active power load oscillating in opposition to the oscillation of the bus where is connected will increase the system damping, and will have more influence in the oscillation as it gets electrically closer [3, 9] to the oscillation mode, indicated by the magnitude of the modal voltage phase angle.

The above analysis framework can be extended readily to multi-machine systems. These arguments suggest that the angle calculated from the modal voltage phase angle variations may be used to locate areas inside the power system with coherent oscillation behavior.

Clearly, the load effect on the mode will depend on its oscillation pattern. Loads with a similar oscillation pattern to the one experienced by the bus where they are connected will decrease damping of the mode of concern. Conversely, loads exhibiting an out of phase oscillation will introduce damping to the system.

Drawing upon these ideas, a general method based on modal analysis, for determining voltage coherent areas associated with a mode of concern is proposed.

2.3 Modal Voltage Control Areas

Identification of modal voltage control areas is done in two steps. In the first step, two dominant areas are identified with angles near 0° and 180°. The largest bus participation is set to 0°.

In the second step clusters of buses within these areas are identified based on electrical distances. Within each group:

a) Group buses which have phase angles within a small range. This will result in several clusters.
b) Within each group sort the buses with decreasing magnitude of phase.
c) Retain only the buses with above a certain threshold of the largest magnitude of bus voltage phase angle. The dominant bus within each group is chosen as the bus with the largest modal voltage deviation.

Figure 2.3 gives a schematic representation of a modal voltage control area.
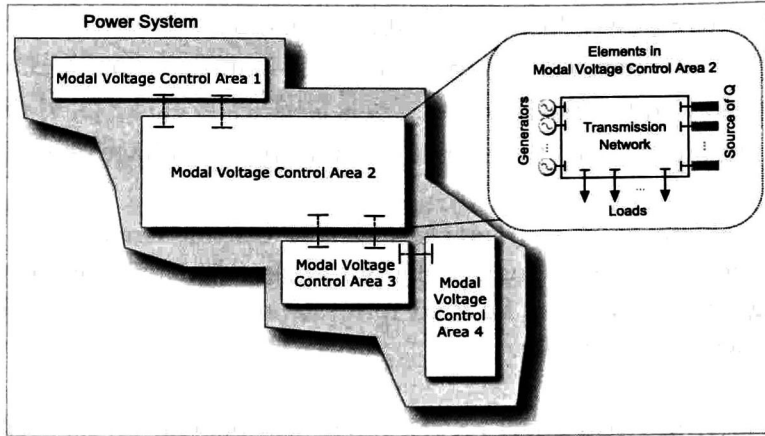
Figure 2.3: Modal voltage control area inside a power system.

2.4 Effect of Active Power Load on System Damping

2.4.1 Load Modeling and Simulation

For the purposes of this discussion, the nonlinear load behavior is represented as function of the bus voltage, with an exponential model [1, 2]. From [1], the voltage dependency of the load may be written

$$P_{Load} = P_{L0}\left(\frac{|V|}{|V_0|}\right)^m \tag{2.10}$$

where P_{Load} is the load active power, P_{L0} is the load active power for initial bus voltage magnitude $|V_0|$; $|V|$ is the magnitude of the bus voltage, and m is the coefficient representing the load sensitivity to bus voltage changes.

After linearization, the variations in active power load demand are expressed as:

$$\Delta P_{Load} = m P_{L0}\left(\frac{|V_0|^{m-1}}{|V_0|^m}\right)\Delta|V| = m P_{L0}\left(\frac{\Delta|V|}{|V_0|}\right) = P_m\left(\frac{\Delta|V|}{|V_0|}\right) \tag{2.11}$$

By substituting equation (2.11) into the differential-algebraic model (2.5) yields

$$
\begin{bmatrix} 2H & 0 & 0 & 0 \\ 0 & 1 & 0 & 0 \\ 0 & 0 & 0 & 0 \\ 0 & 0 & 0 & 0 \end{bmatrix} \frac{d}{dt} \begin{bmatrix} \Delta\omega_r \\ \Delta\delta \\ \Delta\theta \\ \Delta|V|/|V| \end{bmatrix} = \begin{bmatrix} -K_D & -K_1 & K_1 & -K_2 \\ \omega_0 & 0 & 0 & 0 \\ 0 & K_1 & -K_{13} & K_2-K_6-P_m \\ 0 & -K_2 & K_2-K_6 & K_{78} \end{bmatrix} \begin{bmatrix} \Delta\omega_r \\ \Delta\delta \\ \Delta\theta \\ \Delta|V|/|V| \end{bmatrix}
$$

$$(2.12)$$

and reducing the algebraic equations, the ordinary differential equations for the system becomes

$$
\begin{bmatrix} 2H & 0 \\ 0 & 1 \end{bmatrix} \frac{d}{dt} \begin{bmatrix} \Delta\omega_r \\ \Delta\delta \end{bmatrix} = \left[\begin{bmatrix} -K_D & -K_1 \\ \omega_0 & 0 \end{bmatrix} - \begin{bmatrix} 0 & K_1 \\ 0 & -K_2 \end{bmatrix} \begin{bmatrix} -K_{13} & K_2-K_6-P_m \\ K_2-K_6 & K_{78} \end{bmatrix}^{-1} \begin{bmatrix} K_1 & -K_2 \\ 0 & 0 \end{bmatrix} \right] \begin{bmatrix} \Delta\omega_r \\ \Delta\delta \end{bmatrix}
$$

$$
\frac{d}{dt} \begin{bmatrix} \Delta\omega_r \\ \Delta\delta \end{bmatrix} = \begin{bmatrix} -K_D/2H & -K_S/2H \\ \omega_0 & 0 \end{bmatrix} \begin{bmatrix} \Delta\omega_r \\ \Delta\delta \end{bmatrix}
$$

$$(2.13)$$

The characteristic equation is

$$
\lambda^2 + \frac{K_D}{2H}\lambda + \frac{K_S}{2H}\omega_0 = 0
$$

$$(2.14)$$

which can be written

$$
\lambda^2 + 2\zeta\omega_n\lambda + \omega_n^2 = 0
$$

$$(2.15)$$

In terms of undamped natural frequency (ω_n) and damping ratio (ζ) the complex conjugate roots of the characteristic equation are

$$
\lambda_1, \lambda_2 = -\xi\omega_n \pm j\omega_n\sqrt{1-\xi^2}
$$

Where

$$
\omega_n = \sqrt{K_S \frac{\omega_0}{2H}} \; ; \qquad\qquad \zeta = \frac{1}{2}\frac{K_D}{2H\omega_n} = \frac{1}{2}\frac{K_D}{\sqrt{K_S 2H\omega_0}}
$$

From the above expression, it can be seen that as K_S increases, the natural undamped frequency increases and the damping ratio decreases. Similarly, an

increase in K_D increases the damping ratio and an increase in inertia constant decreases both, damping ratio and natural frequency.

To assess the effect of load characteristics on system behavior, coefficient K_S is analyzed for the cases without and with active load deviations ΔP_{Load}, these are as follows:

Without load deviations:

$$K_S = -K_1 + \frac{-K_{13}K_2^2 + 2K_1K_2(K_2 - K_6) + K_1^2 K_{78}}{(K_2 - K_6)^2 + K_{13}K_{78}} \qquad (2.16)$$

With load deviations:

$$K_S = -K_1 + \frac{-K_{13}K_2^2 + 2K_1K_2(K_2 - K_6) + K_1^2 K_{78} - K_1 K_2 P_m}{(K_2 - K_6)^2 + K_{13}K_{78} - (K_2 - K_6)P_m} \qquad (2.17)$$

It follows from equations (2.16) and (2.17) that the active load modifies the expression of the K_S by introducing new terms proportional to P_m. These new terms in (2.17) will decrease or increase the value of coefficient K_S, indirectly decreasing/increasing the natural frequency and increasing/decreasing the damping ratio. The ability of the load to affect damping depends on the load exponent, m.

We expand on the above observations in the following example.

2.4.2 Application to Single Machine-Infinite Bus System.

Consider a single-machine infinite bus system shown in Fig. 2.4. The post fault system conditions in per unit on the 2220 MVA, 24KV system base are shown in the diagram.

The generator is represented by its classical model with K_D = 10, H=3.5 MW-s/MVA and X'_d = 0.3 in per unit on the system base.
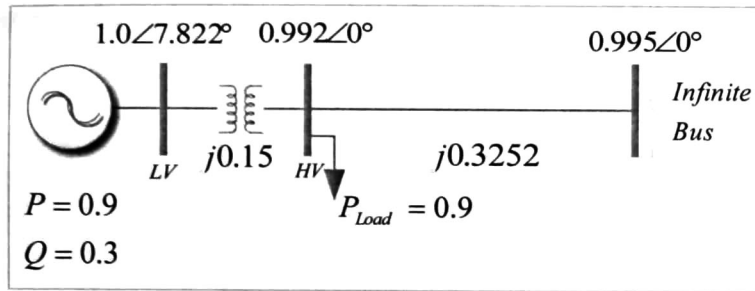
Figure 2.4: Initial conditions for the SMIB system.

Table 2.1:
Mode damping variations for different load characteristics.

Load Characteristic	m	Mode	Damping Ratio	Damped Freq. (Hz)
Constant Impedance	2	-0.7143 + 7.8075i	0.0911	1.2426
Constant Current	1	-0.7143 + 7.9247i	0.0898	1.2613
Constant MVA	0	-0.7143 + 8.0471i	0.0884	1.2807

Table 2.1 shows the system eigenvalues for various load characteristics. It can be seen that as m increases, the damping ratio is increased. These results are in line with the conclusions presented in previous sections.

In large interconnected systems, however, the impact of load on system behavior will depend on several interacting factors such as the load nature and its location relative to voltage control devices and excitation control.

For the purpose of introducing the more general ideas that follow, the active power swing flow, as well as the modal voltage phase angle for all buses associated with the electromechanical mode was computed[1].The special structure of this system allows the easy calculation of the modal distribution.

Following tables and figures show the contribution of each system element to the total oscillation flow associated with the electromechanical mode. The results are presented for three cases: (a) constant impedance load characteristics, (b) constant current characteristics, and (c) constant power characteristics.

---

[1] Values are normalized against the largest magnitude. For modal active power, phase angle near 0° as injecting element and angle near 180° as absorbing element.

Constant Impedance Characteristic

Table 2.2:
Modal voltage phase angle deviations. Constant impedance characteristic.

Modal Voltage Phase Angle Deviations		
	Normalized	
Bus	Relative Mag. (%)	Relative Phase
LV	100	0
HV	68.16784574	0
Infinite Bus	0.2633	0.17

Table 2.3:
Modal active power flow. Constant impedance characteristic.

Modal Active Power Flow		
	Normalized	
Element	Relative Mag. (%)	Relative Phase
Generator	86.6556	180
Infinite bus	100	0
Load	13.345	180
Transmission Line	100	0
Transformer	86.6668	0
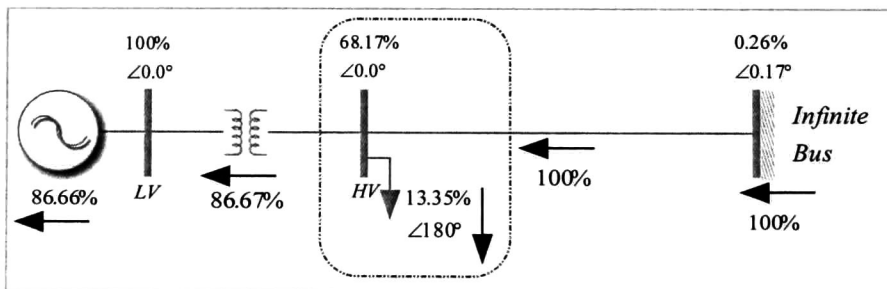
Figure 2.5: Modal power flow and voltage phase angle. Constant impedance characteristic.

Constant Current Characteristic

Table 2.4:
Modal voltage phase angle deviations. Constant current characteristic.

Modal Voltage Phase Angle Deviations		
	Normalized	
Bus	Relative Mag. (%)	Relative Phase
LV	100	0
HV	66.6512	0
Infinite Bus	0.2578	0.16

Table 2.5:
Modal active power flow. Constant current characteristic.

Modal Active Power Flow		
	Normalized	
Element	Relative Mag. (%)	Relative Phase
Generator	92.8514	180
Infinite bus	100	0
Load	7.1496	180
Transmission Line	100	0
Transformer	92.8627	0
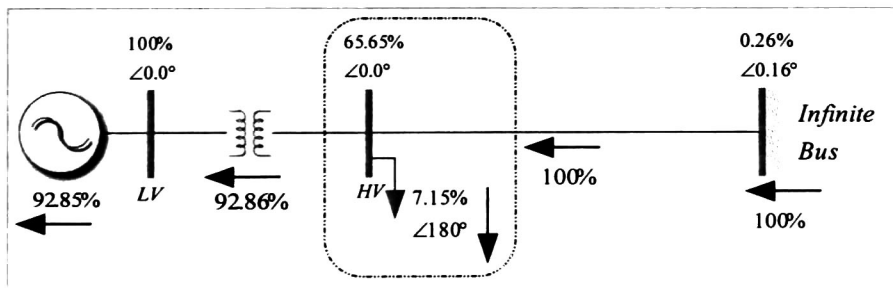
Figure 2.6: Modal power flow and voltage phase angle. Constant current characteristics.

Constant Power Characteristic

Modal Voltage Phase Angle Deviations		
	Normalized	
Bus	Relative Mag. (%)	Relative Phase
LV	100	0
HV	64.9827	0
Infinite Bus	0.2518	0.15

Modal Active Power Flow		
	Normalized	
Element	Relative Mag. (%)	Relative Phase
Generator	100	180
Infinite bus	100	0
Load	0	
Transmission Line	100	0
Transformer	100	0
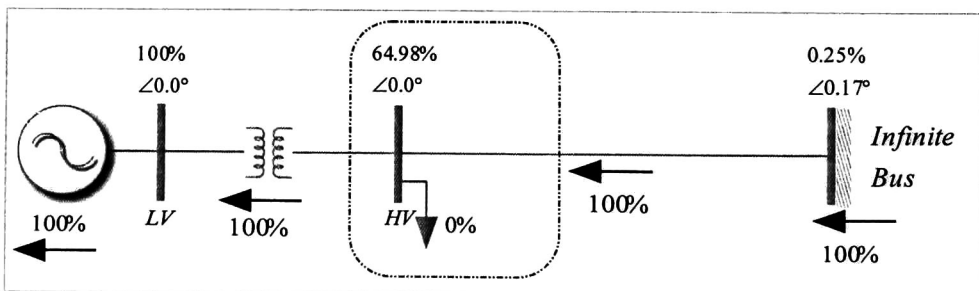
Figure 2.7: Modal power flow and voltage phase angle. Constant power characteristics.

The results in the preceding example have made clear that analyzing the distribution of modal power flow gives insight into the possible patterns of modal behavior that are likely to exist at any particular time across the network.

A few remarks are in order:

1. For the case under study, constant impedance load result in the highest contribution to modal power flow.

2. Static nonlinear load characteristics approaching constant power behavior have no effect on damping and no participation in modal power flow.

3. A load oscillating in opposition to the oscillation of the bus where is connected will have a positive effect on system damping. In contrast, a load oscillating in phase with the bus oscillation will have a positive impact on damping.

4. The extent to which the damping of and specific mode or a combination of modes is affected depends on the arguments of the modal active power flow of the load and modal voltage phase angle variations of the bus where is connected.

For the analysis of large-scale systems a procedure for dominant loads is presented below. Generalizations to this approach to compute power swing flows and modal voltage are discussed in detail in Chapters 3 and 4.

2.4.3 Analytical Procedure to Determine Dominant Loads

A load inside the power system is considered to be dominant for a mode or modes of interest, if variations in its dynamic characteristics result in changes in system damping.

1. More precisely, identification of dominant load requires analysis of two basic aspects:

    1.1. The magnitude of the modal voltage phase angle variations of the buses where a load is connected. The greater the magnitude the greater the effect of the load over the damping.

    1.2. The participation of the load in the exchange of modal active power.

2. Having selected the possible dominant loads it is important to verify the nature of the contribution to modal power. Results suggest that

2.1. If bus voltages and load contributions swing out of phase, the contribution will be positive.

2.2. If modal bus voltage deviations and modal load contributions are in phase the effect will be negative.

Once the dominant loads within the power system have been selected, the voltage dependant characteristic can be changed for one load at a time, leaving the rest unchanged; the effects on damping can then be calculated. This allows the variations of the load model to be considered or neglected.

The advantages of this approach are two-fold. First, loads having a larger impact on system behavior can be identified. Further, the nature of load contribution can be determined.

2.5 References

[1] P. Kundur, "Power System Stability and Control", McGraw-Hill, Inc. Ney York, 1994.

[2] P. W. Sauer and M. A. Pai, "Power System Dynamics and Stability", Prentice Hall, 1998.

[3] O. Samuelsson and B. Eliasson, "Damping of Electro-Mechanical Oscillations in a Multimachine System by Direct Load Control" IEEE Trans. Power Systems. Vol. 12 No. 4, 1997.

[4] O. Samuelsson "Power System Damping, Structural Aspects of Controlling Active Power". Ph. D. Thesis, Dept. of Industrial Electrical Engineering and Automation. Lund University, Lund, Sweden. 1997.

[5] G. Radman and J. Powell, "Dynamic Voltage Stability Improvement Using Coordinated Control of Dynamic VAR-Sources" Bulk Power System Dynamics and Control VII. Revitalizing Operational Reliability, 2007 iREP Symposium . August 19-24, 2007-Charleston, SC, USA.

[6] L. Vanfretti and J. H. Chow, "Computation and Analysis of Power System Voltage Oscillations from Interarea Modes" IEEE Transactions on Power Systems. August 2005.

[7] R. Graham, "Cap Tutorial Power System Structure and Oscillations. IEEE Computer Applications in Power Systems". April 1999. Pages 14-21.

[8]R. L. Bolden, "Use of stabilizing signals in static VAR compensators to enhance the damping of power systems", Symposium on Static VAR Systems, Capricornia Institute, Australia, November 1985.

[9]T. Smed, G. Andersson, "Utilising HVDC to Damp Power Oscillations" IEEE T-PWRD, Vol. 8 No. 2, Aprol 1993, pp 620-627.

Chapter3
Modal Power Oscillation Flow

Modal power flow is an efficient technique for describing spatial modal flow distribution in large power systems. In this chapter the concept of modal oscillation flow is introduced and its application to power system models is discussed. The method incorporates two aspects of conventional small signal analysis: modal analysis and small signal behavior.

The derivation is given of a systematic procedure for determining modal power flows in power systems incorporating synchronous machines, FACTS devices and dynamic loads. The analysis of system dynamic behavior is explored by a modal power oscillation flow algorithm.

Using this approach, a linear state model of an electric power system is developed which considers the representation of synchronous machines and controllers as subsystems of the state model which interact through the network description. The analysis framework also allows for explicit quantification of the impact of loads and system controllers on system behavior.

The potential advantages and limitations are pointed out and notation is established.

3.1 Power System Model and Equations

The power system state representation is seen as constituted of dynamic subsystems interacting through the transmission system. Consider to this end, a network composed of several dynamic subsystems, each of which can be represented by a component connection model [1]. Regardless of the connection structure, it is always possible to construct a composite state space model.

More precisely, each dynamic subsystem is represented by its own partial state model and an algebraic equation expressing its interaction with the power network. All elements are connected to the power network through its own current balance equation in order to obtain the global state representation of the electric power system.

In this representation, the input for every dynamic device and each load in the system is the real and imaginary parts of the terminal voltage variations and the output is the real and imaginary parts of the injected current variations to the power network.

Generalization to these models to include supplementary signals from the system such as frequency deviations, tie-line power or remote bus voltages are discussed below.

3.1.1 Partial Device Representation

In the system model, each dynamic device is represented by its own state representation as

$$\dot{\mathbf{x}}_k = \mathbf{A}_k \mathbf{x}_k + \mathbf{C}_k \Delta \mathbf{V}_k + \mathbf{B}_k \mathbf{u}_k \tag{3.1}$$

$$\Delta \mathbf{I}_k = \mathbf{W}_k \mathbf{x}_k + \mathbf{Y}_k \Delta \mathbf{V}_k \tag{3.2}$$

where

$\mathbf{x}_k$ is the vector of the kth device state variables.

$\Delta\mathbf{V}_k$ is the vector of terminal bus voltages for the kth dynamic device in D-Q reference frame $[\Delta V_{D_k} \ \Delta V_{Q_k}]^T$.

$\Delta\mathbf{I}_k$ is the vector of current injections into the network of the kth dynamic device in D-Q reference frame $[\Delta I_{D_k} \ \Delta I_{Q_k}]^T$

$\mathbf{u}_k$ is the vector of input signals to the kth device.

In what follows, we briefly review the nature of the adopted model. Emphasis is placed on the modeling of synchronous machines and network equations.

Synchronous Machine Equations

For simplicity and clarity of exposition, each synchronous machine is represented by its classical model – refer to Fig. 3.1. More general models follow this representation.
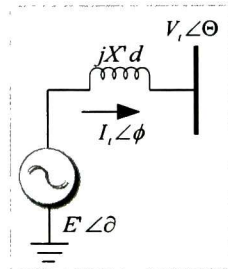
Figure 3.1: Synchronous machine equivalent model

Following Kundur [2], the equations relating the voltage at the terminal of a synchronous machine to that behind the transient reactance can be expressed as follows

$$V_t \angle \theta = V_{t_D} + jV_{t_Q} \tag{3.3}$$

and

$$I_t \angle \phi = I_{t_D} + jI_{t_Q} = \frac{E' \angle \delta - V_t \angle \theta}{jX'_d} \tag{3.4}$$

29

where E' is the voltage behind transient reactance X'_d, and δ is the internal rotor angle. $V_t \angle \theta$ is the terminal voltage and $I_t \angle \emptyset$ is the current injected to the network.

Separating (3.4) in real and imaginary parts and linearizing around an operating point, a linear incremental equation for the current injections of the synchronous machine to the network is given by the following expression

$$
\begin{bmatrix} \Delta I_{t_D} \\ \Delta I_{t_Q} \end{bmatrix} = \begin{bmatrix} \dfrac{e^0_D}{X'd} & 0 \\ \dfrac{e^0_Q}{X'd} & 0 \end{bmatrix} \begin{bmatrix} \Delta \delta \\ \Delta \omega_r \end{bmatrix} + \begin{bmatrix} 0 & -\dfrac{1}{X'd} \\ \dfrac{1}{X'd} & 0 \end{bmatrix} \begin{bmatrix} \Delta V_{t_D} \\ \Delta V_{t_Q} \end{bmatrix} \tag{3.5}
$$

where e^0_D and e^0_Q are the initial condition of the real and imaginary parts of the voltage behind transient reactance in D-Q network coordinates.

Expression (3.5) is in the form given by equation (3.2) with $\Delta \mathbf{X} = [\Delta \delta \, \Delta wr]^T$. Expanding the equations of motion about the initial equilibrium point yields

$$
\frac{d}{dt}\begin{bmatrix} \Delta \delta \\ \Delta \omega_r \end{bmatrix} = \begin{bmatrix} 0 & \omega_0 \\ \dfrac{-K_S}{2H} & \dfrac{-K_D}{2H} \end{bmatrix} \begin{bmatrix} \Delta \delta \\ \Delta \omega_r \end{bmatrix} + \begin{bmatrix} 0 & 0 \\ \dfrac{-e^0_Q}{2HX'd} & \dfrac{e^0_D}{2HX'd} \end{bmatrix} \begin{bmatrix} \Delta V_{t_D} \\ \Delta V_{t_Q} \end{bmatrix} + \begin{bmatrix} 0 \\ \dfrac{1}{2H} \end{bmatrix} \Delta P \tag{3.6}
$$

where, H is the inertia constant, K_D is the damping torque coefficient, K_s is the synchronizing torque coefficient and ω_0 is the rated speed in electrical radians per second. The above procedure can be extended to more complicated machine models.

As indicated in the expressions above a transformation, from the machine d-q reference frame to the network common D-Q reference frame must be applied before linearization.

FACTS Devices Equations

The structure of the dynamic representation of FACTS devices follows that of the system model in equations (3.1) and (3.2). Each dynamic device is represented by its own partial state representation, expressed as a function of its terminal voltage deviations. The interaction with the network can be obtained by a device-network interface equation, representing the FACTS device as current injections of the form presented in equation (3.2). See [3] for further details about this model.

3.1.2 Load Equation

For the purposes of this analysis, nonlinear load behavior can be represented by the following exponential model

$$P_L = P_{L0} \left[\frac{|V|}{|V_0|} \right]^m \tag{3.7}$$

$$Q_L = Q_{L0} \left[\frac{|V|}{|V_0|} \right]^n \tag{3.8}$$

where P_L and Q_L are the load active and reactive power, P_{L0} and Q_{L0} are the load active and reactive power for initial bus voltage magnitude $|V_0|$; $|V|$ is the magnitude of the bus voltage, and m, n are coefficients representing the load sensitivity to bus voltage changes. The static behavior of the loads can be related to the current injection equations from its small signal representation as

$$\begin{bmatrix} \Delta I_{L_D} \\ \Delta I_{L_Q} \end{bmatrix} = \begin{bmatrix} G_{DD} & B_{DQ} \\ -B_{QD} & G_{QQ} \end{bmatrix} \begin{bmatrix} \Delta V_{L_D} \\ \Delta V_{L_Q} \end{bmatrix} \tag{3.9}$$

where G_{DD}, B_{DQ}, B_{QD} and G_{QQ} are entries depending on the load characteristics and initial conditions given in [2].

Finally, the current injections from all loads in the system is given as

$$\Delta \mathbf{I}_L = \mathbf{Y}_L \Delta \mathbf{V}_L \tag{3.10}$$

where the elements of matrix $\mathbf{Y}_L$ contain the effects of nonlinear static loads.

3.1.3 Network Equation

The interconnecting network is represented by the node equations. For a network having n nodes, the interconnecting transmission network can be represented by the node equations

$$\begin{bmatrix} \Delta \mathbf{I}_d \\ \Delta \mathbf{I}_L \end{bmatrix} = \begin{bmatrix} \mathbf{Y}_{dd} & \mathbf{Y}_{dL} \\ \mathbf{Y}_{Ld} & \mathbf{Y}_{LL} \end{bmatrix} \begin{bmatrix} \Delta \mathbf{V}_d \\ \Delta \mathbf{V}_L \end{bmatrix} \tag{3.11}$$

where

$\Delta \mathbf{I}_d$ is the vector of current injections into the network from the devices. In D-Q reference frame.

$\Delta \mathbf{I}_L$ is the vector of current injections into the network from the loads. In D-Q reference frame.

$\Delta \mathbf{V}_d$ is the vector of device bus voltages in D-Q reference frame.

$\Delta \mathbf{V}_L$ is the vector of network bus voltages in D-Q reference frame.

Each entry of the symmetrical admittance matrix of expression (3.11) consists of *2x2* submatrices of the form

$$Y_{km} = \begin{bmatrix} G_{km} & -B_{km} \\ B_{km} & G_{km} \end{bmatrix}$$

for *k, m*=1, 2, 3, …, *n*.

3.2 Augmented System Model

A modified large-scale small-signal stability program is used to determine voltage control areas and reactive power sources having a strong influence on system behavior.

In developing the system equations we assume that each dynamic device is represented by a partial state model. The state space representation of the interconnected system can now be written as

$$\dot{\mathbf{x}}_d = \mathbf{A}_d \mathbf{x}_d + \mathbf{C}_d \Delta \mathbf{V}_d + \mathbf{B}_d \mathbf{u}_d \tag{3.12}$$

$$\Delta \mathbf{I}_d = \mathbf{W}_d \mathbf{x}_d + \mathbf{Y}_d \Delta \mathbf{V}_d \tag{3.13}$$

where the subscript "*d*" is used to indicate equations for dynamic devices. Matrices $\mathbf{A}_d$ and $\mathbf{C}_d$ are block diagonal matrices composed of the individual state models.

Substitution of equation (3.10) into the section of expression (3.11) for the load current variations gives

$$0 = \mathbf{Y}_{Ld}\Delta\mathbf{V}_d + (\mathbf{Y}_{LL} - \mathbf{Y}_L)\Delta\mathbf{V}_L \qquad (3.14)$$

With the connection of the loads represented by above expression, the interconnecting transmission network is now represented by

$$\Delta\mathbf{I} = \mathbf{Y'}_{BUS}\,\Delta\mathbf{V} \qquad (3.15)$$

where

$$\Delta\mathbf{I} = \begin{bmatrix} \Delta\mathbf{I}_d \\ \mathbf{0} \end{bmatrix}; \qquad \mathbf{Y'}_{BUS} = \begin{bmatrix} \mathbf{Y}_{dd} & \mathbf{Y}_{dL} \\ \mathbf{Y}_{Ld} & (\mathbf{Y}_{LL} - \mathbf{Y}_L) \end{bmatrix}; \qquad \Delta\mathbf{V} = \begin{bmatrix} \Delta\mathbf{V}_d \\ \Delta\mathbf{V}_L \end{bmatrix}$$

The subsystem equations can be combined as follows:

$$\begin{bmatrix} \mathbf{x} \\ \mathbf{0} \end{bmatrix} = \begin{bmatrix} \mathbf{A_d} & \mathbf{C} \\ -\mathbf{W} & \mathbf{Y}_{BUS}^m \end{bmatrix} \begin{bmatrix} \mathbf{x} \\ \Delta\mathbf{V} \end{bmatrix} + \begin{bmatrix} \mathbf{B}_d \\ \mathbf{0} \end{bmatrix} \mathbf{u} \qquad (3.16)$$

$$[\mathbf{y}] = \begin{bmatrix} \mathbf{C}_x & \mathbf{C}_v \end{bmatrix} \begin{bmatrix} \mathbf{x} \\ \Delta\mathbf{V} \end{bmatrix} \qquad (3.17)$$

where $\mathbf{x}$ is the state vector, $\Delta\mathbf{V}$ is the voltage deviations vector, $\mathbf{y}$ is the vector of outputs, and $\mathbf{u}$ is the vector of control inputs, and matrices $\mathbf{W}$, $\mathbf{C}$ and $\mathbf{Y}_{BUS}^m$ are defined as follows

$$\mathbf{W} = \begin{bmatrix} \mathbf{W}_d \\ \mathbf{0} \end{bmatrix}; \qquad \mathbf{Y}_{BUS}^m = \begin{bmatrix} (\mathbf{Y}_{dd} - \mathbf{Y}_d) & \mathbf{Y}_{dL} \\ \mathbf{Y}_{Ld} & (\mathbf{Y}_{LL} - \mathbf{Y}_L) \end{bmatrix}; \qquad \mathbf{C} = \begin{bmatrix} \mathbf{C}_d & \mathbf{0} \end{bmatrix}$$

In above equations, sub-matrices $\mathbf{A}_d$, $\mathbf{B}_d$, $\mathbf{C}_d$, $\mathbf{W}_d$ and $\mathbf{Y}_d$ represent the physical relations describing the interconnection of variables and the effects of controllers. In what follows this model is used to compute modal power flow studies. In the next chapter this model will help us to determine the modes of concern and the modal voltage deviations in a more efficient way for large power systems.

Figure 3.2 gives a block diagram representation of the dynamic model of power system in (3.16). As suggested in the diagram, the feedback signals ($\mathbf{K}_x$, $\mathbf{K}_v$) can be obtained from any measurement made to the power system, and are

represented by dotted lines. From this diagram we can define transfer functions and sensitivity functions between variables of concern.

Figure 3.2: Block diagram for the dynamic model of the power system.

3.3 Modal Deviations Analysis of Voltage and Current

Useful insight into the effect of voltage control on small signal stability can be found from the analysis of modal voltage solutions. As discussed in previous sections, the augmented system model shows the interaction between the internal parameters of the power system. These interactions are the basis of the modal power flow algorithm presented on this chapter.

Before introducing this technique, an interesting approach of the model proposed can be obtained, by defining the notion of modal deviations as matrices representing the interaction inside the power system.   In   the   next   two subsections, the notion of modal voltage deviations and modal current deviations are introduced and their practical application is analyzed in order to establish the best path for the analysis.

3.3.1 Modal Voltage Deviations

Useful insight into the effect of voltage control on small signal stability can be found from the analysis of modal voltage solutions.

34

Solving for the bus voltage deviations in (3.16) yields

$$
\begin{bmatrix} \Delta \mathbf{V}_d \\ \Delta \mathbf{V}_L \end{bmatrix} = \begin{bmatrix} (\mathbf{Y}_{dd} - \mathbf{Y}_d) & \mathbf{Y}_{dL} \\ \mathbf{Y}_{Ld} & (\mathbf{Y}_{LL} - \mathbf{Y}_L) \end{bmatrix}^{-1} \begin{bmatrix} \mathbf{W}_d \\ 0 \end{bmatrix} \mathbf{x} = \mathbf{S}_{vx} \Delta \mathbf{X}
\tag{3.18}
$$

where $\mathbf{S}_{vx}$ is a sensitivity matrix that relates the changes in the bus terminal voltages to the changes in the state vector deviations. In order to develop the concept of modal voltage deviations it is important to introduce the notion of system modes.

The Notion of System Modes.

Consider the linear system representation

$$
\dot{x}(t) = \mathbf{A} \ \mathbf{x}(t)
\tag{3.19}
$$

where $\mathbf{A}$ is the $n_A \times n_A$ state matrix and $\mathbf{x}$ is the perturbed n_A-vector.

From linear system theory [5] it follows that the free system response is given by

$$
\mathbf{x}(t) = e^{\mathbf{A}t} \mathbf{x(0)}
\tag{3.20}
$$

Matrices $\mathbf{A}$ and $e^{\mathbf{A}t}$ may be written as dynamic expansions

$$
\mathbf{A} = \sum_{i=1}^{n_A} \lambda_i \mathbf{U}_i \mathbf{V}_i^T
\tag{3.21}
$$

$$
e^{\mathbf{A}t} = \sum_{i=1}^{n_A} e^{\lambda_i t} \mathbf{U}_i \mathbf{V}_i^T
\tag{3.22}
$$

Equation (3.20) may then be written as

$$
\mathbf{x}(t) = \sum_{i=1}^{n_A} (\mathbf{V}_i^T \mathbf{x(0)}) \mathbf{U}_i e^{\lambda_i t} = \sum_{i=1}^{n_A} (c_i) \mathbf{U}_i e^{\lambda_i t}
\tag{3.23}
$$

where λ_i $(i=1, 2, \ldots, n_A)$ are the system eigenvalues and $\mathbf{U}_i$ and $\mathbf{V}_i$ are the corresponding left and right eigenvectors: $\mathbf{x(0)}$ is the initial state condition.

Inserting (3.23) into (3.18) yields

$$\Delta\mathbf{V}(\lambda_i) = (\mathbf{Y}_{BUS}^m)^{-1}(\mathbf{W})\sum_{i=1}^{nmc}(c_i)\mathbf{U}_i e^{\lambda_i t} \tag{3.24}$$

where *nmc* is the number of modes of concern.

For a swing mode of concern, (3.24) allows modal voltages to be computed as a function of modal quantities. Because of its linearity, modal solutions can be associated with a single mode or mode combinations.

Several possibilities exist in the analysis process. These are briefly described below.

An interesting physical interpretation can be given to the above equation as the product of impedance and modal current injections

$$\Delta\mathbf{V}(\lambda_i) = (\mathbf{Y}_{BUS}^m)^{-1}\mathbf{I}_{mod}(\lambda_i) \tag{3.25}$$

in which $\mathbf{I}_{mod}$ is the modal current injection from every dynamic device defined as

$$\mathbf{I}_{mod}(\lambda_i) = \begin{pmatrix} \mathbf{W}_d \\ \mathbf{0} \end{pmatrix}\sum_{i=1}^{nmc}(c_i)\mathbf{U}_i e^{\lambda_i t} \tag{3.26}$$

Now, letting t=0 in equation (3.26) the modal voltage deviations associated with each combination of motion modes or energy modes can be determined by solving equation (3.25) for different $\mathbf{I}_{mod}$. Thanks to the linearity of the model proposed the sum of the modal voltage for each motion mode gives the total solution. For the case of stable systems, the expression for modal current injections is analyzed at time t=0 because for a stable mode of the system the maximum values are found at that time.

Once the modal voltage is obtained, the modal current deviations experienced by all dynamic devices within the power system can be calculated from (3.13)

$$\Delta\mathbf{I}_d(\lambda_i) = \mathbf{W}_d\,\mathbf{x}(\lambda_i) + \mathbf{Y}_d\,\Delta\mathbf{V}_d(\lambda_i) = \mathbf{I}_{mod_d}(\lambda_i) + \mathbf{Y}_d\Delta\mathbf{V}_d(\lambda_i) \tag{3.27}$$

Figure 3.3 sketches the nature of the adopted model.
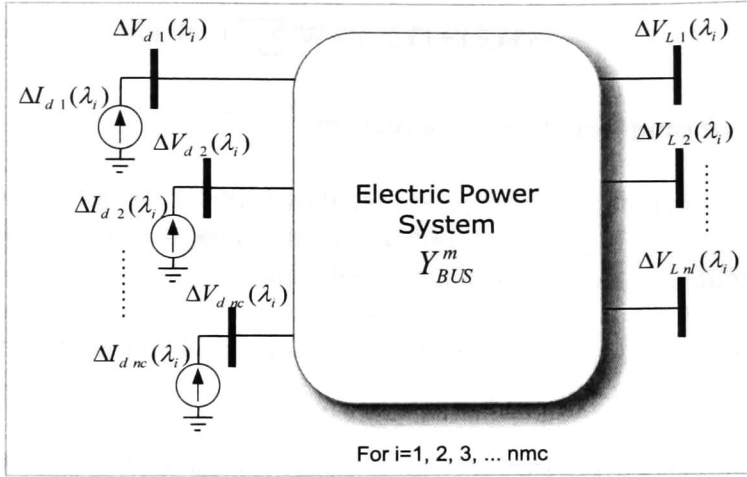
Figure 3.3: Equivalent model for the modal voltage analysis of the power system.

For the algorithm developed the $\mathbf{I}_{mod}$ is selected as a combination of motion modes or energy modes. Table 3.1 illustrates the nature of the modal current injections for specific modes of interest, as defined in [9].

Table 3.1:
Evaluation of modal current injections.

Mode	Description	Modal Current Injection
λ_i	Motion Mode	$\mathbf{I}_{mod}(\lambda_i) = \begin{pmatrix} \mathbf{W}_d \\ \mathbf{0} \end{pmatrix}(\mathbf{V}_i^T\mathbf{x}(0))\mathbf{U}_i e^{\lambda_i t}$
$\lambda_i + \lambda_i^*$	Energy Mode	$\mathbf{I}_{mod}(\lambda_i, \lambda_i^{\check{}}) = \begin{pmatrix} \mathbf{W}_d \\ \mathbf{0} \end{pmatrix}\{(\mathbf{V}_i^T\mathbf{x}(0))\mathbf{U}_i e^{\lambda_i t} + (\mathbf{V}_i^T\mathbf{x}(0))\mathbf{U}_i e^{\lambda_i^{\check{}} t}\}$
$\lambda_i + \lambda_j$	Energy Mode	$\mathbf{I}_{mod}(\lambda_i, \lambda_j) = \begin{pmatrix} \mathbf{W}_d \\ \mathbf{0} \end{pmatrix}\{(\mathbf{V}_i^T\mathbf{x}(0))\mathbf{U}_i e^{\lambda_i t} + (\mathbf{V}_j^T\mathbf{x}(0))\mathbf{U}_j e^{\lambda_j t}\}$
$(\lambda_i + \lambda_i^*)$ $+ (\lambda_j + \lambda_j^*)$	Energy Mode	$\mathbf{I}_{mod}(\lambda_i, \lambda_i^{\check{}}, \lambda_j, \lambda_j^{\check{}}) = \begin{pmatrix} \mathbf{W}_d \\ \mathbf{0} \end{pmatrix}\{(\mathbf{V}_i^T\mathbf{x}(0))\mathbf{U}_i e^{\lambda_i t} + (\mathbf{V}_i^T\mathbf{x}(0))\mathbf{U}_i e^{\lambda_i^{\check{}} t}$ $+ (\mathbf{V}_j^T\mathbf{x}(0))\mathbf{U}_j e^{\lambda_j t} + (\mathbf{V}_j^T\mathbf{x}(0))\mathbf{U}_j e^{\lambda_j^{\check{}} t}\}$

It should be noted that the modal voltage may be real or complex numbers depending on the nature of the modal current injections.

A few remarks are in order in the interpretation of the system model:

1. Relation (3.18) involves a transformation from the eigenvalue/vector reference frame to the common D-Q network reference frame [8].

2. An efficient computational technique for the analysis of power systems and it allows the use of conventional analysis tools.

The information from (3.26) is calculated as real and imaginary parts, in order to exploit the ideas presented in chapter 2, the voltage magnitude and phase angle deviations need to be calculated.

Let the bus voltages be expressed in terms of the real and imaginary components as:

$$|V_k| = \sqrt{V_{D_k}^2 + V_{Q_k}^2} \tag{3.28}$$

$$\theta_{V_k} = \arctan\left(\frac{V_{D_k}}{V_{Q_k}}\right) \tag{3.29}$$

From (3.28) and (3.29) the voltage magnitude and angle deviations for a k bus in the system can be calculated using

$$\Delta|V_k| = \begin{bmatrix} \dfrac{V_{D_k}^0}{|V_k^0|} & \dfrac{V_{Q_k}^0}{|V_k^0|} \end{bmatrix} \begin{bmatrix} \Delta V_{D_k} \\ \Delta V_{Q_k} \end{bmatrix} \tag{3.30}$$

$$\Delta\theta_{V_k} = \begin{bmatrix} \dfrac{-V_{Q_1}^0}{|V_1^0|^2} & \dfrac{V_{D_1}^0}{|V_1^0|^2} \end{bmatrix} \begin{bmatrix} \Delta V_{D_k} \\ \Delta V_{Q_k} \end{bmatrix} \tag{3.31}$$

Substitutions of (3.25) in (3.30) and (3.31) the modal contribution in voltage magnitude and angle for all buses in the system is given as:

$$\Delta|\mathbf{V}|(\lambda_i) = |\Delta|\mathbf{V}||\angle\varphi_{\Delta|V|} = \mathbf{M}_{|V|}(\mathbf{Y}_{BUS}^m)^{-1}\mathbf{I}_{mod}(\lambda_i) \tag{3.32}$$

$$\Delta\mathbf{\theta}_V(\lambda_i) = |\Delta\mathbf{\theta}_V|\angle\varphi_{\Delta\theta_V} = \mathbf{M}_{\theta_V}(\mathbf{Y}_{BUS}^m)^{-1}\mathbf{I}_{mod}(\lambda_i) \tag{3.33}$$

where $\mathbf{M}_{|V|}$ and $\mathbf{M}_{\theta_V}$ are block diagonal matrices containing the initial bus voltage values in D-Q reference frame and are represented as

$$\mathbf{M}_{|V|} = diag \left\{ \begin{bmatrix} \dfrac{V_{D_1}^0}{|V_1^0|} & \dfrac{V_{Q_1}^0}{|V_1^0|} \end{bmatrix} \begin{bmatrix} \dfrac{V_{D_2}^0}{|V_2^0|} & \dfrac{V_{Q_2}^0}{|V_2^0|} \end{bmatrix} \cdots \begin{bmatrix} \dfrac{V_{D_n}^0}{|V_n^0|} & \dfrac{V_{Q_n}^0}{|V_n^0|} \end{bmatrix} \right\}$$

$$\mathbf{M}_{\theta_V} = diag \left\{ \begin{bmatrix} \dfrac{-V_{Q_1}^0}{|V_1^0|^2} & \dfrac{V_{D_1}^0}{|V_1^0|^2} \end{bmatrix} \begin{bmatrix} \dfrac{-V_{Q_2}^0}{|V_2^0|^2} & \dfrac{V_{D_2}^0}{|V_2^0|^2} \end{bmatrix} \cdots \begin{bmatrix} \dfrac{-V_{Q_n}^0}{|V_n^0|^2} & \dfrac{V_{D_n}^0}{|V_n^0|^2} \end{bmatrix} \right\}$$

Once modal voltages are computed, the phase of modal contributions can be used to identify geographical areas showing coherent behavior. Buses experiencing the largest magnitude of oscillations indicate zones where voltage support is expected to have the largest influence on the inter-area modes of concern. These buses are grouped together using the phase information to form a voltage control area.

With the purpose of comparing an alternative procedure is developed and presented in the following section.

3.3.2 Modal Current Deviations

In this procedure, the current deviations on terminals of dynamic devices within the power system are calculated as the main variable. From (3.14) modal voltage deviations at load buses can be expressed in terms of $\Delta \mathbf{V}_d$ as follows:

$$\Delta \mathbf{V}_L = -(\mathbf{Y}_{LL} - \mathbf{Y}_L)^{-1} \mathbf{Y}_{Ld} \Delta \mathbf{V}_d \tag{3.34}$$

and

$$\Delta \mathbf{I}_d = \left[\mathbf{I}_n - \mathbf{Y}_d \left[\mathbf{Y}_{dd} - \mathbf{Y}_{dL}(\mathbf{Y}_{LL} - \mathbf{Y}_L)^{-1} \mathbf{Y}_{Ld} \right]^{-1} \right]^{-1} \mathbf{W}_d \ \mathbf{x} = \mathbf{S}_{ix} \ \mathbf{x} \tag{3.35}$$

where $\mathbf{I}_n$ is the identity matrix. Here matrix $\mathbf{S}_{ix}$ represents the sensitivity of current injections from the dynamic devices to changes in the state vector.

Substituting (3.23) into (3.35) we can write

$$\Delta \mathbf{I}_d(\lambda_i) = \mathbf{S}_{ix} \sum_{i=1}^{nmc} (c_i) \mathbf{U}_i e^{\lambda_i t} \tag{3.36}$$

39

Now, letting t=0 in equation (3.36) the modal current deviations associated with each mode or combination of modes can be determined.

It then follows that

$$\Delta \mathbf{V}_d = \mathbf{Y}_d^{-1}(\Delta \mathbf{I}_d - \mathbf{W}_d \, \Delta \mathbf{X}) \qquad (3.37)$$

And the solution for (3.37) is substituted into equation (3.35) to obtain the modal voltages for load buses. This analysis requires great amount of calculation effort and evaluation time.

Alternatives to compute modal quantities are discussed in Chapter 4.

3.4 Modal Active and Reactive Power

Modal power flow analysis provides a general framework for the analysis of kinetic energy exchange in complex systems. It establishes the variations of power from any element inside the electric power system due to the excitation of a specific system mode or a combination of modes.

Before proceeding with the analysis of modal power flow, some basic concepts are briefly revisited. Let $V_{D_k}, V_{Q_k}, I_{D_k}$ and I_{Q_k} be the real and imaginary parts of the voltage and current at bus k. It follows that

$$P_k = V_{D_k} I_{D_k} + V_{Q_k} I_{Q_k} \qquad (3.38)$$

$$Q_k = V_{Q_k} I_{D_k} - V_{D_k} I_{Q_k} \qquad (3.39)$$

3.4.1 Contribution of Synchronous Machines and Control Devices to the Modal Power Flow

Expanding equations (3.38) and (3.39) around an initial condition of interest and neglecting terms involving second and higher orders, the modal active and reactive power for any k-device can be expressed as

$$\Delta P_{d_k} = \begin{bmatrix} I_{D_k}^0 & I_{Q_k}^0 \end{bmatrix} \begin{bmatrix} \Delta V_{D_k} \\ \Delta V_{Q_k} \end{bmatrix} + \begin{bmatrix} V_{D_k}^0 & V_{Q_k}^0 \end{bmatrix} \begin{bmatrix} \Delta I_{D_k} \\ \Delta I_{Q_k} \end{bmatrix} \qquad (3.40)$$

$$\Delta Q_{d_k} = \begin{bmatrix} -I_{Q_k}^0 & I_{D_k}^0 \end{bmatrix} \begin{bmatrix} \Delta V_{D_k} \\ \Delta V_{Q_k} \end{bmatrix} + \begin{bmatrix} V_{Q_k}^0 & -V_{D_k}^0 \end{bmatrix} \begin{bmatrix} \Delta I_{D_k} \\ \Delta I_{Q_k} \end{bmatrix} \tag{3.41}$$

where $V_{D_k}^0, V_{Q_k}^0, I_{D_k}^0$ and $I_{Q_k}^0$ represent the initial operating conditions for the voltages and currents at the device terminals. Inserting the expression for modal current deviations (3.27) in the above equations gives after some simplifications

$$\begin{aligned} \Delta \mathbf{P}_d(\lambda_i) &= |\Delta \mathbf{P}_d| \angle \varphi_{Pd} = \\ &\quad (\mathbf{I}_{gd}^0 + \mathbf{V}_{gd}^0 \mathbf{Y}_d)\, \Delta \mathbf{V}_d(\lambda_i) + \mathbf{V}_{gd}^0\, \mathbf{W}_d\, \mathbf{x}(\lambda_i) \end{aligned} \tag{3.42}$$

$$\begin{aligned} \Delta \mathbf{Q}_d(\lambda_i) &= |\Delta \mathbf{Q}_d| \angle \varphi_{Qd} = \\ &\quad (\mathbf{I}_{gq}^0 + \mathbf{V}_{gq}^0 \mathbf{Y}_d)\, \Delta \mathbf{V}_d(\lambda_i) + \mathbf{V}_{gq}^0\, \mathbf{W}_d\, \mathbf{x}(\lambda_i) \end{aligned} \tag{3.43}$$

where nc is the number of dynamic devices and $\mathbf{I}_{gd}^0$, $\mathbf{I}_{gq}^0$, $\mathbf{V}_{gd}^0$ and $\mathbf{V}_{gq}^0$ are the real and imaginary parts of the initial values for currents and voltages in the system, given by

$$\mathbf{I}_{gd}^0 = diag\left\{ \begin{bmatrix} I_{D_1}^0 & I_{Q_1}^0 \end{bmatrix} \begin{bmatrix} I_{D_2}^0 & I_{Q_2}^0 \end{bmatrix} \cdots \begin{bmatrix} I_{D_{nc}}^0 & I_{Q_{nc}}^0 \end{bmatrix} \right\}$$

$$\mathbf{I}_{gq}^0 = diag\left\{ \begin{bmatrix} -I_{q_1}^0 & I_{d_1}^0 \end{bmatrix} \begin{bmatrix} -I_{q_2}^0 & I_{d_2}^0 \end{bmatrix} \cdots \begin{bmatrix} -I_{q_{nc}}^0 & I_{d_{nc}}^0 \end{bmatrix} \right\}$$

$$\mathbf{V}_{gd}^0 = diag\left\{ \begin{bmatrix} V_{d_1}^0 & V_{q_1}^0 \end{bmatrix} \begin{bmatrix} V_{d_2}^0 & I_{q_2}^0 \end{bmatrix} \cdots \begin{bmatrix} V_{d_{nc}}^0 & V_{q_{nc}}^0 \end{bmatrix} \right\}$$

$$\mathbf{V}_{gq}^0 = diag\left\{ \begin{bmatrix} V_{q_1}^0 & -V_{d_1}^0 \end{bmatrix} \begin{bmatrix} V_{q_2}^0 & -V_{d_2}^0 \end{bmatrix} \cdots \begin{bmatrix} V_{q_{nc}}^0 & -V_{d_{nc}}^0 \end{bmatrix} \right\}$$

The second term on each of the above equations contains the vector of modal current injections associated with the mode or modes of interest. Defining

$$\Delta P_d(\lambda_i) = \begin{bmatrix} \Delta P_{d_1} & \Delta P_{d_2} & \cdots & \Delta P_{d_{nc}} \end{bmatrix}^T$$

$$\Delta Q_d(\lambda_i) = \begin{bmatrix} \Delta Q_{d_1} & \Delta Q_{d_2} & \cdots & \Delta Q_{d_{nc}} \end{bmatrix}^T$$

the participation of each device in the modal power oscillation flow is calculated by substituting the expression for modal voltage (3.25) and modal current injections (3.26) associated to the modes of concern into equations (3.42) and (3.43).

The following conclusions can be drawn from the above analysis:

For modal active power:

1. In general, modal powers are complex quantities. The magnitude related to a specific mode allows identifying the contribution of each machine in the system to the inter-area oscillation phenomenon. The largest magnitude indicates which device has the higher contribution.

2. The phase angle indicates the power exchange pattern between machines in the power system. The power exchange pattern can be established by grouping those generators that shows coherent behavior (similar angle phase) and determine which group of machines oscillates respect to another group of machines inside the system.

3. The balance of modal active power is equal to zero for every node of the system.

4. The modal active power is related with the acceleration power of the system.

For modal reactive power:

1. Normalized magnitudes indicate the participation of the dynamic devices in modal reactive power flow. The dependence of reactive power deviations of the dynamic devices due to variations in voltage, represented by equation (3.21), which in turn depend on changes in the states of the system.

2. Phase angle indicates the behavior of the dynamic device in the modal reactive power exchange. Devices with angle near 0° can be grouped as generating units and devices with angle phase near 180° as absorbing devices).

3. The balance of modal reactive power flow is equal to zero for every node of the system.

4. Information from the modal reactive power is important in voltage stability because indicates which devices will experience the highest variation of reactive power due to changes in voltage magnitude.

3.4.2 Contribution of Loads to the Modal Power Flow

From (3.7) and (3.8) we can write

$$\Delta P_{L_k} = \begin{bmatrix} L_{P11_k} & L_{P12_k} \end{bmatrix} \begin{bmatrix} \Delta V_{D_k} \\ \Delta V_{Q_k} \end{bmatrix} = \mathbf{P}_{LV_k} \Delta \mathbf{V}_{L_k} \tag{3.44}$$

$$\Delta Q_{L_k} = \begin{bmatrix} L_{Q11_k} & L_{Q12_k} \end{bmatrix} \begin{bmatrix} \Delta V_{D_k} \\ \Delta V_{Q_k} \end{bmatrix} = \mathbf{Q}_{LV_k} \Delta \mathbf{V}_{L_k} \tag{3.45}$$

in which the model coefficients are given by

$$L_{P11_k} = V_{D_k}^0 G_{DD} - V_{Q_k}^0 B_{QD} + I_{D_k}^0$$
$$L_{P12_k} = V_{D_k}^0 B_{DQ} + V_{Q_k}^0 G_{QQ} + I_{Q_k}^0$$
$$L_{Q11_k} = V_{Q_k}^0 G_{DD} + V_{D_k}^0 B_{QD} - I_{Q_k}^0$$
$$L_{Q12_k} = V_{Q_k}^0 B_{DQ} - V_{D_k}^0 G_{QQ} + I_{D_k}^0$$

where the sensitivity coefficients G_{DD}, B_{DQ}, B_{QD} and G_{QQ} depend on load characteristics and operation conditions. The initial values for load currents can be obtained from the following expressions:

$$I_{D_k}^0 = \frac{P_{L_k}^0 V_{D_k}^0 + Q_{L_k}^0 V_{Q_k}^0}{\left(V_k^0\right)^2} \; ; \quad I_{Q_k}^0 = \frac{P_{L_k}^0 V_{Q_k}^0 - Q_{L_k}^0 V_{Q_k}^0}{\left(V_k^0\right)^2}$$

$$\left|V_k^0\right| = \sqrt{(V_{D_k}^0)^2 + (V_{Q_k}^0)^2}$$

Substituting expression (3.25) into equations (3.44) and (3.45) the contribution of the *nl* loads of the power system in modal power is obtained as

$$\Delta \mathbf{P}_L(\lambda_i) = |\Delta \mathbf{P}_L| \angle \varphi_{PL} = \mathbf{P}_{LV} \Delta \mathbf{V}_L(\lambda_i) = \mathbf{P}_{LV} \left(\mathbf{Y}_{BUS}^m\right)^{-1} \mathbf{W} \; \mathbf{x}(\lambda_i) =$$
$$= \mathbf{P}_{LV} \; \mathbf{S}_{VX} \mathbf{x}(\lambda_i) = \mathbf{P}_{LV} \left(\mathbf{Y}_{BUS}^m\right)^{-1} \mathbf{I}_{mod}(\lambda_i) \tag{3.46}$$

43

$$\Delta \mathbf{Q}_L(\lambda_i) = |\,\Delta \mathbf{Q}_L\,| \angle \boldsymbol{\varphi}_{QL} = \mathbf{Q}_{LV}\, \Delta \mathbf{V}_L(\lambda_i) = \mathbf{Q}_{LV}\, \left(\mathbf{Y}_{BUS}^m\right)^{-1} \mathbf{W}\ \mathbf{x}(\lambda_i) =$$
$$= \mathbf{Q}_{LV}\, \mathbf{S}_{VX}\, \mathbf{x}(\lambda_i) = \mathbf{Q}_{LV}\, \left(\mathbf{Y}_{BUS}^m\right)^{-1} \mathbf{I}_{\mathrm{mod}}(\lambda_i)$$
(3.47)

where

$$\mathbf{P}_{LV} = diag\left\{ \begin{bmatrix} L_{P11_1} & L_{P12_1} \end{bmatrix} \begin{bmatrix} L_{P11_2} & L_{P12_2} \end{bmatrix} \cdots \begin{bmatrix} L_{P11_{nl}} & L_{P12_{nl}} \end{bmatrix} \right\}$$

$$\mathbf{Q}_{LV} = diag\left\{ \begin{bmatrix} L_{Q11_1} & L_{Q12_1} \end{bmatrix} \begin{bmatrix} L_{Q11_2} & L_{Q12_2} \end{bmatrix} \cdots \begin{bmatrix} L_{Q11_{nl}} & L_{Q12_{nl}} \end{bmatrix} \right\}$$

and

$$\Delta \mathbf{P}_L(\lambda_i) = \begin{bmatrix} \Delta P_{L_1} & \Delta P_{L_2} & \cdots & \Delta P_{L_{nl}} \end{bmatrix}^T$$

$$\Delta \mathbf{Q}_L(\lambda_i) = \begin{bmatrix} \Delta Q_{L_1} & \Delta Q_{L_2} & \cdots & \Delta Q_{L_{nl}} \end{bmatrix}^T$$

According to previous chapter the load contribution to the active oscillation flow depends on the following factors;

1. Characteristics of loads model: Loads with constant impedance characteristic have the higher participation, while with constant MVA the participation is equal to zero.

2. Location of the loads: Depending of the oscillation of the load and the bus where is connected the contribution can be in a positive way, contrary oscillation, or in a negative way, coherent oscillation.

3. Location of control devices: According to [8], Loads with poor voltage regulation characteristics may contribute very significantly to modal power flow.

As in the dynamic devices, for the modal reactive power flow, the argument indicates the loads in the system experiencing the highest participation and the angle indicates if those loads are injecting, with angle near 0°, modal reactive power or consuming, with angle near 180°.

3.4.3 Contribution of Transmission Lines to the Modal Power Flow

Consider a line transmission represented by its equivalent Π circuit:
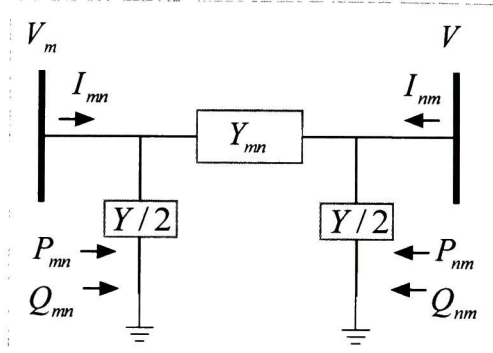
Figure 3.4: Transmission line model.

From figure 3.4 the complex power can be expressed as:

$$S_{mn} = P_{mn} + jQ_{mn} = V_m I_{mn}^* \qquad (3.48)$$

where * indicates conjugate. Linearazing above equation around an operating point gives

$$\Delta P_{R_k} = \begin{bmatrix} P_{11_k} & P_{12_k} \end{bmatrix} \begin{bmatrix} \Delta V_{D_m} \\ \Delta V_{Q_m} \end{bmatrix} + \begin{bmatrix} P_{21_k} & P_{22_k} \end{bmatrix} \begin{bmatrix} \Delta V_{D_n} \\ \Delta V_{Q_n} \end{bmatrix} \qquad (3.49)$$

$$\Delta Q_{R_k} = \begin{bmatrix} Q_{11_k} & Q_{12_k} \end{bmatrix} \begin{bmatrix} \Delta V_{D_m} \\ \Delta V_{Q_m} \end{bmatrix} + \begin{bmatrix} Q_{21_k} & Q_{22_k} \end{bmatrix} \begin{bmatrix} \Delta V_{D_n} \\ \Delta V_{Q_n} \end{bmatrix} \qquad (3.50)$$

where coefficients P_{11}, P_{12}, P_{21}, P_{22} and Q_{11}, Q_{12}, Q_{21}, Q_{22} depend on parameters of the transmission line: series resistance and reactance and the shunt susceptance as well as the initial voltages for bus "m" and "n".

Substituting expression for modal voltage deviations into above equations and for a system with L transmission links and B buses the modal active and reactive power are given by:

$$\Delta \mathbf{P}_R(\lambda_i) = | \Delta \mathbf{P}_R | \angle \varphi_{PR} = \mathbf{P} \, \Delta \mathbf{V}(\lambda_i) = \mathbf{P} \left(\mathbf{Y}_{BUS}^m \right)^{-1} \mathbf{W} \, \mathbf{x}(\lambda_i) = \mathbf{P} \left(\mathbf{Y}_{BUS}^m \right)^{-1} \mathbf{I}_{\text{mod}}(\lambda_i) \qquad (3.51)$$

45

$$\Delta \mathbf{Q}_R(\lambda_i) = |\Delta \mathbf{Q}_R| \angle \varphi_{QR} = \mathbf{Q} \, \Delta \mathbf{V}(\lambda_i) = \mathbf{Q} \left(Y^m_{BUS}\right)^{-1} \mathbf{W} \, \mathbf{x}(\lambda_i) = \mathbf{Q} \left(\mathbf{Y}^m_{BUS}\right)^{-1} \mathbf{I}_{mod}(\lambda_i) \quad (3.52)$$

where $\mathbf{P}$ and $\mathbf{Q}$ are $L \times 2B$ block diagonal matrices numerically depending on transmission line parameters and initial operation conditions.

The following conclusions in transmissions lines can be established:

1. Magnitude of modal active power for transmission lines indicates the stress level of the branches in the power system. Lines having greater magnitude of oscillation are, generally, those that connect machines showing the largest participation in the mode of concern.

2. Normalized phase angle, for active power, indicates if the modal flow proposed is correct (angle = 0°) or is in the opposite direction (angle=180°).

3. Transmission lines, like loads and dynamic elements, injects or absorbs modal reactive power, having a different behavior to that seen in the modal active power, where only work as the connection between generating units and absorbing units.

4. The phase angle of reactive power indicates the direction of the modal reactive power flow, injecting to or absorbing from a specific node.

It is important to mention that the analysis for transmission lines presented in this section is from bus "m" to bus "n" but, and specially for modal reactive power, an analysis from bus "n" to bus "m" is necessary to be performed.

3.4.4 Contribution of Transformers to the Modal Power Flow

Consider a transformer represented by the following circuit
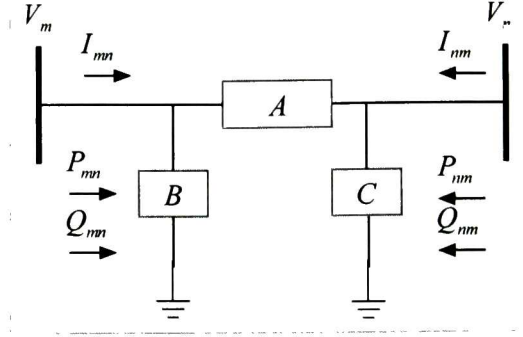
Figure 3.5: Transformer model.

Where *A*, *B* and *C* are the parameters of the transformer expressed in terms of admittance and off-nominal turns ratio given in reference [4] as

$$A = \frac{Y_{mn}}{tap}; \qquad B = \frac{1}{tap}(\frac{1}{tap} - 1)Y_{mn}; \qquad C = (1 - \frac{1}{tap})Y_{mn}$$

Following the same procedure as for transmission lines, the expressions for modal active and reactive power for the kth transformer are given by:

$$\Delta P_{T_k} = \begin{bmatrix} P_{11_k} & P_{12_k} \end{bmatrix} \begin{bmatrix} \Delta V_{D_m} \\ \Delta V_{Q_m} \end{bmatrix} + \begin{bmatrix} P_{21_k} & P_{22_k} \end{bmatrix} \begin{bmatrix} \Delta V_{D_n} \\ \Delta V_{Q_n} \end{bmatrix} \qquad (3.53)$$

$$\Delta Q_{T_k} = \begin{bmatrix} Q_{11_k} & Q_{12_k} \end{bmatrix} \begin{bmatrix} \Delta V_{D_m} \\ \Delta V_{Q_m} \end{bmatrix} + \begin{bmatrix} Q_{21_k} & Q_{22_k} \end{bmatrix} \begin{bmatrix} \Delta V_{D_n} \\ \Delta V_{Q_n} \end{bmatrix} \qquad (3.54)$$

where coefficients P_{11}, P_{12}, P_{21}, P_{22} and Q_{11}, Q_{12}, Q_{21}, Q_{22} depend on parameters of the transformer: turns ratio, resistance and reactance as well as the initial voltages.

Equations (3.53) and (3.54) can be integrated to the expression for transmission lines (3.51) and (3.52) and the same conclusions applied for transformers.

3.5 Closed-Form Solution

In previous sections of this chapter the solution proposed for modal power oscillation study was assumed in open loop. However the influence of feedback signals over the modal power flow can also be evaluated by following the proposed

closed-loop representation of the augmented system model. It is obtained by expressing the input signals in control devices as function of the state variables and terminal voltage deviations.

The augmented state model with the system output signals is expressed as

$$
\begin{bmatrix} \mathbf{x} \\ \mathbf{0} \end{bmatrix} = \begin{bmatrix} \mathbf{A_d} & \mathbf{C} \\ -\mathbf{W} & \mathbf{Y}^m_{BUS} \end{bmatrix} \begin{bmatrix} \mathbf{x} \\ \mathbf{\Delta V} \end{bmatrix} + \begin{bmatrix} \mathbf{B_d} \\ \mathbf{0} \end{bmatrix} \mathbf{u}
\tag{3.55}
$$

$$
[\mathbf{y}] = [\mathbf{C_x} \quad \mathbf{C_v}] \begin{bmatrix} \mathbf{x} \\ \mathbf{\Delta V} \end{bmatrix}
\tag{3.56}
$$

where the output vector $\mathbf{y}$ contains measured signals, namely line power and current, and terminal bus voltages.

The feedback signals are introduced to the system through the input signals vector $\mathbf{u}$, this is

$$
\mathbf{u} = \mathbf{K}[\mathbf{y}] = \mathbf{K}[\mathbf{C_x} \quad \mathbf{C_v}] \begin{bmatrix} \mathbf{x} \\ \mathbf{\Delta V} \end{bmatrix} = [\mathbf{K_x} \quad \mathbf{K_v}] \begin{bmatrix} \mathbf{x} \\ \mathbf{\Delta V} \end{bmatrix}
\tag{3.57}
$$

where $\mathbf{K}$ is the matrix of feedback gains and $\mathbf{K_x}$, $\mathbf{K_v}$ are appropriate connecting matrices. Substitution of (3.57) into (3.55) yields

$$
\begin{bmatrix} \mathbf{x} \\ \mathbf{0} \end{bmatrix} = \begin{bmatrix} \mathbf{A_d} & \mathbf{C} \\ -\mathbf{W} & \mathbf{Y}^m_{BUS} \end{bmatrix} \begin{bmatrix} \mathbf{x} \\ \mathbf{\Delta V} \end{bmatrix} + \begin{bmatrix} \mathbf{B_d} \\ \mathbf{0} \end{bmatrix} [\mathbf{K_x} \quad \mathbf{K_v}] \begin{bmatrix} \mathbf{x} \\ \mathbf{\Delta V} \end{bmatrix}
$$

$$
\begin{bmatrix} \mathbf{x} \\ \mathbf{0} \end{bmatrix} = \underbrace{\begin{bmatrix} \mathbf{A_d} & \mathbf{C} \\ -\mathbf{W} & \mathbf{Y}^m_{BUS} \end{bmatrix}}_{\mathbf{A}_{OL}} \begin{bmatrix} \mathbf{x} \\ \mathbf{\Delta V} \end{bmatrix} + \underbrace{\begin{bmatrix} \mathbf{B_d K_x} & \mathbf{B_d K_v} \\ \mathbf{0} & \mathbf{0} \end{bmatrix}}_{\mathbf{\Delta A}_{FS}} \begin{bmatrix} \mathbf{x} \\ \mathbf{\Delta V} \end{bmatrix}
\tag{3.58}
$$

Closed-loop solution is given as

$$
\begin{bmatrix} \mathbf{x} \\ \mathbf{0} \end{bmatrix} = \underbrace{\begin{bmatrix} \mathbf{A_d + B_d K_x} & \mathbf{C + B_d K_v} \\ -\mathbf{W} & \mathbf{Y}^m_{BUS} \end{bmatrix}}_{\mathbf{A}_{CL}} \begin{bmatrix} \mathbf{x} \\ \mathbf{\Delta V} \end{bmatrix}
\tag{3.59}
$$

Proposition 3.1: The variations in the open-loop system eigenvalues and eigenvectors depend on the nominal (undisturbed) values of $\mathbf{A}_{OL}$, and matrix $\Delta \mathbf{A}_{FS}$ as well as the eigenvalues and eigenvectors of the open-loop system.

Proof:

Linear systems (3.58) and (3. 59) can be rewritten as

$$\mathbf{M}\dot{\mathbf{x}} = \mathbf{A}_{OL}\mathbf{x} + \Delta \mathbf{A}_{FS}\mathbf{x} \qquad (3.60)$$

$$\mathbf{M}\dot{\mathbf{x}} = \mathbf{A}_{CL}\mathbf{x} \qquad (3.61)$$

where $\mathbf{M}$ is a constant diagonal matrix with entry "1" for differential equations and entry "0" for algebraic equations.

The nominal characteristic polynomial is represented as

$$f(\lambda_{OL},\mathbf{M},\mathbf{A}_{OL}) = \det(\lambda_{OL}\mathbf{M} - \mathbf{A}_{OL}) = 0 \qquad (3.62)$$

and λ_{OLi} a finite and distinct root of (3.62). The problem is to find the root variations $\Delta\lambda_i$, such that

$$\lambda_{CL_i} = \lambda_{OL_i} + \Delta\lambda_i$$

is a finite and distinct root of the characteristic polynomial of (3.61), expressed as

$$f(\lambda_{CL},\mathbf{M},\mathbf{A}_{CL}) = \det(\lambda_{CL}\mathbf{M} - \mathbf{A}_{CL}) = 0 \qquad (3.63)$$

Expanding (3.63) in Taylor series about the nominal values λ_{OL} and $\mathbf{A}_{OL}$ one obtains (sub-index "0" indicates nominal values)

$$f(\lambda_{CL},\mathbf{M},\mathbf{A}_{CL}) = f(\lambda_{CL},\mathbf{M},\mathbf{A}_{CL})\big|_0 + \sum_{k=1}^{\infty} \frac{1}{k!}\partial^k f(\lambda_{CL},\mathbf{M},\mathbf{A}_{CL})\big|_0 = 0 \qquad (3.64)$$

Since

$$f(\lambda_{CL},\mathbf{M},\mathbf{A}_{CL})\big|_0 = f(\lambda_{OL},\mathbf{M},\mathbf{A}_{CL}) = \det(\lambda_{OL}\mathbf{M} - \mathbf{A}_{CL}) = 0$$

and if the variations of $\Delta\mathbf{A}_{FS}$ are sufficiently small, then the terms under summation sign in (3.64) for k>1 may be neglected, relation (3.64) becomes

$$f(\lambda_{CL}, \mathbf{M}, \mathbf{A}_{CL}) = \partial f(\lambda_{CL}, \mathbf{M}, \mathbf{A}_{CL})\big|_0 = 0 \qquad (3.65)$$

From references [7,13], for any square matrix $\mathbf{D}$,

$$\partial(\det(\mathbf{D})) = adj(\mathbf{D}) \bullet \partial\mathbf{D} \qquad (3.66)$$

where $\bullet$ denotes the inner product of two equidimensional square matrices, i. e., $\mathbf{C} \bullet \mathbf{D} = trace(\mathbf{CD})$, [7]. Applying (3.66) to (3.65) yields

$$f(\lambda_{CL}, \mathbf{M}, \mathbf{A}_{CL}) = \partial f(\lambda_{CL}, \mathbf{M}, \mathbf{A}_{CL})\big|_0 = \partial \det(\lambda_{CL}, \mathbf{M}, \mathbf{A}_{CL})\big|_0 = 0$$

$$adj(\lambda_{CL}, \mathbf{M}, \mathbf{A}_{CL})\big|_0 \bullet \partial(\lambda_{CL}, \mathbf{M}, \mathbf{A}_{CL})\big|_0 = 0$$

$$adj(\lambda_{OL}\mathbf{M} - \mathbf{A}_{OL}) \bullet (\mathbf{M}\Delta\lambda - \Delta\mathbf{A}_{FS}) = 0 \qquad (3.67)$$

Solving for the particular characteristic root λ_{OL_i}, variations are given by

$$\Delta\lambda_i = \left(adj(\lambda_{OL_i}\mathbf{M} - \mathbf{A}_{OL}) \bullet (\mathbf{M})\right)^{-1} adj(\lambda_{OL_i}\mathbf{M} - \mathbf{A}_{OL}) \bullet \Delta\mathbf{A}_{FS} \qquad (3.68)$$

The paper at reference [7] was used to derive this expression.

Definition 3.1 [6]: Let $\mathbf{A}$, $\mathbf{M}$ be n x n matrices with real or complex components. The number λ (real or complex) is called an eigenvalue of $\mathbf{A}$, $\mathbf{M}$ if there is a nonzero vector $\mathbf{u}$ in $\mathbb{C}^n$ such that:

$$\mathbf{A}\mathbf{u}_i = \lambda_i\mathbf{M}\mathbf{u}_i \qquad (3.69)$$

The vector $\mathbf{u}_i \neq 0$ is called an eigenvector of $\mathbf{A}$, $\mathbf{M}$ corresponding to the eigenvalue λ_i.

Linearizing (3.69) around nominal values yields

$$\left(\mathbf{A}_{OL} - \mathbf{M}\lambda_{OL_i}\right)\Delta\mathbf{u}_i = (\Delta\lambda_i\mathbf{M}\mathbf{u}_{OL_i} - \Delta\mathbf{A}_{FS}\mathbf{u}_{OL_i}) \qquad (3.70)$$

For the left eigenvector a similar expression is found

$$\Delta \mathbf{v}_i^T \left(\mathbf{A}_{OL} - \mathbf{M} \lambda_{OL_i} \right) = (\mathbf{v}_{OLi}^T \mathbf{M} \Delta \lambda_i - \mathbf{v}_{OL_i}^T \Delta \mathbf{A}_{FS}) \tag{3.71}$$

Variations in eigenvalues and eigenvectors from the open loop model depend on the feedback signals of the proposed close loop representation.

End of proof.

3.6 Non-Homogeneous Response

In applying modal power flow to system analysis, it is desirable to relate the open loop formulation to the non-homogeneous case. In section 3.3.1 the homogenous response was used in order to calculate firstly the modal current injections associated to a mode of concern and secondly the modal voltage deviations. In this section the non-homogenous response is presented as a different approach in the modal power flow analysis.

In order to examine these relationships, consider a linear system

$$\dot{\mathbf{x}}(t) = \mathbf{A} \ \mathbf{x}(t) + \mathbf{B} \ \mathbf{u}(t) \tag{3.72}$$

where $\mathbf{A}$ is the $n_A \ x \ n_A$ state matrix and $\mathbf{x}$ is the perturbed n_A-vector, $\mathbf{B}$ is the $n_A \ x \ r$ input matrix and $\mathbf{u}$ is the perturbed input r-vector.

The non-homogenous solution in time for above system is given by

$$\mathbf{x}(t) = e^{\mathbf{A}t}\mathbf{x}(0) + \int_0^t e^{\mathbf{A}t}\mathbf{B} \ \mathbf{u}(\tau)d\tau \tag{3.73}$$

where the first term is the response to the initial conditions, and the second term is the response to the input vector $\mathbf{u}$.

Substitution of (3.22) into (3.73) yields

$$\mathbf{x}(t) = \sum_{i=1}^{n_A} \left[\mathbf{U}_i \left[\mathbf{V}^T \mathbf{x}(0) + \mathbf{V}^T \mathbf{B} \int_0^t e^{-\lambda_i \tau} \mathbf{u}(\tau)d\tau \right] e^{\lambda_i t} \right] \tag{3.74}$$

By eigenvalue analysis the eigenvalues λ_i (i=1, 2,..., n_A) and the right and left eigenvectors, $\mathbf{U}_i$ and $\mathbf{V}_i$ respectively, can be obtained.

By replacing equation (3.74) into (3.18) a new equation for modal voltage deviations with the effect of the input vector is obtained.

From (3.23) the response for the ith mode at time t=0 is given as

$$\mathbf{x}(\lambda_i) = (c_i)\mathbf{U}_i e^{\lambda_i 0} = (c_i)\mathbf{U}_i \tag{3.75}$$

and from expression (3.74) the solution is given by

$$\mathbf{x}(\lambda_i) = \mathbf{U}_i \left[\mathbf{V}_i^T \mathbf{x}(0) + \mathbf{V}_i^T \mathbf{B} \int_0^0 e^{-\lambda_i \tau} \mathbf{u}(\tau) d\tau \right] e^{\lambda_i 0}$$

$$\mathbf{x}(\lambda_i) = \mathbf{U}_i \left[\mathbf{V}^T \mathbf{x}(0) \right] = \mathbf{U}_i (c_i)$$

$$\mathbf{x}(\lambda_i) = (c_i)\mathbf{U}_i \tag{3.76}$$

At time t=0 the data obtained from a modal power flow analysis performed with homogenous and non-homogenous response is the same, expressions (3.75) and (3.76). The effect of the input vector in the modal power flow can be analyzed in a time range of interest.

These findings provide basic insight into the linear behavior of large-scale dynamic systems. The results may be useful for understanding and predicting the dynamic behavior of inter-area oscillations.

We briefly summarize the standard modal power flow algorithm.

3.7 Computation Procedure for Modal Power Oscillation Flow

Computation of modal power flow is straightforward.

Step 1: Modal power oscillation flow analysis starts by choosing a steady-state operating point by performing a load flow study of the power system.

Step 2: Form the state matrix and find the eigenvalues and eigenvectors.

Step 3: Select motion modes and energy modes of concern.

For each mode of concern follow the next steps:

Step 4: Calculate the modal voltage deviations using equation (3.24).

Due to the computer calculation time and effort needed to obtain the inverse of the modified admittance matrix, an algorithm is proposed in [9] for numerical calculation of the modal voltage deviations.

Step 5: Calculate the modal voltage magnitude and phase angle deviations.

Step 6: Calculate modal current deviations according to equation (3.27).

Step 7: With modal and current contributions determined as in eqs. (3.24) and (3.27), calculate modal power oscillation flow for:

- Each synchronous machine in the power system.
- Each control device within the system.
- Each load.
- Each Transmission line and transformer in the power system.
- And other elements connected to the system.

Step 8: Normalize modal power deviations and modal voltage deviations

Power oscillation flows and modal voltage solutions are obtained based on the eigenvector, whose entries are relative values. Therefore the solutions are relative values too, and need to be normalized. For each mode of concern there always exist some elements of the power system which are experiencing the largest magnitude of oscillation, servicing as the bottleneck of the power system flow.

1. The magnitudes and phase angles of the modal active and reactive power calculated for the dynamic devices in the power system are normalized against the machine with the largest contribution.

$$\left|\Delta P_{d_k}^N\right| = \frac{\left|\Delta P_{d_k}\right|}{\left|\Delta P_{d_{REF}}\right|}; \qquad \left|\Delta Q_{d_k}^N\right| = \frac{\left|\Delta Q_{d_k}\right|}{\left|\Delta Q_{d_{REF}}\right|}$$

53

$$\angle\phi_{Pd_k}^{N} = \angle\phi_{Pd_k} - \angle\phi_{Pd\,REF}\ ; \qquad\qquad \angle\phi_{Qd_k}^{N} = \angle\phi_{Qd_k} - \angle\phi_{Qd\,REF}$$

for $k=1, 2, 3, \ldots, nc$: number of dynamic devices

Here, subscript "REF" indicates the dynamic device with the largest contribution to the modal power oscillation flow and superscript "N" represents normalized values. The reference machine will have a modal power magnitude equal to 100.0% and modal power phase angle of 0°.

2. Participation of transmission lines and transformers in modal power flow

$$\left|\Delta P_{R_k}^{N}\right| = \frac{\left|\Delta P_{R_k}\right|}{\left|\Delta P_{d_{REF}}\right|}\ ; \qquad\qquad \left|\Delta Q_{R_k}^{N}\right| = \frac{\left|\Delta Q_{R_k}\right|}{\left|\Delta Q_{d_{REF}}\right|}$$

$$\angle\phi_{PR_k}^{N} = \angle\phi_{PR_k} - \angle\phi_{Pd\,REF}\ ; \qquad\qquad \angle\phi_{QR_k}^{N} = \angle\phi_{QR_k} - \angle\phi_{Qd\,REF}$$

for $k=1, 2, 3, \ldots, nr$: number of branches.

3. Participation of loads in modal power flow

$$\left|\Delta P_{L_k}^{N}\right| = \frac{\left|\Delta P_{L_k}\right|}{\left|\Delta P_{d_{REF}}\right|}\ ; \qquad\qquad \left|\Delta Q_{L_k}^{N}\right| = \frac{\left|\Delta Q_{L_k}\right|}{\left|\Delta Q_{d_{REF}}\right|}$$

$$\angle\phi_{PL_k}^{N} = \angle\phi_{PL_k} - \angle\phi_{Pd\,REF}\ ; \qquad\qquad \angle\phi_{QL_k}^{N} = \angle\phi_{QL_k} - \angle\phi_{Qd\,REF}$$

for $k=1, 2, 3, \ldots, nl$: number of loads.

4. Modal voltage solutions are also normalized. This will be done against the bus experiencing the largest argument of modal voltage deviations.

$$\left|\Delta V^{N}\right| = \frac{\left|\Delta V_k\right|}{\left|\Delta V_{REF}\right|}\ ; \qquad \angle\phi_{V_k}^{N} = \angle\phi_{V_k} - \angle\phi_{V\,REF}$$

for $k=1, 2, 3, \ldots, n$: number of buses in the electric power system.

Step 9: Select information of concern for future analysis.

A schematic depiction of the method is given in Fig. 3.6. As described in Chapter 4, the general form of the modal power flow problem is very amenable to analysis, especially using sparsity-based analysis techniques.
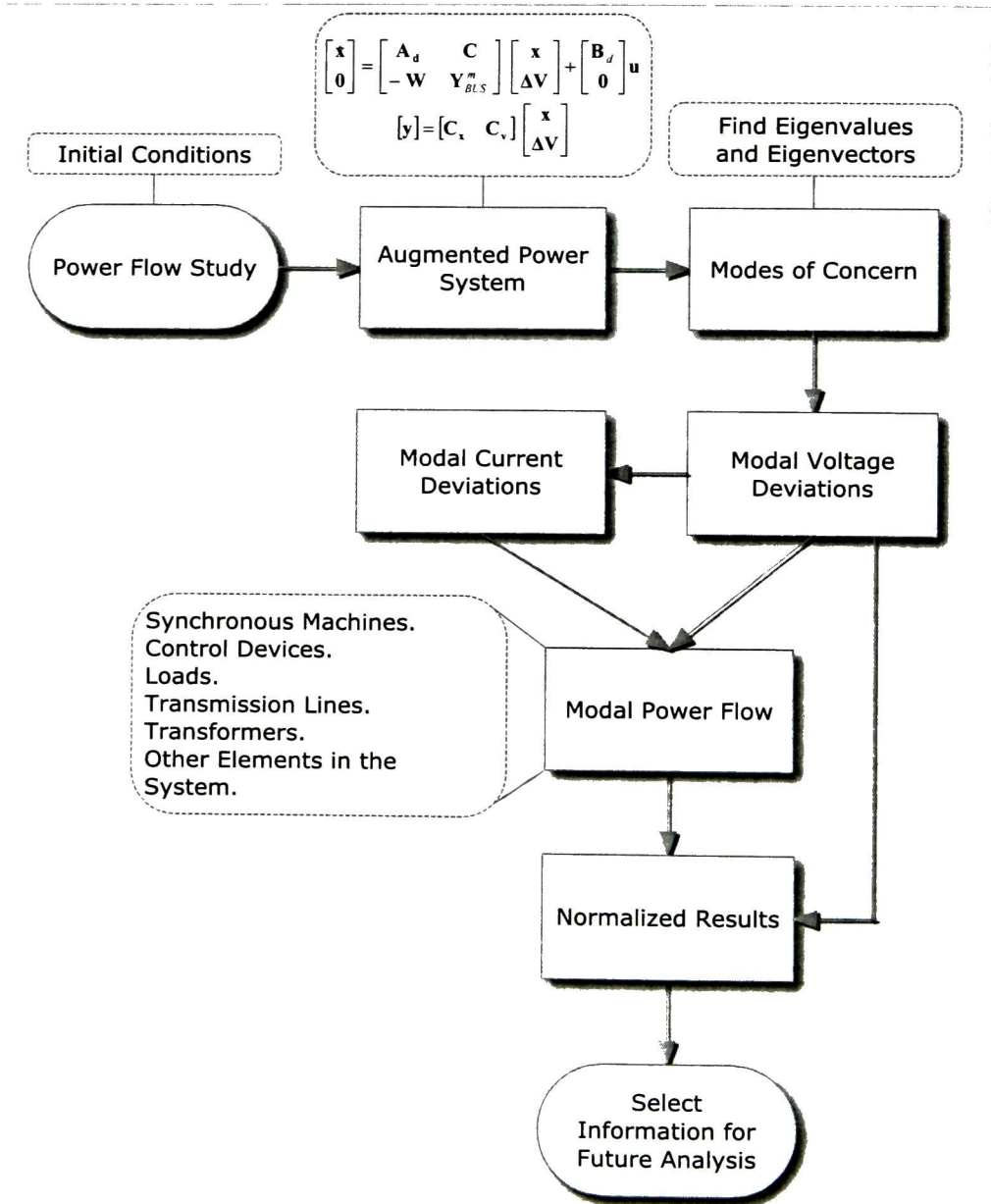

Figure 3.6: Modal power oscillation flow computation procedure.

3.8 References

[1] O. Wasynczuk, R. A. Decarlo, "The component connection model and structure preserving model order reduction", Automatica, vol. 17, no. 4, 619-626, 1981.

[2] P. Kundur, "Power System Stability and Control", McGraw-Hill, Inc. Ney York, 1994.

[3] P. W. Sauer and M. A. Pai, "Power System Dynamics and Stability", Prentice Hall, 1998.

[4] G. W. Stagg and A. H. El-Abiad, "Computer Methods in Power System Analysis", *McGraw-Hill, Inc. 1968*

[5] C. T. Chen. "Linear System Theory and Design" Third Edition. Oxford University Press, Inc. 1999.

[6] J. H. Wilkinson, "The Algebraic Eigenvalue Problem", Oxford University Press, Oxford, U.K., 1965.

[7] F. Ayres Jr. "Theory and Problems of Matrices". Ney York: McGraw-Hill. 1974

[8] E. Z. Zhou, "Power Oscillation Study of Electric Power Systems", Electrical Power and Energy Systems. Vol. 12. No. 2, pp 143-150, 1995.

[9] M. Ochoa, "Aplicación de Métodos de Potencia y Energía Modal al Análisis de Oscilaciones Interárea". Centro de Investigación y Estudios Avanzados del I.P.N. (CINVESTAV), Unidad Guadalajara. Guadalajara Jalisco. June 2001.

[10] A. R. Messina, S. Vazquez, A. L. Rios, and B. J. Betancourt., "Coordination of Secondary Voltage-VAR Controls to Enhance Overall System Stability".

[11] F. R. Segundo, and A. R. Messina, "Modeling and Simulation of Interline Power Flow Controllers: Application to Enhance System Damping" North American Power Symposium (NAPS), Oct 4-6, 2009, pp 1-6.

[12] A. R. Messina, H. Hernández, E. Barocio, M. Ochoa, and J. Arroyo, "Coordinated Application of FACTS Controllers to Damp Out Inter-area Oscillations". Electric Power Systems Research, Vol. 62, pp 55-53. 2002.

[13]   P. N. Paraskevopoulos, M. A. Christodoloulou, M. A. Tsakiris, "Eigenvalue-Eigenvector Sensitivity Analysis of Linear Time.Invariant Singular Systems" IEEE Transactions on Automatic Control, VOL. AC-29 No. 4. April 1984.

Chapter 4
Advanced Power Oscillation Flow Methodologies

In chapter 3 the method of modal power oscillation flow was presented and discussed. Standard modal power flow algorithms rest upon reduced-order representations in which the algebraic equations representing the network behavior are included in the set of differential equations.

In this chapter, a new approach based on modal analysis is proposed for modeling of power systems described by differential-algebraic equations. This approach leads to new insights into the DAE modeling problem.

Criteria for the proposed representation are derived and implementation issues are then discussed. The proposed techniques offer a compact description of the system dynamics, and are especially useful for the study of electromechanical oscillations since they preserve the essential features of system behavior in terms of actual observational data.

Extensions to the basic algorithm to compute modal power flow from measured data are finally proposed based on least-squares optimization. Relations between the standard approach and the proposed methodology are provided.

4.1 Problem Statement

The difficulties associated with analyzing large linear power system models have long been recognized [12]-[14]. In addition to sparsity, large DAE models may result in a vast amount of information that needs to be monitored and analyzed.

Consider a power system linear model described by a DAE system (3.16) and (3.17). Assuming that matrix $\mathbf{Y}_{BUS}^m$ is non-singular, elimination of the algebraic variables from equation (3.16) yields the following reduced system

$$\mathbf{x} = \mathbf{A}\mathbf{x} + \mathbf{B}_d\mathbf{u} \tag{4.1}$$

where

$$\mathbf{A} = \left(\mathbf{A}_d + \mathbf{C}(\mathbf{Y}_{BUS}^m)^{-1}\mathbf{W} \right)$$

This approach is not satisfactory in most cases, because the information it provides is restricted to the physical states. As a result, the network structure is destroyed thus preventing the analysis of the impact of transmission elements on system behavior.

Alternative approaches to extract modal information are of interest to this research. In order to explain the proposed procedure we introduce important definitions and theorems.

Definition 4.1 [2]: Let $\mathbf{A}$ be an $n \times n$ matrix with real or complex components. The number λ (real or complex) is called an eigenvalue of $\mathbf{A}$ if there is a nonzero vector $\mathbf{u}$ in $\mathbb{C}^n$ such that:

$$\mathbf{A}\,\mathbf{u} = \lambda\,\mathbf{u} \tag{4.2}$$

The vector $\mathbf{u} \neq 0$ is called an eigenvector of $\mathbf{A}$ corresponding to the eigenvalue λ.

The small-signal stability of the power system can be analyzed by calculating the eigenvalues λ of $\mathbf{A}$, i.e. solving equation (4.2). More precisely, we have the following theorem.

Theorem 4.1 [6]: The eigenvalue problem of equation (4.2) is equivalent to:

$$\begin{bmatrix} (\mathbf{A_d} - \lambda\mathbf{I_n}) & \mathbf{C} \\ -\mathbf{W} & \mathbf{Y}_{BUS}^m \end{bmatrix} \begin{bmatrix} \mathbf{u} \\ \mathbf{v} \end{bmatrix} = \begin{bmatrix} \mathbf{0} \\ \mathbf{0} \end{bmatrix} \tag{4.3}$$

That is, $\mathbf{u}$ is a solution of (4.3) if and only if $\mathbf{u}$ is a solution of (4.2).

Proof . *See reference [6].*

Theorem 4.1 is important because it provides explicit criteria that can be used to compute modal properties of large power system models.

4.2 DAE Power System Model

Power system models are naturally very sparse. As discussed in Chapter 3, a linear DAE power system model can be expressed in the general form

$$\begin{bmatrix} \mathbf{x} \\ \mathbf{0} \end{bmatrix} = \begin{bmatrix} \mathbf{A_d} & \mathbf{C} \\ -\mathbf{W} & \mathbf{Y}_{BUS}^m \end{bmatrix} \begin{bmatrix} \mathbf{x} \\ \Delta\mathbf{V} \end{bmatrix} + \begin{bmatrix} \mathbf{B_d} \\ \mathbf{0} \end{bmatrix} \mathbf{u} \tag{4.4}$$

$$[\mathbf{y}] = [\mathbf{C_x} \quad \mathbf{C_v}] \begin{bmatrix} \mathbf{x} \\ \Delta\mathbf{V} \end{bmatrix} \tag{4.5}$$

where $\mathbf{y}$ is the vector of output variables and $\mathbf{C}_x$ and $\mathbf{C}_v$ are appropriate connection matrices.

The study of DAE models presents significant problems in simulation and analysis. In what follows, important properties of these models are investigated.

4.2.1 Reduced Order Models

It is apparent that if the admittance matrix $\mathbf{Y}_{BUS}^m$ is non-singular, the system model can be rewritten in the form

$$\mathbf{x} = \mathbf{A}_{ODE}\ \mathbf{x} + \mathbf{B}_{ODE}\ \mathbf{u} \qquad (4.6)$$

$$\mathbf{y} = \mathbf{C}_{ODE}\ \mathbf{x} \qquad (4.7)$$

where

$$\mathbf{A}_{ODE} = (\mathbf{A}_d + \mathbf{C}(\mathbf{Y}_{BUS}^m)^{-1}\mathbf{W})$$

$$\mathbf{B}_{ODE} = \mathbf{B}_d$$

$$\mathbf{C}_{ODE} = (\mathbf{C}_x + \mathbf{C}_v(\mathbf{Y}_{BUS}^m)^{-1}\mathbf{W})$$

and

$$(\mathbf{Y}_{BUS}^m)^{-1} = \mathbf{Z}_{BUS}^m = \begin{bmatrix} \mathbf{Z}_{dd} - \mathbf{Z}_d & \mathbf{Z}_{dL} \\ \mathbf{Z}_{Ld} & \mathbf{Z}_{LL} - \mathbf{Z}_L \end{bmatrix} \qquad (4.8)$$

From the above expression we see that the new state matrix $\mathbf{A}_{ODE}$ is composed of two submatrices; the first submatrix, $\mathbf{A}_d$, is the individual state matrix associated with each of the dynamic devices. The second submatrix represents the interaction between the dynamic devices through the transmission network.

Figure 4.1 shows a standard block diagram representation of the reduced-order model of the system.
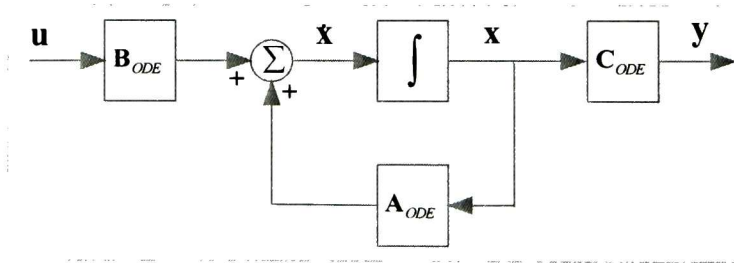

Figure 4.1: Block diagram of the ODE model of the power system.

From *definition 4.1* it follows that the eigenvalue λ_i and the right eigenvector $\mathbf{U}_i$ of $\mathbf{A}_{ODE}$ can be calculated as

$$\mathbf{A}_{ODE}\ \mathbf{U}_i = \lambda_i \mathbf{U}_i \qquad (4.9)$$

Further, the eigenvalue λ_i and left eigenvector $\mathbf{V}_i$ can be found from the definition

$$\mathbf{V}_i \, \mathbf{A}_{ODE} = \lambda_i \mathbf{V}_i \tag{4.10}$$

A disadvantage of this formulation is that the sparsity of the system matrix is destroyed. Techniques for computing the eigenvalues/vectors for large power systems are discussed next in the context of sensitivity analyzes in power systems in [7].

4.2.2 Differential-Algebraic Equation (DAE) Model

The augmented system of equations (4.4) and (4.5) preserves system structure and therefore the sparsity of the model. In this section, we introduce simple analytical relations between the modal properties of reduced-order models and DAE models.
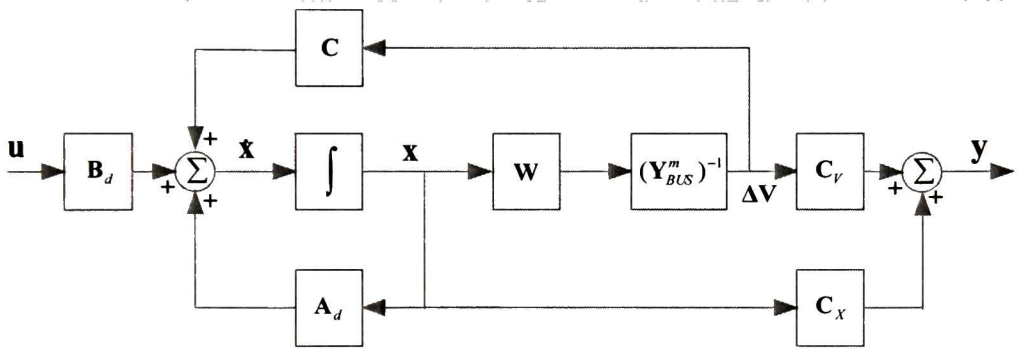
Figure 4.2: Block diagram of the DAE model of the power system.

In the light of these observations, an important property of a linear model can be defined.

Definition 4.2 [5]: Let $\mathbf{A}$, $\mathbf{M}$ be $n \times n$ matrices with real or complex components. The number λ (real or complex) is called an eigenvalue of $\mathbf{A}$, $\mathbf{M}$ if there is a nonzero vector $\mathbf{u}$ in $\mathbb{C}^n$ such that:

$$\mathbf{Au} = \lambda \, \mathbf{Mu} \tag{4.11}$$

The vector $\mathbf{u} \neq 0$ is called an eigenvector of $\mathbf{A}$, $\mathbf{M}$ corresponding to the eigenvalue λ.

Clearly, if $\mathbf{M}$ is invertible, then (4.11) can be solved as (4.2).

Using *definition 4.2* the eigenvalue λ_i and the right eigenvector $\mathbf{U}_{DAE_i}$ of $\mathbf{A}_{DAE}$ can be computed as

$$\mathbf{A}_{DAE}\mathbf{U}_{DAE_i} = \lambda_i \mathbf{M}\ \mathbf{U}_{DAE_i} \tag{4.12}$$

where

$$\mathbf{M} = \begin{bmatrix} \mathbf{I}_n & \mathbf{0} \\ \mathbf{0} & \mathbf{0} \end{bmatrix}$$

Partitioning the right eigenvectors, $\mathbf{U}_{DAE_i}$, in (4.12) as $\mathbf{U}_{DAE_i} = \left[\mathbf{U}_{DAE_{xi}}, \mathbf{U}_{DAE_{vi}}\right]^{\mathsf{T}}$ the eigenvalue problem in (4.12) can be rewritten as

$$\begin{bmatrix} \mathbf{A_d} & \mathbf{C} \\ -\mathbf{W} & \mathbf{Y}_{BUS}^m \end{bmatrix} \begin{bmatrix} \mathbf{U}_{DAE_{xi}} \\ \mathbf{U}_{DAE_{vi}} \end{bmatrix} = \lambda_i \begin{bmatrix} \mathbf{I}_n & \mathbf{0} \\ \mathbf{0} & \mathbf{0} \end{bmatrix} \begin{bmatrix} \mathbf{U}_{DAE_{xi}} \\ \mathbf{U}_{DAE_{vi}} \end{bmatrix}$$

or, in a more convenient form,

$$\begin{bmatrix} (\mathbf{A}_d - \lambda_i\mathbf{I_n}) & \mathbf{C} \\ -\mathbf{W} & \mathbf{Y}_{bus}^m \end{bmatrix} \begin{bmatrix} \mathbf{U}_{DAE_{xi}} \\ \mathbf{U}_{DAE_{vi}} \end{bmatrix} = \begin{bmatrix} \mathbf{0} \\ \mathbf{0} \end{bmatrix} \tag{4.13}$$

By *theorem 4.1*, expression (4.13) and (4.9) are equivalent. Therefore, $\mathbf{U}_{DAE_{xi}}$ and $\mathbf{U}_i$ are solutions for both eigenproblems.

Proof: Solving (4.13) for $\mathbf{U}_{DAE_{xi}}$ yields

$$\underbrace{(\mathbf{A_d} + \mathbf{C}(\mathbf{Y}_{BUS}^m)^{-1}\mathbf{W})}_{\mathbf{A}_{ODE}}\mathbf{U}_{DAE_{xi}} = \lambda_i \mathbf{U}_{DAE_{xi}} \tag{4.14}$$

where the term within parenthesis is the reduced system matrix, $\mathbf{A}_{ODE}$.

Clearly, the DAE model shares the eigenvalues and the correspondent right eigenvectors related to the dynamic states of the ODE model. Hence, the algebraic part of the DAE eigenvector can be expressed in terms of the dynamic part as

$$\mathbf{U}_{DAE_{xi}} = (\mathbf{Y}_{BUS}^m)^{-1} \mathbf{W} \mathbf{U}_{DAE_{di}} \tag{4.15}$$

Similarly, one has for the left eigenvectors

$$\mathbf{V}_{DAE_i} \mathbf{A}_{DAE} = \lambda_i \mathbf{V}_{DAE_i} \mathbf{M} \tag{4.16}$$

or, in terms of the dynamic and static subvectors,

$$\begin{bmatrix} \mathbf{V}_{DAE_{di}} & \mathbf{V}_{DAE_{xi}} \end{bmatrix} \begin{bmatrix} \mathbf{A_d} & \mathbf{C} \\ -\mathbf{W} & \mathbf{Y}_{BUS}^m \end{bmatrix} = \lambda_i \begin{bmatrix} \mathbf{V}_{DAE_{di}} & \mathbf{V}_{DAE_{xi}} \end{bmatrix} \begin{bmatrix} \mathbf{I}_n & \mathbf{0} \\ \mathbf{0} & \mathbf{0} \end{bmatrix}$$

$$\begin{bmatrix} \mathbf{V}_{DAE_{di}} & \mathbf{V}_{DAE_{xi}} \end{bmatrix} \begin{bmatrix} (\mathbf{A_d} - \lambda_i \mathbf{I_n}) & \mathbf{C} \\ -\mathbf{W} & \mathbf{Y}_{bus}^m \end{bmatrix} = \begin{bmatrix} \mathbf{0} & \mathbf{0} \end{bmatrix} \tag{4.17}$$

By **theorem 4.1** expressions (4.17) and (4.10) are equivalent; $\mathbf{V}_{DAE_{xi}}$ and $\mathbf{V}_i$ are solutions for both eigenproblems.

Proof: Solving (4.17) for $\mathbf{V}_{DAE_{xi}}$ gives

$$\mathbf{V}_{DAE_{di}} \underbrace{(\mathbf{A}_d + \mathbf{C}(\mathbf{Y}_{BUS}^m)^{-1} \mathbf{W})}_{\mathbf{A}_{ODE}} = \lambda_i \mathbf{V}_{DAE_{di}} \tag{4.18}$$

It is straightforward to verify that the DAE model shares the eigenvalues and dynamic part of the left eigenvectors of the reduced-order model. Consequently, $\mathbf{V}_{DAE_{vi}}$ can be calculated as

$$\mathbf{V}_{DAE_{xi}} = \mathbf{C}(\mathbf{Y}_{BUS}^m)^{-1} \mathbf{V}_{DAE_{di}} \tag{4.19}$$

This discussion demonstrates that the reduced-order model (4.6) can be analyzed as a DAE system, thus preserving the structure of the modified admittance matrix as well as the sparsity of the system. More importantly, the augmented representation preserves valuable information regarding the interaction between the algebraic and dynamic components of the right eigenvector.

4.3 Computation of Modal Voltage Deviations from Right Eigenvector

Given a particular mode of oscillation λ_i the modal voltage deviations in (3.18) can be expressed in terms of the time evolution of the state vector as

$$\mathbf{\Delta V}(\lambda_i) = (\mathbf{Y^m_{BUS}})^{-1} \mathbf{W} \ \mathbf{x}(\lambda_i) \tag{4.20}$$

in which, for the homogeneous case,

$$\mathbf{x}(\lambda_i) = (\mathbf{V_i^T}\mathbf{x}(0))\mathbf{U}_i e^{\lambda_i t} = (c_i)\mathbf{U}_i e^{\lambda_i t} \tag{4.21}$$

where $\mathbf{U}_i$ and $\mathbf{V}_i$ are the right and left eigenvectors of the eigenvalue λ_i and $\mathbf{x}(0)$ is a vector of the initial conditions of the variable states of the system.

The solution of (4.21) at time t=0 is then given by

$$\mathbf{x}(\lambda_i) = (c_i)\mathbf{U}_i \tag{4.22}$$

Substituting (4.22) into (4.20), the modal voltage deviations at t=0 yields

$$\mathbf{\Delta V}(\lambda_i) = (\mathbf{Y^m_{BUS}})^{-1}\mathbf{W}(c_i)\mathbf{U}, \tag{4.23}$$

Comparing equations (4.15) and (4.23), it can be observed that the expressions for modal voltage deviations are a particular case of the solution based on the right eigenvector; the latter model is weighted only by the scalar c_i in (4.23).

Theorem 4.2 [3]: If $\mathbf{u}$ is an eigenvector of the matrix $\mathbf{A}$ with eigenvalue λ then any scalar multiple $\alpha \neq 0$ is also an eigenvector of $\mathbf{A}$ with the same eigenvalue

Proof:

$$\mathbf{A}(\alpha\mathbf{u}) = \alpha\mathbf{A}\mathbf{u} = \alpha\lambda\mathbf{u} = \lambda(\alpha\mathbf{u}) \tag{4.24}$$

By *theorem 4.2* it can be concluded that the subvector of the right eigenvector $U_{DAE_{vi}}$ is proportional to the modal bus voltage deviations, i.e.

1. $U_{DAE_{vi}} = \Delta V(\lambda_i)$ if $c_i = 1$.

2. $U_{DAE_{vi}} = \left(\dfrac{1}{c_i}\right) \Delta V(\lambda_i)$ if $c_i \neq 1$ and $c_i \neq 0$.

Based on the above results, it is clear that both quantities lead to identical results since the factor c_i affects all entries of the right eigenvector. DAE models, however, allow the full potential of modal power flow algorithms to be reached. Further, the modal bus voltage deviations are calculated from the algebraic component of the right eigenvector. The inverse of the modified admittance matrix is not calculated.

Table 4.1 illustrates the nature of the modal voltage deviations for specific modes of interest.

Table 4.1:
Evaluation of modal voltage deviations.

Modes	Description	Modal Voltage Deviations from Right Eigenvector
λ_i	Motion Mode	$\Delta V(\lambda_i) = U_{DAE_{vi}}$
$\lambda_i + \lambda_i^*$	Energy Mode	$\Delta V(\lambda_i, \lambda_i^*) = U_{DAE_{vi}} + U_{DAE_{vi}}^*$
$\lambda_i + \lambda_j$	Energy Mode	$\Delta V(\lambda_i, \lambda_j) = U_{DAE_{vi}} + U_{DAE_{vj}}$
$(\lambda_i + \lambda_i^*)$ $+ (\lambda_j + \lambda_j^*)$	Energy Mode	$\Delta V(\lambda_i, \lambda_i^*, \lambda_j, \lambda_j^*) = U_{DAE_{vi}} + U_{DAE_{vi}} + U_{DAE_{vj}} + U_{DAE_{vj}}^*$

Given the linearity of the model, we can write

$$\Delta V = \sum_{i=1}^{n} (c_i) U_{DAE_{vi}} \tag{4.25}$$

where n is the number of eigenvalues of the system, and

$$c_i = \begin{bmatrix} \mathbf{V}_{i_1} & \mathbf{V}_{i_2} & \cdots & \mathbf{V}_{i_n} \end{bmatrix} \begin{bmatrix} x_1(0) \\ x_2(0) \\ \\ x_n(0) \end{bmatrix}$$

Extensions to this approach are discussed later in this document.

In the proposed approach, the modal bus voltage deviations, magnitude and phase angle, can be expressed in terms of the right eigenvectors as

$$\Delta |\mathbf{V}|(\lambda_i) = |\Delta|\mathbf{V}|\angle \boldsymbol{\varphi}_{\Delta|V|} = \mathbf{M}_{|V|} \sum_{i=1}^{nmc} \mathbf{U}_{DAE_{vi}} \qquad (4.26)$$

$$\Delta \boldsymbol{\theta}_V(\lambda_i) = |\Delta \boldsymbol{\theta}_V|\angle \boldsymbol{\varphi}_{\Delta\theta_V} = \mathbf{M}_{\theta_V} \sum_{i=1}^{nmc} \mathbf{U}_{DAE_{vi}} \qquad (4.27)$$

where $\mathbf{M}_{|V|}$ and $\mathbf{M}_{\theta_V}$ depend on the initial values of the terminal voltages as indicated in previous chapter.

4.4 Computation of Modal Power Flow from Right Eigenvector

In order to exploit the advantages of calculating the eigenvalues/vectors directly from the augmented system, a modified power flow algorithm is proposed.

4.4.1 Modal Current Injections

In an extension to the above model, modal current injections are computed using modal information. Straightforward analysis results in

$$\mathbf{I}_{mod}(\lambda_i) = \mathbf{Y}_{BUS}^m \sum_{i=1}^{nmc} \mathbf{U}_{DAE_{vi}} \qquad (4.28)$$

where $\mathbf{Y}_{BUS}^m$ is the modified admittance matrix and $\mathbf{U}_{DAE_{vi}}$ is the dynamic voltage component of the right eigenvector.

The modal current deviations experienced by all dynamic devices within the power system can be calculated from (3.27) as

$$\Delta \mathbf{I}_d(\lambda_i) = \mathbf{I}_{\text{mod}_d}(\lambda_i) + \mathbf{Y_d} \mathbf{U}_{DAE_{vdi}} \tag{4.29}$$

where $\mathbf{I}_{\text{mod}_d}$ is the modal current injection of dynamic devices and $\mathbf{U}_{DAE_{vdi}}$ is the subvector of the right eigenvector section related with the voltage deviations in buses where dynamic devices are connected.

With these equations, the system model needed for power flow analysis is complete. Once the modal voltages and currents are calculated, the modal power flow can be computed as discussed below.

4.4.2 Contribution of Dynamic Devices

From expressions (3.42) and (3.343) the contribution of dynamic devices to the modal power flow for the *i*th mode of interest become

$$\Delta \mathbf{P}_d(\lambda_i) = |\Delta \mathbf{P}_d| \angle \varphi_{Pd} = (\mathbf{I}_{gd}^0 + \mathbf{V}_{gd}^0 \mathbf{Y_d}) \mathbf{U}_{DAE_{vdi}} + \mathbf{V}_{gd}^0 \mathbf{I}_{\text{mod}_d}(\lambda_i) \tag{4.30}$$

$$\Delta \mathbf{Q}_d(\lambda_i) = |\Delta \mathbf{Q}_d| \angle \varphi_{Qd} = (\mathbf{I}_{gq}^0 + \mathbf{V}_{gq}^0 \mathbf{Y_d}) \mathbf{U}_{DAE_{vdi}} + \mathbf{V}_{gq}^0 \mathbf{I}_{\text{mod}_d}(\lambda_i) \tag{4.31}$$

where $\mathbf{I}_{gd}^0$, $\mathbf{I}_{gq}^0$, $\mathbf{V}_{gd}^0$ and $\mathbf{V}_{gq}^0$ are the initial values for currents and voltages in the system reference frame.

Similar expressions can be derived for other control devices such as FACTS controllers. This is not discussed here.

4.4.3 Contribution of Loads

Assuming we know the modal voltages and currents, we get

$$\Delta \mathbf{P}_L(\lambda_i) = |\Delta \mathbf{P}_L| \angle \varphi_{PL} = \mathbf{P}_{LV} \mathbf{U}_{DAE_{vLi}} \tag{4.32}$$

$$\Delta \mathbf{Q}_L(\lambda_i) = |\Delta \mathbf{Q}_L| \angle \varphi_{QL} = \mathbf{Q}_{LV} \mathbf{U}_{DAE_{vLi}} \tag{4.33}$$

where $\mathbf{P}_{LV}$ and $\mathbf{Q}_{LV}$ are *2nl x 2nl* block diagonal matrices depending on the initial conditions, voltage and current, besides the voltage depending load characteristic. $\mathbf{U}_{DAE_{vLi}}$ is related with the voltage deviations in buses where loads are connected.

4.4.4 Contribution of the Transmission Network

Given the models of transmission lines and transformers in Chapter 3, the modal contributions can be expressed as

$$\Delta\mathbf{P_R}(\lambda_i) = |\Delta\mathbf{P_R}| \angle \varphi_{PR} = \mathbf{PU}_{DAE_{vi}} \tag{4.34}$$

$$\Delta\mathbf{Q_R}(\lambda_i) = |\Delta\mathbf{Q_R}| \angle \varphi_{QR} = \mathbf{QU}_{DAE_{vi}} \tag{4.35}$$

where $\mathbf{P}$ and $\mathbf{Q}$ are *Lx2B* matrices numerically depending on the parameters of the transmission lines and transformers as well as on the initial voltage for buses *"m"* and *"n"*

4.5 Modified Power Oscillation Flow Algorithm

Computation of modal power flow using the proposed approach is as follows:

Step 1: Given an initial operating point, construct the DAE model in (4.12).

Step 2: Compute right and left eigenvectors using sparsity-based techniques.

Step 3: Select modes or combination of modes for analysis.

For each mode or modes of concern follow the next steps.

Step 4: Extract from the right eigenvector the subvector associated with the algebraic states (voltage deviations).

Step 5: Calculate the modal voltage magnitude and phase angle deviations.

Step 6: Calculate modal current deviations from expression (4.29).

Step 7: Calculate the active and reactive contributions for

- Each synchronous machine in the power system.
- Each control device within the system.
- Each load
- Each Transmission line and transformer in the power system
- And other elements connected to the system.

Step 8: Normalize modal power deviations and modal voltage deviations as discussed in Chapter 3.

Step 9: Select information of concern for future analysis.

Now attention is turned to the problem of estimating modal power flow from measured data.

4.6 Modal Power Flow from Measured Data

The recent advent of phasor measurement units has opened the way to compute modal power flow from measured data. The viability of the proposed method depends to a great extent of efficient modal estimation methods

4.6.1 Modal Voltage Deviations

Assume, without loss of generality, that measurements are taken at all load buses. Shown in Fig. 4.3 is a conceptual representation of the proposed method.
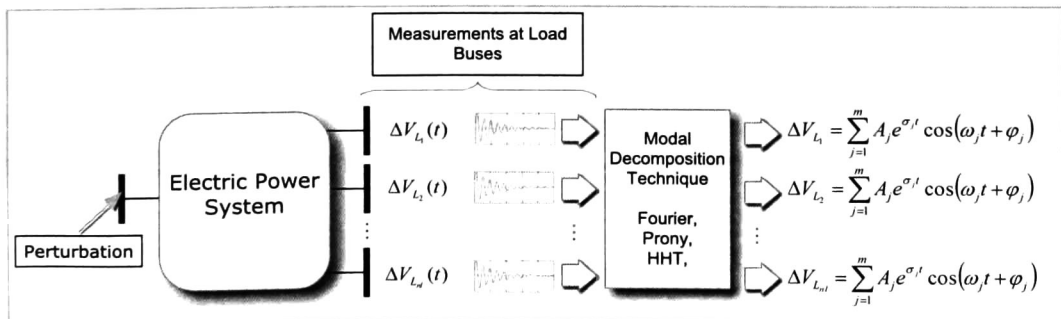

Figure 4.3: Conceptual representation of modal decomposition of PMUs.

As a first step towards the implementation of the method, let a vector of measured voltages be defined as

$$\Delta \mathbf{V_L} = \begin{bmatrix} \Delta V_{L1_D} \\ \Delta V_{L1_Q} \\ \vdots \\ \Delta V_{Lnl_D} \\ \Delta V_{Lnl_Q} \end{bmatrix} \tag{4.36}$$

and it is assumed that each element in (4.36) is decomposed into a sum of modal components:

$$\Delta V_{L_{D\,j}} = \mathrm{Re}\left[\sum_{j=1}^{m} A_j e^{\sigma_j t} \cos\left(\omega_j t + \varphi_j\right) \right]$$

and

$$\Delta V_{L_{Q\,j}} = \mathrm{Im}\left[\sum_{j=1}^{m} A_j e^{\sigma_j t} \cos\left(\omega_j t + \varphi_j\right) \right]$$

by an appropriate modal decomposition technique.

The power system represented by the augmented state model (4.4) can be written as

$$\begin{bmatrix} \dot{\mathbf{x}} \\ \mathbf{0} \\ \mathbf{0} \end{bmatrix} = \begin{bmatrix} \mathbf{A}_d & \mathbf{C}_d & \mathbf{0} \\ -\mathbf{W}_d & (\mathbf{Y}_{dd} - \mathbf{Y}_d) & \mathbf{Y}_{dL} \\ \mathbf{0} & \mathbf{Y}_{Ld} & (\mathbf{Y}_{LL} - \mathbf{Y}_L) \end{bmatrix} \begin{bmatrix} \mathbf{x} \\ \Delta \mathbf{V}_d \\ \Delta \mathbf{V}_L \end{bmatrix} + \begin{bmatrix} \mathbf{B}_d \\ \mathbf{0} \\ \mathbf{0} \end{bmatrix} \mathbf{u} \tag{4.37}$$

It then follows that the bus voltage deviations can be expressed in terms of the load bus voltage deviations as

$$\mathbf{Y}_{Ld} \Delta \mathbf{V}_d = -(\mathbf{Y}_{LL} - \mathbf{Y}_L)\, \Delta \mathbf{V}_L \tag{4.38}$$

where $\mathbf{Y}_{Ld}$ is an $nl \times nc$ matrix, nc is the number of dynamic devices and nl is the number of load buses.

Normally, $\mathbf{Y}_{Ld}$ is a rectangular matrix, unless the number of load buses is equal to the number of terminals with dynamic devices. $(\mathbf{Y}_{LL}\text{-}\mathbf{Y}_L)$ is a $nl \times nl$ matrix, $\Delta \mathbf{V}_d$ is a $nc \times 1$ vector and $\Delta \mathbf{V}_L$ is an $nc \times 1$ vector.

The linear system can be represented by:

$$\mathbf{Ax = b}$$

where $\mathbf{A} = \mathbf{Y}_{Ld} \in \mathfrak{R}^{nl \times nc}$, and

$$\mathbf{b} = -(\mathbf{Y}_{LL} - \mathbf{Y}_L) \, \Delta \mathbf{V}_L \in \mathfrak{R}^{nl \times 1}$$
$$\mathbf{x} = \Delta \mathbf{V}_d \in \mathfrak{R}^{nc \times 1}$$

Lemma 4.1 [4]: Suppose that the rank of $\mathbf{A} \in \mathbf{R}^{nl \times nc}$ is $r < nc$. Then a general solution to the least-square problem can be written as

$$\min_{\mathbf{x} = \in \mathfrak{R}^{nc \times 1}} \|\mathbf{Ax} - \mathbf{b}\|$$

with $\mathbf{A} \in \mathfrak{R}^{nl \times nc}$, and $\mathbf{b} = \in \mathfrak{R}^{nl \times 1}$

is given by

$$\mathbf{x} = \mathbf{A}^+ \mathbf{b} + (\mathbf{I}_n - \mathbf{A}^+ \mathbf{A})\mathbf{z}; \; \forall \; \mathbf{z} \in \mathfrak{R}^{nc \times 1}$$

The important point to note here is that $\mathbf{x} = \mathbf{A}^+\mathbf{b}$ is the unique minimum norm solution, where $\mathbf{A}^+$ is the Moore-Penrose generalized inverse or pseudoinverse [11].

By this lemma the solution for the modal voltage deviations of dynamic devices can be solved by a least-square method.

4.6.2 Modal Current Injections

From system (4.37) the modal current injections in terms of the voltage variations

$$\mathbf{I}_{\mathrm{mod}} = \begin{bmatrix} \mathbf{w}_d \\ \mathbf{0} \end{bmatrix} \mathbf{x} = \begin{bmatrix} (\mathbf{Y}_{dd} - \mathbf{Y}_d) & \mathbf{Y}_{dL} \\ \mathbf{Y}_{Ld} & (\mathbf{Y}_{LL} - \mathbf{Y}_L) \end{bmatrix} \begin{bmatrix} \Delta \mathbf{V}_d \\ \Delta \mathbf{V}_L \end{bmatrix} \qquad (4.39)$$

4.6.3 Modal Current Deviations

Modal current deviations from each dynamic device terminal can be expressed as:

$$\Delta \mathbf{I}_d = \begin{bmatrix} \mathbf{w}_d \\ \mathbf{0} \end{bmatrix} \mathbf{x} + \begin{bmatrix} \mathbf{Y}_d & \mathbf{0} \end{bmatrix} \begin{bmatrix} \Delta \mathbf{V}_{d_k} \\ \Delta \mathbf{V}_{L_k} \end{bmatrix} = \mathbf{I}_{\mathrm{mod}_d} + \mathbf{Y}_d \Delta \mathbf{V}_d \qquad (4.40)$$

$\mathbf{I}_{\mathrm{mod}_d}$ is the section of the modal current injections related to the dynamic devices; the rest of this vector is full of zeros and is related to the loads.

It follows that

$$\mathbf{I}_{\mathrm{mod}_d} = \mathbf{w}_d \mathbf{x}$$

and

$$\Delta \mathbf{I}_L = \mathbf{Y}_L \Delta \mathbf{V}_L \qquad (4.41)$$

where

$$\mathbf{Y}_L = \begin{pmatrix} \begin{bmatrix} \mathbf{G}_{DD_1} & \mathbf{B}_{DQ_1} \\ -\mathbf{B}_{QD_1} & \mathbf{G}_{QQ_1} \end{bmatrix} & \cdots & \mathbf{0} \\ \vdots & & \vdots \\ \mathbf{0} & \cdots & \begin{bmatrix} \mathbf{G}_{DD_{nl}} & \mathbf{B}_{DQ_{nl}} \\ -\mathbf{B}_{QD_{nl}} & \mathbf{G}_{QQ_{nl}} \end{bmatrix} \end{pmatrix}$$

in which $\mathbf{G}_{DD}$, $\mathbf{B}_{DQ}$, $\mathbf{B}_{QD}$ and $\mathbf{G}_{QQ}$ are dependent on the load characteristics and initial conditions.

From the linearized node equations, the current deviations in terminals where dynamic devices are connected can be calculated as, (3.11):

$$\begin{bmatrix} \Delta \mathbf{I}_d \\ \Delta \mathbf{I}_L \end{bmatrix} = \begin{bmatrix} \mathbf{Y}_{dd} & \mathbf{Y}_{dL} \\ \mathbf{Y}_{Ld} & \mathbf{Y}_{LL} \end{bmatrix} \begin{bmatrix} \Delta \mathbf{V}_d \\ \Delta \mathbf{V}_L \end{bmatrix} \qquad (4.42)$$

As mentioned in the previous chapter, each entry of the symmetrical admittance matrix consists of elementary *2x2* submatrices.

Once the modal and current deviations are obtained, the contribution of each system element to the oscillation flow can be computed.

4.6.4 Modal Power Flow

We present below a description of how to compute the power oscillation flow; for more details the reader is referred to Chapter 3.

Participation of dynamic devices

$$\Delta \mathbf{P}_d = (\mathbf{I}_{gd}^0 + \mathbf{V}_{gd}^0 \mathbf{Y}_d) \, \Delta \mathbf{V}_{d_k} + \mathbf{V}_{gd}^0 \, \mathbf{I}_{\mathrm{mod}\,d} \qquad (4.48)$$

$$\Delta \mathbf{Q}_d = (\mathbf{I}_{gq}^0 + \mathbf{V}_{gq}^0 \mathbf{Y}_d) \, \Delta \mathbf{V}_{d_k} + \mathbf{V}_{gq}^0 \, \mathbf{I}_{\mathrm{mod}\,d} \qquad (4.49)$$

where I_{gd}^0, I_{gq}^0, V_{gd}^0 and V_{gq}^0 are the real and imaginary parts of the initial values for currents and voltages in the system as presented in chapter 3, at time t_0.

Participation of loads

In this case,

$$\Delta \mathbf{P}_L = \mathbf{P}_{LV} \, \Delta \mathbf{V}_L \qquad (4.50)$$

$$\Delta \mathbf{Q}_L = \mathbf{Q}_{LV} \, \Delta \mathbf{V}_L \qquad (4.51)$$

where $\mathbf{P}_{LV}$ and $\mathbf{Q}_{LV}$ are *2nlx2nl* block diagonal matrices depending on the conditions at t_0, voltages and currents at terminals and load characteristic.- see chapter 3 for more details.

Participation of transmission links

For a transmission system consisting of L branches and b buses, the contribution from transmission lines and transformers can be expressed as

$$\Delta \mathbf{P}_R = \mathbf{P} \, \Delta \mathbf{V} \tag{4.52}$$

$$\Delta \mathbf{Q}_R = \mathbf{Q} \, \Delta \mathbf{V} \tag{4.53}$$

where $\mathbf{P}$ and $\mathbf{Q}$ are $L \times 2b$ matrices numerically depending on the parameters of the transmission lines or on the parameters of the transformers as well as the initial voltages for the end terminals.

These matrices are defined in Section 3.4.3 for transmission lines and 3.4.4 for transformers and are not repeated here.

4.7 Numerical Implementation

Based on the above representation, a computer algorithm was developed for modal analysis of power system models described by DAEs.

The main steps in the method are described below.

Step 1: Calculate the modal voltage deviations of loads from the measured data, as indicated by expression (4.36).

Step 2: Construct the DAE model around an initial condition t_0.

Step 3: Using least-squares techniques, compute modal voltage deviations at dynamic devices.

Step 4: Calculate modal current injections as presented in section 4.7.2

Step 5: Calculate modal current deviations for dynamic devices and loads.

Step 6: Calculate the participation in modal active and reactive power for:

- Each synchronous machine in the power system.

- Each control device within the system.
- Each load
- Each Transmission line and transformer in the power system
- And other elements connected to the system.

Step 7: Normalize modal power deviations against the maximum value of modal active and reactive power.

The data can be calculated for all the time interval of the measurements, with the initial condition at t_0.

4.8 References

[1] P. Kundur, "Power System Stability and Control", McGraw-Hill, Inc. Ney York, 1994.

[2] S. I. Grossman, "Álgebra Lineal", Quinta Edición. McGraw-Hill/Interamericana de México S.A. de C.V. 1996.

[3] S. Lipschutz, "Theory and Problems of Linear Algebra Second Edition" Shaum's Outline Series, McGrall-Hill. 1991.

[4] T. Katayama, "Subspaces Methods for System Identification" Springer-Verlag London Limited 2005.

[5] J. H. Wilkinson, "The Algebraic Eigenvalue Problem", Oxford University Press, Oxford, U.K., 1965.

[6] G. L. G. Sleijpen, A. G. L. Booten, D. R. Fokkema, And H. A Van Der Vorst. "Jacobi-Davidson Type Methods For Generalized Eigen problems And Polynomial Eigen Problems". BIT 36:3, 595-633,1996.

[7] T. Smed, "Feasible Eigenvalue Sensitivity for Large Power Systems", IEEE Trans. Power Systems, Vol. 8 No. 2 May 1993.

[8]   O. Samuelsson, "Power System Damping, Structural Aspects of Controlling Active Power, Ph. D. Thesis", Dept. of Industrial Electrical Engineering and Automation. Lund University, Lund, Sweden. 1997.

[9]   E. Z. Zhou, "Power Oscillation Study of Electric Power Systems" Electrical Power and Energy Systems. Vol. 12. No. 2, pp 143-150, 1995.

[10]   M. Ochoa, "Aplicación de Métodos de Potencia y Energía Modal al Análisis de Oscilaciones Interárea" Centro de Investigación y Estudios Avanzados del I.P.N. (CINVESTAV), Unidad Guadalajara. Guadalajara Jalisco. June 2001.

[11]   A. J. Laub, "The Moore-Penrose Pseudoinverse" (Math 33A:Laub) Notes on Moore-Pwnrose Pseudoinverse. Dept. of Mathematics/electrical Engineering. www.math.ucla.edu/~Laub.

[12]   P. Kundur, "A Comprehensive Computer Program Packagefor Small Signal Stability Analysis of Power Systems" IEEE 1990 Power Winter Meeting. Atlanta, Georgia.

[13]   N. Martins, "Efficient Eigenvalue and Frequency Response Methods Applied to Power Systems Small.Signal Stability Studies". IEEE Trans. on Power Systems Vol. PWEA-1 No.1 1986, pp. 217-226.

[14]   A. Semlyen and L. Wang, "Sequential Computation of the Complete Eigensystem for the study Zone in Small Signal Stability Analysis of Large Power Systems" IEEE Transactions on Power Systems, Vol. PWRS-3, No. 2 1988, pp. 715-725.

Chapter5
Application.

This chapter describes the application of the proposed modal power flow algorithm to the study of small signal stability of power systems.

The method is tested on two power systems. The first test system is a 6-machine, 10-bus system; the second system is a 46-machine, 191-bus simplified equivalent of the Mexican Interconnected System.

First, the ability of the technique to identify modal voltage control areas is investigated. The reactive modal contribution is computed and the effect of generators, SVCs and loads to the reactive power swing flow is determined.

The application of the method to the 6-machine system and the Mexican system also focuses on the analysis of the impact of load on system behavior.

5.1 Outline of the Study

The proposed methodology of coherency and dominant loads identification was tested on two power networks. These are:

1. A 6-machine, 10-bus test system. Voltage support is provided by a synchronous compensator at a major transmission bus.

2. A 5-area simplified equivalent of the Mexican interconnected system. This system consists of 46 machines and 191 buses and 2 SVCs.

5.2 Application to the 6-Machine System

Figure 5.1 shows the 6-machine test system used in this research work. The machine and excitation control data used in the system are given in Ref. [1]. The system has two inter-area modes of interest.

For the present discussion, attention is focused on the inter-area modes 4, -0.1430 ± 5.6635i, and 5, 0.0088 ± 3.1272i. Mode 4 is of interest to system behavior as it represents an interarea oscillation involving machines GEN-006 and GEN-001 swinging against the rest of the system. Mode 5 represents an oscillation involving GEN-001 and the rest of the machines in the system.

5.2.1 Modal Voltage Control Areas

Interarea mode 4

Using modal analysis, the system can be divided into three main voltage control areas. The first area is formed by buses experiencing phase angles around 0°. Area 2 is formed only with bus 1, whilst area 3 is formed with bus 4. Bus 2 and 9 can be considered inside area 1 because their oscillation pattern is closer to this area. Figure 5.1 gives a schematic representation of the system showing voltage control areas.

For this mode, the dominant generator is GEN-012 with a modal active power of 100% with an angle of 0° GEN-001 and GEN-006, with participations on modal active power of 59% angle of 180.06° and 77.23% angle of 175.09° respectively.
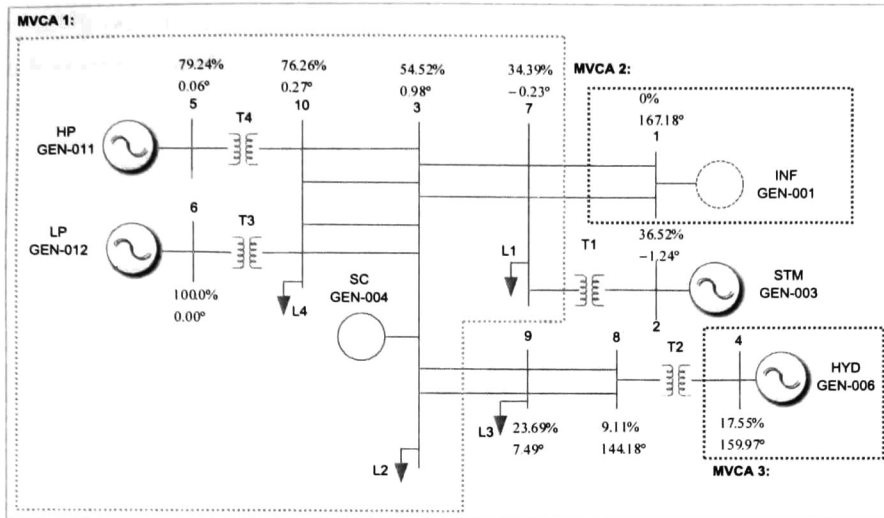
Figure 5.1: Modal voltage control areas for mode 4.

The analysis of modal line contributions shows that transmission paths linking machine GEN-006 with bus 3 have a large participation to the modal power flow.

Table 5.1:
Modal active power flow in transmission elements.

| | Modal Active Power Flow | |
| | Normalized | |
Line	Relative Mag. (%)	Relative P. Angle
3 -- 9	35.38	-4.46
3 -- 9	35.38	-4.46
9 -- 8	35.49	-4.95
9 -- 8	35.49	-4.95
8 -- 4	75.95	-4.911

For MCVA 1, the machines having the largest deviations in modal reactive power, on the other hand, are GEN-012 (100%) and GEN-004 (93.03%). Loads inside this area have a participation of 12.03% (L3), 10.08% (L2), 8.65% (L1) and 8.12% (L4). In turn, for MCVA 3, GEN-006 has an important participation (98.1%) while for MCVA 2, the participation of GEN-001 is 67.39%.

Insight into the nature of modal voltage behavior can be gleaned from the study of modal bus voltage magnitudes in Fig. 5.2. As shown, buses 9 and 8 show the largest modal deviations.
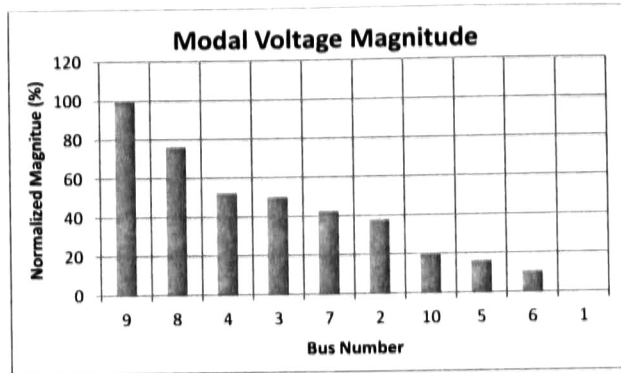

Figure 5.2: Normalized arguments for voltage magnitude deviations. Mode 4.

From above results can be observed that buses 9 and 8 are between MVCA 1 and MVCA 3. Being the link that connects two areas with different oscillation may be the reason why the oscillation has more effect in those buses.

Interarea mode 5

The analysis of mode 5 suggests that the system can be divided into two modal voltage control areas. Where the exchange of modal active power is between area 1, with the largest participation coming from GEN-006 (61.62% angle of 180.44°) and GEN-012 (21.38% angle of 178.75°), and area 2, where the infinite bus is experiencing 100% angle of 0° All generators are oscillating against the infinite bus, represented by GEN-001.

The first area is formed with all the buses experiencing angles around 0° and second area is formed only by bus 1, with an angle around 180°. Figure 5.3 depicts the modal voltage areas for this mode.
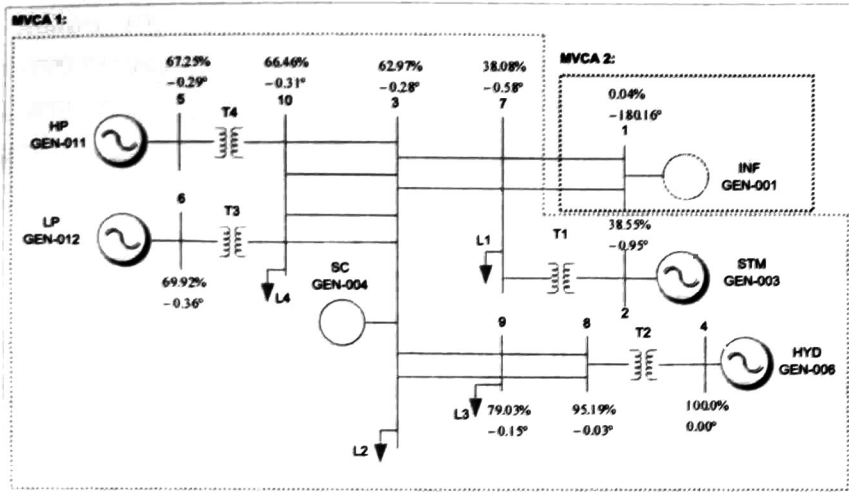
Figure 5.3: Modal voltage control areas for mode 5.

The analysis of modal power flow in Table 5.2 reveals that the transmission lines with the largest participation in the mode is the lines between buses 1 and 7 (100%). The analysis of bus voltage magnitudes in Fig. 5.4 identifies buses 9 and 8 with the largest deviations.

Table 5.2:
Modal active power flow in transmission elements.

| Line | Modal Active Power Flow | |
| | Normalized | |
	Relative Mag. (%)	Relative P. Angle
1 -- 7	50	0
1 -- 7	50	0
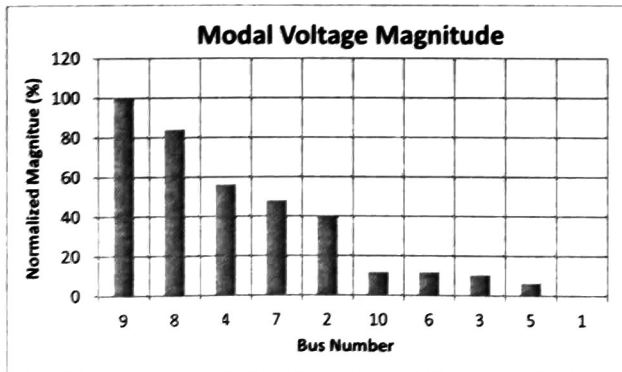
Figure 5.4: Normalized arguments for voltage magnitude deviations. Mode 5.

Inside MVCA 1, GEN-006, GEN-003 and GEN-004 exhibit the largest deviations of reactive power with normalized values of 100%, 57.09%, and 29.83%. The participation of GEN-001 in MVCA 2 is high with value of 86.20%. All loads are inside MVCA 1, and the largest participation is from load L3 with 12.07%.

5.2.2 Dominant Loads

The studies were carried out for modes 4 and 5. For the latter mode, the damping variations calculated were very small and the analysis is not shown. The study is then only presented and discussed for mode 4.

Interarea mode 4

The results for voltage phase angle deviations are presented in figure 5.5[2] and for modal active power in table 5.3 for all the loads in the system. These results suggest, due especially for the large contribution of this mode to the bus voltage deviations, that load at bus 10 is the dominant load.

Bus voltage and load contribution are swinging out of phase, the contribution of load 10 to the system is positive with the greatest damping found with load modeled as constant impedance.
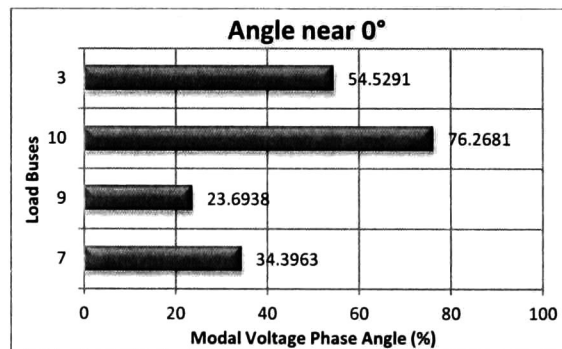

Figure 5.5: Modal voltage phase angle deviations. Mode 4.

_____

[2] (+) Phase angle near 0°and (-) phase angle near 180°.

| Modal Active Power Flow | | |
| Normalized | | |
Load	Relative Mag. (%)	Relative Phase
Bus 3	5.2043	202.36
Bus 7	4.4655	201.36
Bus 9	3.1054	187.17
Bus 10	4.1986	228.25

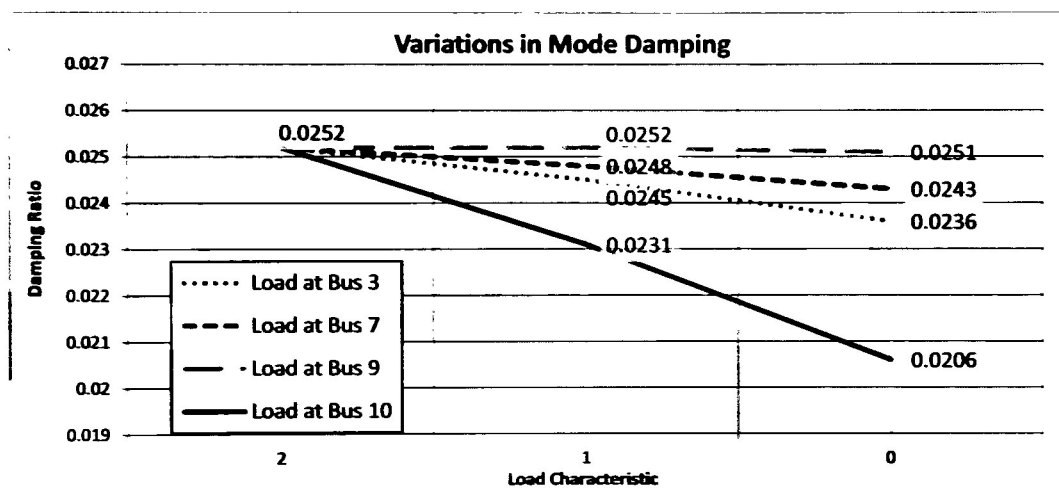The results of varying the load characteristic in the four loads of test system 2 are presented at figure 5.6.

Figure 5.6: Variations in mode damping due to variations in load characteristic. Mode 4.

Examination of above results indicates that load at 10 is having a large influence over mode 4, where the variation of load characteristic produces the highest variations in mode damping.

5.3 Application to a Large System

In this section, the modal power swing flow technique is applied to a larger test system. See Ref. [2] for further details about this system.

For reference and comparison, standard small signal analyzes were conducted to assess system behavior. Table 5.4 summarizes the 3 slowest modes of the system showing swing patterns and dominant generators, calculated with a modal active power flow analysis.

<p style="text-align:center">Table 5.4:
Slowest modes for large power system.</p>

Mode	Eigenvalue	Damping Ratio.	Damped Freq. (Hz)	Dominant Generators[3]
1	-0.1331 ± 2.6795i	0.0496	0.4265	GEN 33 (+100%), GEN 32 (+95.25%), GEN 28 (+51.00%), GEN 40 (+46.34%), GEN 41 (+46.22%), GEN 25 (+42.17%).
2	-0.2176 ± 3.7647i	0.0577	0.5992	GEN 33 (+100%), GEN 32 (+90.86%), GEN 25 (-39.87%), GEN 26 (-34.48%), GEN 31 (+32.93%), GEN 29 (-31.14%).
3	-0.0877 ± 4.6273i	0.0190	0.7365	GEN 19 (+100%), GEN 35 (+94.15%), GEN 36 (+93.85%), GEN 24 (+88.61%), GEN 23 (+84.48%), GEN 22 (+81.00%).

5.3.1 Modal Voltage Control Areas

Interarea mode 1

Application of the modal power flow technique for this mode results in 6 modal voltage control areas. The modal areas and the interconnected regional systems are illustrated in figure 5.7. For this swing mode the machines in the north (N) and north-eastern (NE) systems are oscillating coherently against the machines in central (C), western (W) and south-eastern (SE).

Table 5.5 lists the transmission buses belonging to MVCA 1. This area is formed mainly by buses with angles around 9° and magnitudes of the modal voltage phase angle from 45% to 12%. Buses located in the north and north-eastern system of the MIS. Figure 5.8 shows the normalized modal voltage magnitude. This information suggests possible locations of voltage control devices. The largest modal

---

[3] Values are normalized against the generator with largest magnitude. (+) Phase angle near 0° and (-) phase angle near 180°.

deviations are 100% (bus 185) and bus 90.94% (186) followed by 8 buses with relative values between 80% and 89%.

MVCA 1 includes 10 generators and 1 SVC. It is noteworthy that the SVC at bus 48 exhibits a modal reactive power participation of 100%. Generators 39, 38, 37 and 34 show relative participation of 56.89%, 28.41%, 21.26% and 19.46% respectively. Shunt elements connected inside this area show contributions below 9%, whilst the load participation is less than 4% to the modal reactive power flow.
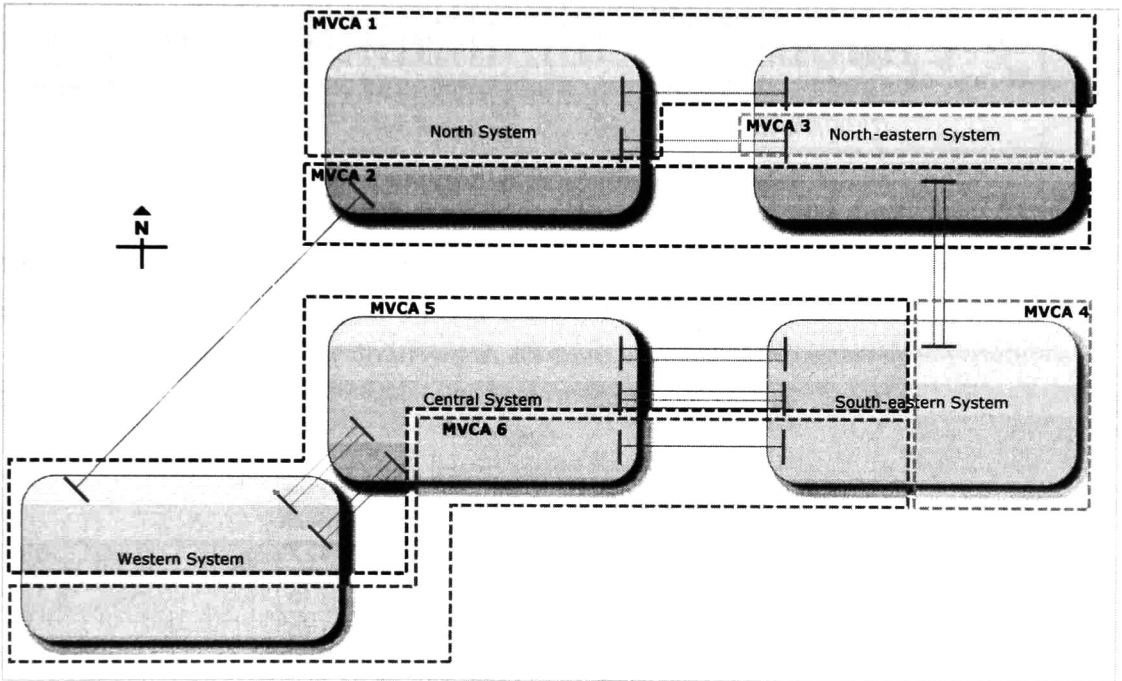

Figure 5.7: Diagram of modal voltage control areas for mode 1 and the 5 regional systems of the MIS.

Table 5.5:
Buses inside modal voltage control area 1 for mode 1.

MVCA:	Buses									
	25	34	48	139	144	155	160	165	170	*185*
	26	37	135	140	145	156	161	166	171	186
1	27	38	136	141	146	157	162	167	180	187
	29	39	137	142	149	158	163	168	183	188
	30	42	138	143	150	159	164	169	184	189

MVCA 2 is formed by 4 sub-areas with angles around 5°, 6°, 7° and 8° each one. Argument of modal voltage phase angle deviations has a maximum value of

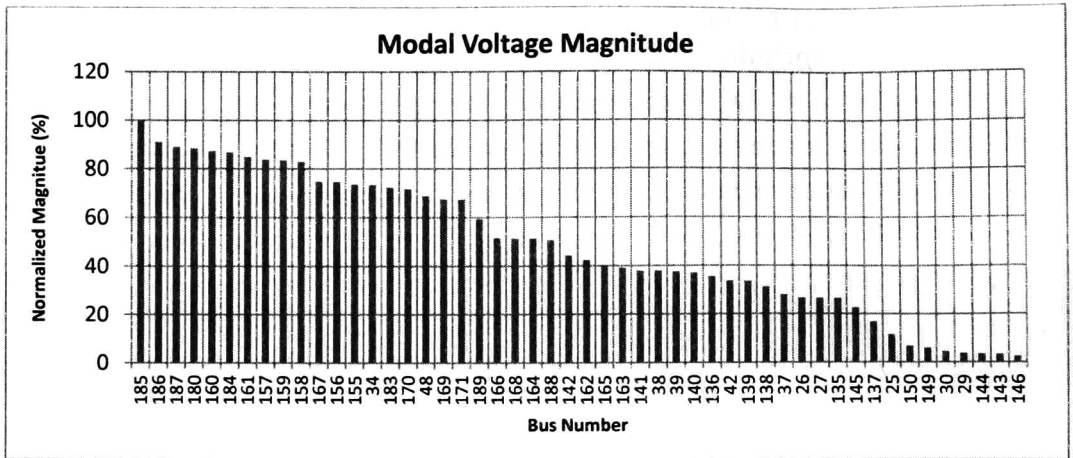54% and a minimum of 39%. Buses inside area 2 are listed at table 5.6.

Figure 5.8: Normalized arguments for voltage magnitude deviations. MCVA 1. Mode 1.

Modal analysis of the reactive power shows that dynamic devices in MCVA 2 are having deviations of less than 6% as well as negligible variations from shunt element and loads (0.47% and less than 1% respectively).

Table 5.6:
Buses inside modal voltage control area 2 for mode 1.

MVCA	Buses					
	28	41	151	154	174	177
2	31	147	152	172	175	178
	40	148	153	173	176	179

Modal contribution on voltage magnitudes deviations are shown at figure 5.9 with a maximum value of 32.57% at bus 178.
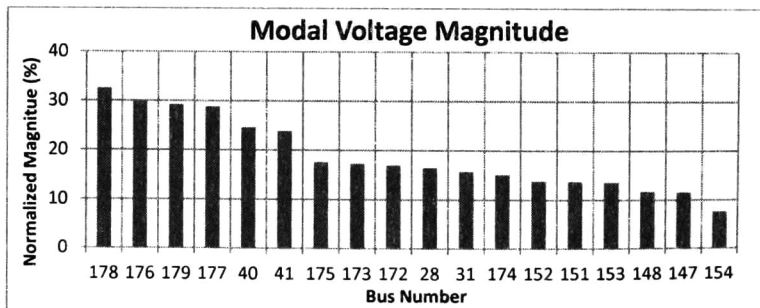

Figure 5.9: Normalized arguments for voltage magnitude deviations. MCVA 2. Mode 1.

Finally, MVCA 3 is formed by 4 buses in the northeast region with a maximum value of modal voltage phase angle of 100% and phase angles around 0°

Table 5.7:
Buses inside modal voltage control area 3 for Mode 1.

MVCA	Buses			
3	32	33	181	182

Participation of generators in reactive power flow inside area 3 has a maximum value of 4.89%. Load and shunt element connected to bus 181 have also small participations. The variations of the modal voltage magnitude are 39.03%, 40.18%, 38.69% and 37.55% for buses 32, 33, 181 and 182 respectively.

The following control areas are showing phase angles near 180° and are formed with buses located inside the C, W and SE regional systems. The first MCVA, denoted as area 4, consists of 4 sub-areas with angles around -171°, -172°, -173° and -174° each one. Magnitudes of voltage angle deviations inside this area are from 25% to 18%.

Table 5.8:
Buses inside modal voltage control area 4 for mode 1.

MVCA	Buses							
	1	6	49	52	55	58	67	75
4	2	46	50	53	56	59	71	84
	3	47	51	54	57	65	72	

Examination of modal reactive power shows that SVC at bus 47 has a participation of 20.85% followed by generators 1, 2 and 3 with 19.99%, 15.34% and 14.48%. Shunt elements and loads show contributions of less than 2.14% (Bus 50) and less than 2.52% (Load at bus 52). The maximum value of bus voltage magnitude deviations is located at bus 58 as it can be observed from figure 5.10.

Table 5.9 lists the buses grouped inside MVCA 5, with all buses with angles around -175° and relative magnitudes of voltage phase angle from 16% to 25%.

The studies of modal reactive power showed low participations of generators,

shunt elements and loads inside this area with values of less than 5%, 1% and 1.5% respectively.
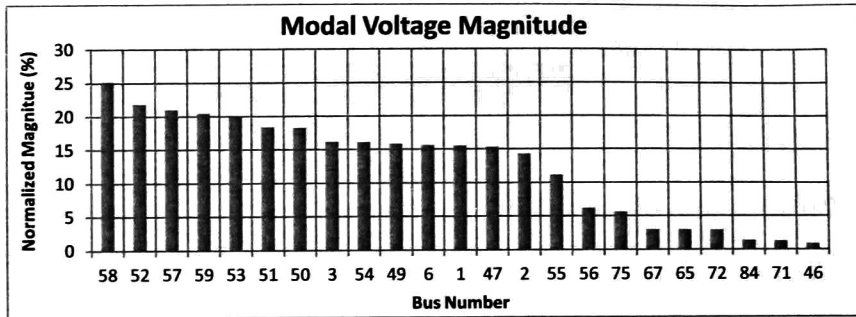

Figure 5.10: Normalized arguments for voltage magnitude deviations. MCVA 4. Mode 1.

Figure 5.11 depicts the information of voltage magnitude deviations due to mode 1 for buses inside area 5. Maximum values experienced by buses 74 and 70.

Table 5.9:
Buses inside modal voltage control area 5 for mode 1.

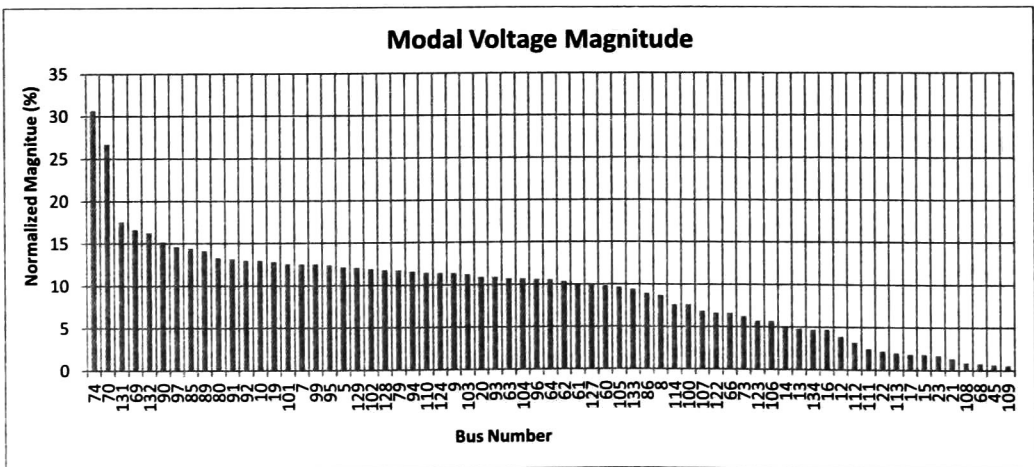| MVCA:	Buses													
	5	12	17	23	63	70	85	92	97	103	108	113	127	133
	7	13	19	45	64	73	86	93	99	104	109	114	128	134
5	8	14	20	60	66	74	89	94	100	105	110	122	129	
	9	15	21	61	68	79	90	95	101	106	111	123	131	
	10	16	22	62	69	80	91	96	102	107	112	124	132	

Figure 5.11: Normalized arguments for voltage magnitude deviations. MCVA 5. Mode 1.

MCVA 6 exhibits voltage phase angle deviations from 25% to 14%, with angles mainly around -176° as well as some buses experiencing angles of -177°. The buses inside this are listed in Table 5.10.

GEN-4 has 42% of participation in modal reactive flow, the rest of the devices are only participating with less than 5%. Low deviations of shunt elements with less than 2% (bus 76) and loads with less than 1.24% (bus 81). Contribution of oscillation mode 1 on bus voltage magnitude can be seen from figure 5.12.

Table 5.10:
Buses inside modal voltage control area 6 for mode 1.

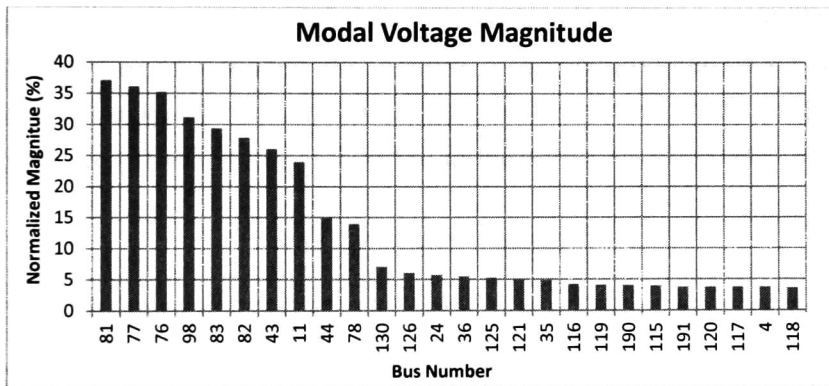| MVCA	Buses								
	4	35	44	78	83	116	119	125	190
6	11	36	76	81	98	117	120	126	191
	24	43	77	82	115	118	121	130	

Figure 5.12: Normalized arguments for voltage magnitude deviations. MCVA 6. Mode 1.

Buses 88, 87 and 18 were not grouped because their phase angles are not near any of the areas described before (-211°, -254° and -271°). GEN-18 is experiencing 18% on modal reactive power. The shunt element at bus 87 is experiencing 9.06% and loads are showing magnitudes of 2.24% at bus 87 and 4.82% at bus 88. The voltage magnitude variations for these buses are high with values of 63.41%, 56.79% and 52.26% for 87, 88, and 18.

Buses 18 and 88 are connected to bus 87 and are located in between two areas with complete different oscillation pattern. Transmission line from bus 183 to bus 88 is experiencing a large participation in modal active power flow with a normalized

magnitude of 311.49%, bus 183 is part of MVCA 1, while bus 88 is connected to bus 81, which is grouped inside MVCA 6.

Study results show that the bus voltage magnitude is higher in area 1 and within this group the higher variations of modal reactive power are experienced. The mode influence over the voltage magnitude is low for MVCAs 2 and 3 and the participation of dynamic devices within these areas are also small. MCVAs 4, 5 and 6 exhibit small modal voltage magnitude deviations and participation in modal reactive power flow as well, with the exception of GEN-4 located in area 6 and GEN-1 in area 4. Special attention must be taken for the 3 non-grouped buses, where the voltage magnitude variations are considerable high.

Interarea mode 2

The analysis of interarea mode 2 reflects a more complex oscillation behavior due to the exchange of modal active power between the south-eastern, central and western systems as well as two generators of the north-eastern system (GEN 32 and GEN 33) oscillating against the machines in the north and north-eastern systems. The areas formed for this mode are represented in the diagram at the figure below.
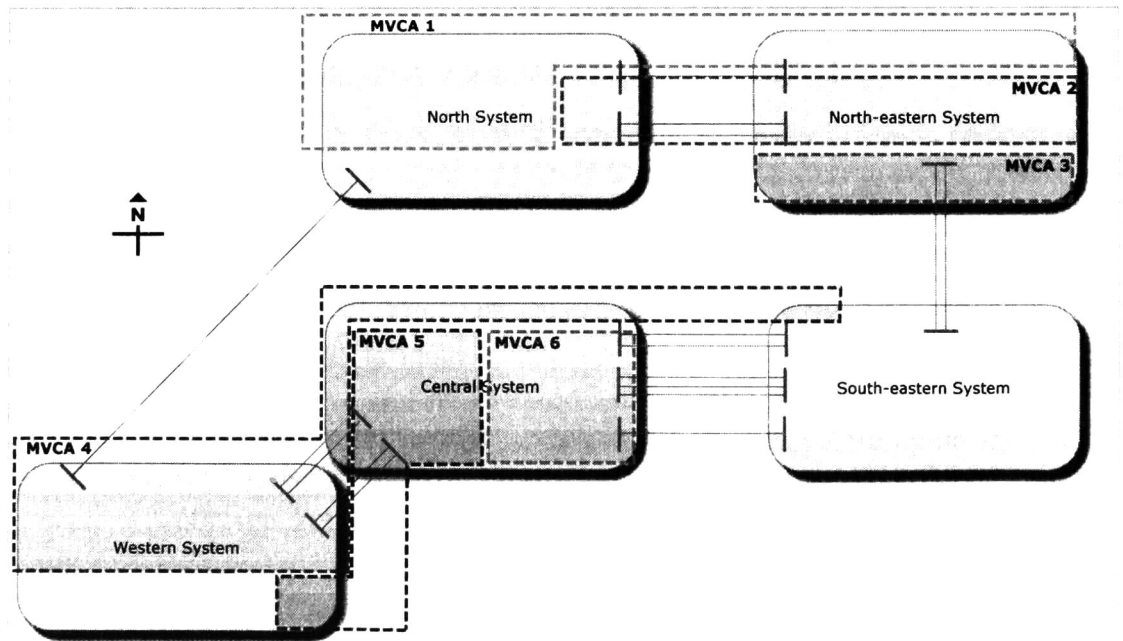

Figure 5.13: Diagram of modal voltage control areas for mode 2 and the 5 regional systems of the MIS.

MVCA 1 is formed with buses in the N and NE regions experiencing angles of modal voltage phase angle deviations of 172° and 173° with the larger cluster formed around 172°. Modal voltage phase angle has relative values from 43.54% to 12.59%. The buses inside this area are shown at table 5.11.

SVC at bus 48 is showing the highest magnitude of modal reactive power with 100% followed by generator 25 with 16.47%. Except for these devices the shunt element at bus 183 is showing participation greater than those shown by the rest of the dynamic devices with 8.35%. Loads variations are small, with maximum value of 3.34% at load connected to bus 151.

Table 5.11:
Buses inside modal voltage control area 1 for mode 2.

MVCA	Buses										
	25	29	48	137	140	143	146	149	152	183	189
1	26	30	135	138	141	144	147	150	153	185	
	27	31	136	139	142	145	148	151	154	188	

Voltage magnitude deviations within MVCA 1 are small with 10 buses experiencing magnitudes from 32% to 34% as is depicted by graphic at figure 5.14.
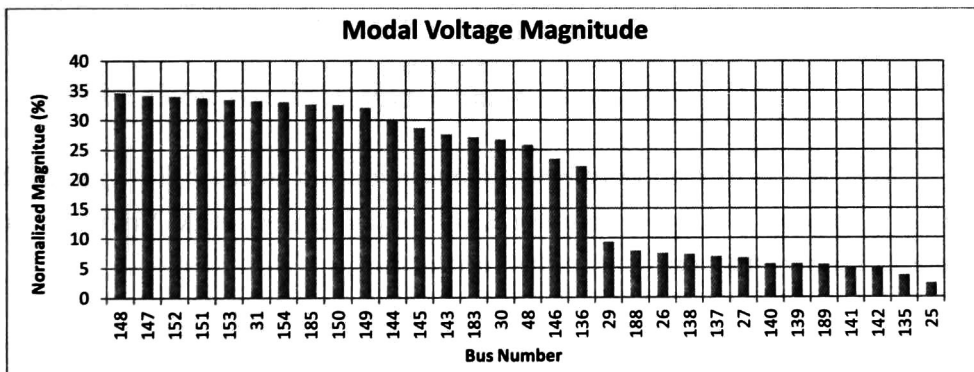

Figure 5.14: Normalized arguments for voltage magnitude deviations. MCVA 1. Mode 2.

Buses showing angles around 171°, mainly from the NE system, are grouped together inside MCVA 2, with arguments of modal voltage phase angle from 25.54% to 21.14%. The buses grouped inside are listed below

MVCA	Buses								
2	34	39	156	159	162	165	168	171	186
	37	42	157	160	163	166	169	180	187
	38	155	158	161	164	167	170	184	

Modal reactive power studies carried out show generators 39, 34, 37 and 28 with values of 79.88%, 28.40%, 28.15% and 25.98% respectively. Negligible participation from loads inside area 2 and the higher participation of shunt elements from those at buses 159 and 170 with values of 4.16% and 4.06%.

Deviations in bus voltage magnitude for this area are depicted in figure 5.15.
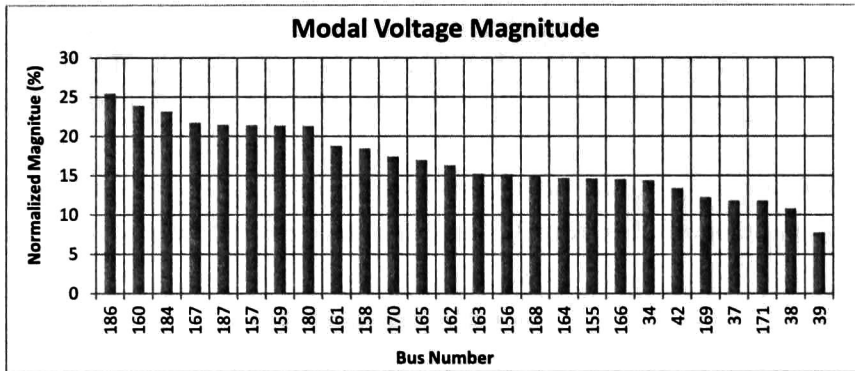
Figure 5.15: Normalized arguments for voltage magnitude deviations. MCVA 2. Mode 2.

MVCA 3 is formed only by four buses located in the NE region of the MIS, with angles around 0° and arguments of voltage phase angle from 87% to 100%. Table 5.13 shows the buses inside this control area.

MVCA	Buses			
3	32	33	181	182

GEN-32 and GEN-33 show low modal reactive power deviations with values of 13.81% and 16.11% respectively. Load participation is 15.97% (bus 181) and shunt element at the same bus with 6.32%. Variations of modal voltage magnitude are

high with values of 77.97%, 69.13%, 68.79% and 68.61% for buses 182, 33, 32 and 181 respectively.

The next area, denominated as MCVA 4, is formed with buses in the C, W and SE systems showing angles around -20° and magnitudes of modal voltage phase angle with a maximum value of 7.40% at bus 36. Buses within this area are listed in table 5.14.

Generators inside this area exhibit minor participation in modal reactive power with GEN-19 showing the maximum contribution (6.05%). Load and shunt elements participations are negligible with magnitudes of less than 1%.

Table 5.14:
Buses inside modal voltage control area 4 for mode 2.

MVCA	Buses												
	15	19	23	36	108	112	116	119	122	125	128	133	191
4	16	21	24	68	109	113	117	120	123	126	129	134	
	17	22	35	86	111	115	118	121	124	127	130	190	

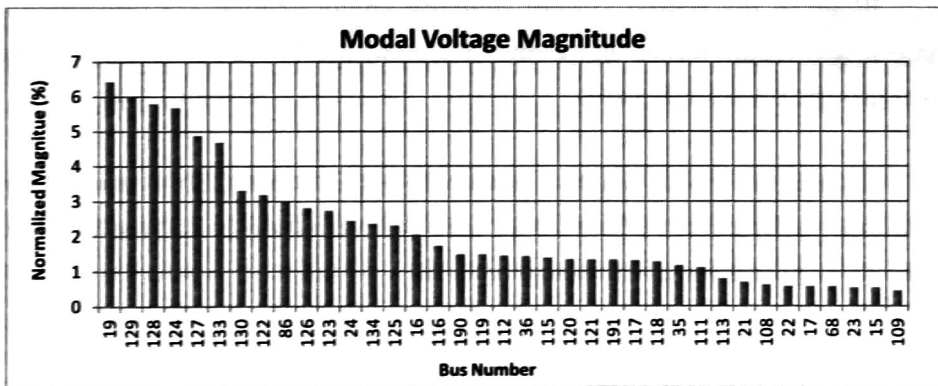Graphic at figure 5.16 shows the contribution of mode 2 on the bus voltage magnitude for MVCA 4.

Figure 5.16: Normalized arguments for voltage magnitude deviations. MCVA 4. Mode 2.

MVCA 5 is formed only with buses experiencing angles around -21° and showing magnitudes of modal voltage phase angle not greater than 6%. Buses inside area 5 are listed in table 5.15.

MVCA	Buses					
	12	20	62	93	105	114
5	13	60	63	96	106	131
	14	61	64	104	107	

Low contributions of modal reactive power in this area all elements, with generators contributing with less than 2%, loads with less than 1.5% and shunt elements with less than 0.5%
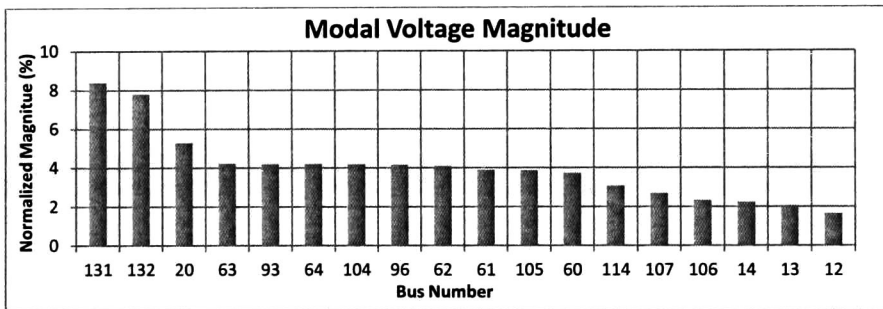

Figure 5.17: Normalized arguments for voltage magnitude deviations. MCVA 5. Mode 2.

Figure 5.17 shows that the variations in bus voltage magnitude due to mode 2.

Buses of the central system showing angles around -22° and modal voltage phase angle variations of less than 3.3% compose MVCA 6. Table 5.16 enlists the buses grouped within this area.

Results for modal reactive power flow show that GEN-9 is experiencing the maximum participation with 6.22%., load's contribution is 2.5% and shunt element at bus 90 is contributing with less than 0.5%.

Table 5.16:
Buses inside modal voltage control area 6 for mode 2.

MVCA	Buses					
	7	10	89	92	97	101	110
6	8	79	90	94	99	102	
	9	80	91	95	100	103	

The modal voltage magnitude deviations are depicted in figure 5.18, small variations are observed for this area.
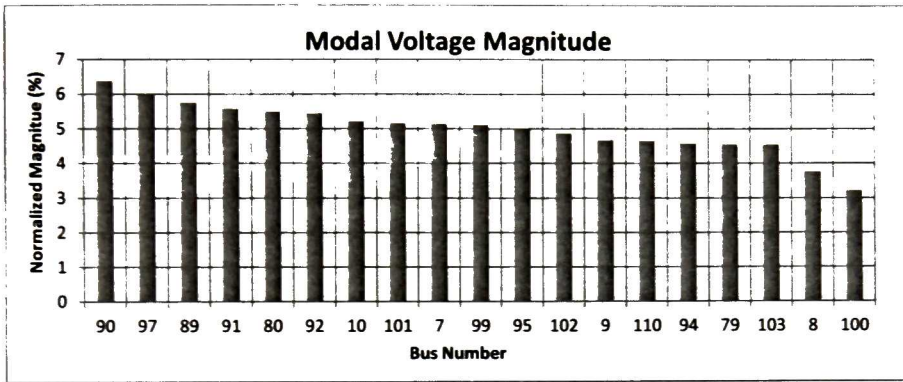

Figure 5.18: Normalized arguments for voltage magnitude deviations. MCVA 6. Mode 2.

The oscillation behavior of the rest of the buses in the system exhibit larger angular distances from the areas mentioned before. From these buses there are some buses where the contribution of mode 2 has an important effect on the bus voltage magnitudes, as seen from figure 5.19. The identified buses are grouped together as sub-areas in the system, and are listed in table 5.17.

Buses inside sub-groups 1 and 2 have oscillation pattern more similar to that experienced by MCVA 2, but both sub groups are connected to sub group 3, which is exhibiting an out of phase oscillation with them. Sub-group 1 is formed with angles between 167° and 163°, sub-area 2 with angles from 158° to 153° and sub-group 3 with angles around 32°

Modal reactive power calculations show small participation from GEN-40 and GEN-41 with values of 10.75% and 3.65% respectively, and negligible participations of loads in sub-area 2. Also small contributions are found from GEN-28 in sub-area 3.

Table 5.17:
Buses inside modal sub-areas for Mode 2.

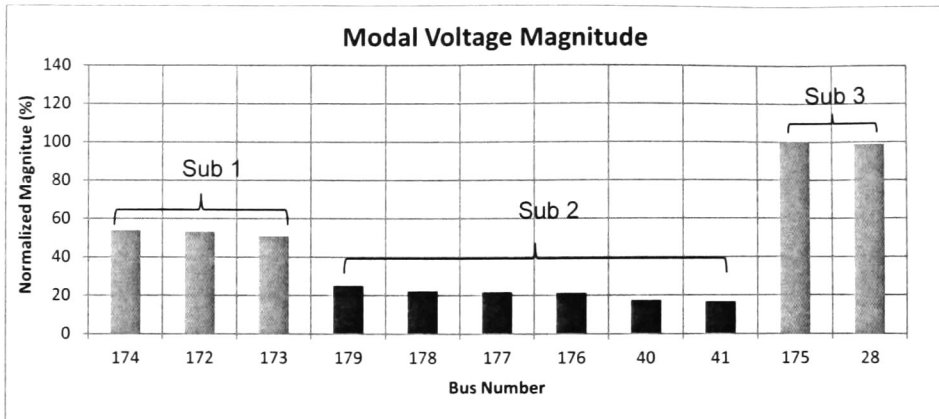| Sub	Buses		
1	172	173	174
2	40	176	178
	41	177	179
3	28	175	

Figure 5.19: Normalized arguments for voltage magnitude deviations. Sub areas. Mode 2.

Important participations in the exchange of modal reactive power are found in devices at buses outside the voltage areas, these are: generators 4, 47, 1, 18 and 2 with 50.04%, 37.72%, 30.09%, 24.30% and 20.74% respectively.

Results exposed above show that MVCA 1 and MVCA 2 has the highest variations of modal reactive power, with SVC at bus 48 with 100% and GEN-39 with 79.88%. Other devices with good participation are found outside the MVCAs formed, GEN-4 and SVC at 47 with 50.04% and 37.72% respectively. Best locations for parallel voltage control are located in sub-area 3 and MVCA 3.

5.3.2 Dominant Loads

Interarea mode 1

Modal voltage phase angle results are depicted in the following figures, with those buses experiencing an angle near 0° with positive magnitude and those with angles near 180° as negative. The maximum contribution is found at bus 181.
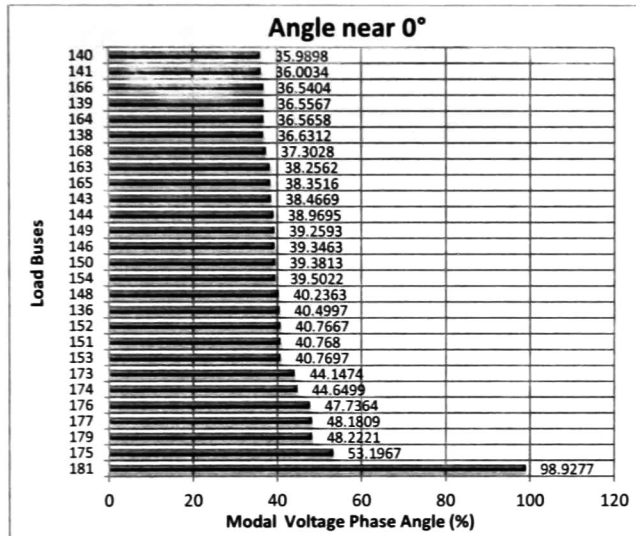

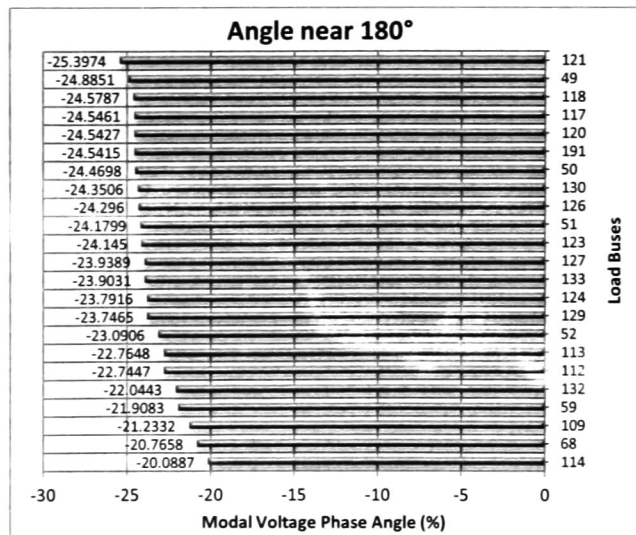Figure 5.20: Modal voltage phase angle deviations, angle near 0°. Mode 1.

Figure 5.21: Modal voltage phase angle deviations, angle near 180°. Mode 1.

The voltage phase angle variations of buses with angles near 0° goes from 30% to 98.92% and buses 185 and 183 with less than 30% whilst the participations of buses with angles near 180° goes from 1% to 25%.

The participation of the loads in modal active power flow is shown in table 5.18, only participations higher than 10% are listed.

Table 5.18:
Modal active power flow for loads. Mode 1.

Modal Active Power Flow		
Load	Normalized	
Bus	Magnitude	Angle
88	28.9725	-3.0219
184	20.4403	-3.9133
181	19.8447	225.7401
52	15.3421	197.3764
157	14.6596	-3.7451
161	14.0580	-4.5977
87	13.5525	-3.1641
97	12.4664	-5.3211
169	10.9479	-2.3293
180	10.6186	-4.7611

Examination of relative magnitudes and phase angles of modal active power and modal voltage phase angle it is expected that load at 181 be the dominant load for mode 1, where the variations in load's characteristic will result in significant variations in mode damping. On the other hand, loads at bus 179 and 175 have low modal power participation (3.66% and 0.48%) and variations in damping are expected to be small even when the magnitude of bus voltage angle is high.

As shown in fig. 5.22, the influence of load at bus 181 is significant. With this load modeled as constant impedance the mode damping is close to 5%, value that may be considered as a minimum acceptable. But with constant current the damping calculated is equal to 3.97% and 2.81% for constant MVA.
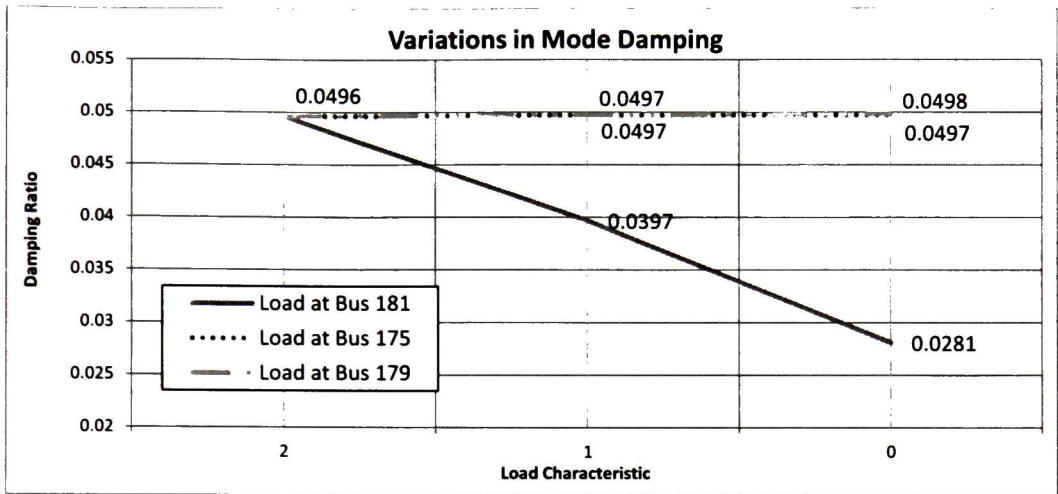
Figure 5.22: Variations in mode damping due to variations in load characteristic, Mode 1.

Analysis as the ones presented for buses 181, 175 and 179 where performed for loads at buses with modal voltage phase angle from 30% to 47% and participations in modal active power flow from 4.7% to 15%. As expected, the variations were small.

The analysis presented before were performed for buses experiencing high magnitudes of voltage phase angles, now the studies are focused on loads with high contribution to modal active power flow, loads at buses 88, 184 and 181.
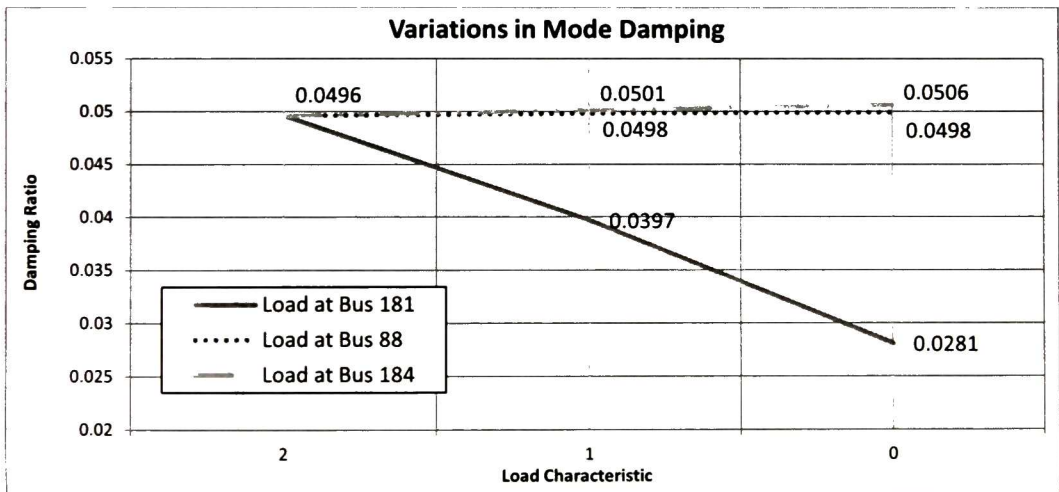

Figure 5.23: Variations in mode damping due to variations in load characteristic, mode 1.

From this analysis it can be determined that load at bus 181 has an important influence over mode 1. The variations in the model representing this loads produces

significant changes in damping of mode 1. In this way it is important to have a well representation of the behavior of load 181.

Interarea mode 2

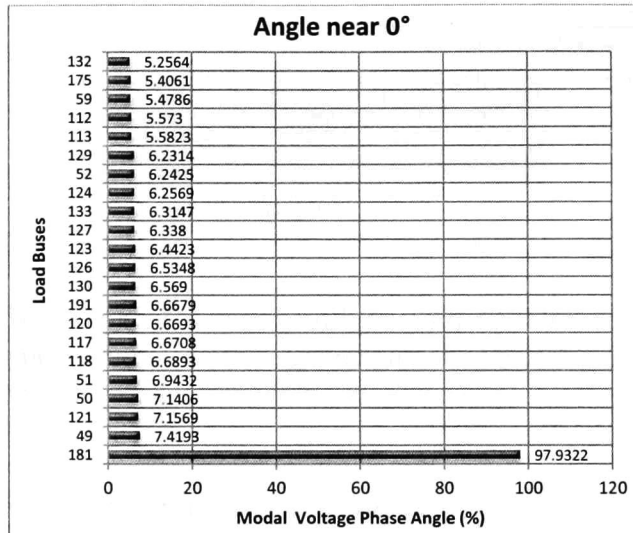Values of voltage phase angle are exhibit in the following graphics

Figure 5.24: Modal voltage phase angle deviations, angle near 0°. Mode 2.
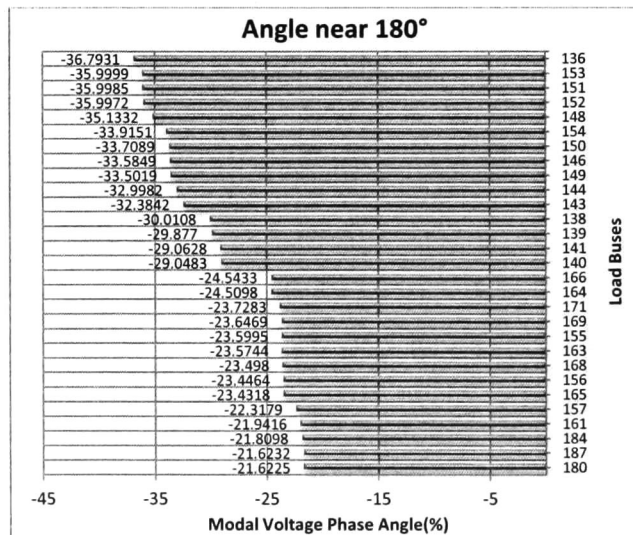

Figure 5.25: Modal voltage phase angle deviations, angle near 180°. Mode 2.

From a modal voltage analysis it is observed that load at bus 181 is experiencing the largest magnitude, the angle at this bus is near 0°

The load's participation in the exchange of modal active power are presented in the following table, only loads with magnitudes greater than 4% are listed.

Table 5.19:
Modal active power flow for loads, mode 2

Modal Active Power Flow		
Load Bus	Normalized	
	Magnitude	Angle
181	23.7519317	208.329982
88	7.75176608	165.879385
52	6.49498752	10.2203516
151	4.69557501	2.03274486
153	4.31193871	2.01696284

The modal analysis performed shows that load at bus 181 may have a significant influence over the mode damping, with important participation in voltage phase angle and also in modal power. Other loads that are analyzed are located at bus 136, 151 and 153, but with lower values. Figure 5.26 depicts the variations in damping from variations in load dynamics characteristic.
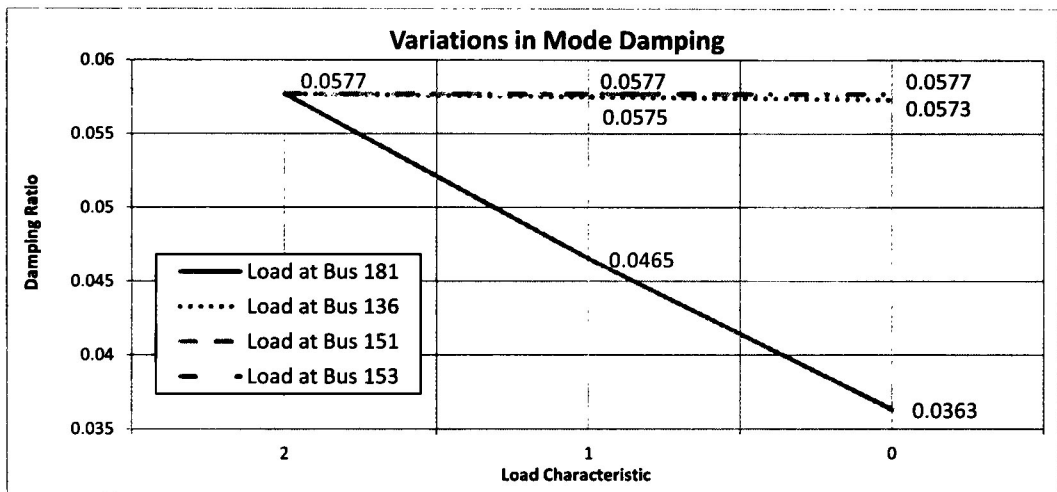

Figure 5.26: Variations in mode damping due to variations in load characteristic. Mode 2.

From these results is determined that load at bus 181 is the dominant load for mode 2 and attention to the model of this load must be taken into account.

5.4 Concluding Remarks

In this chapter, the practical application of the modal voltage variations and modal power flow from the right eigenvector to the study small disturbances stability has been presented for 2 different systems.

Modal bus voltage calculation can be helpful in the identification of areas with coherent oscillation, denominated in this work as modal voltage control areas, as well as possible location for voltage control. Modal reactive power flow, on the other hand, can indicate the dynamic devices, loads and elements inside the power system with larger participation on the reactive power due to one mode or combination of modes of concern.

The analysis of the argument of modal voltage phase angle and the study of modal active power helps to locate loads in the system with significant influence over the system damping. After the selection of the possible dominant loads, the influences were proven by varying the dynamic characteristic at one load at time and calculating the effects over system damping.

5.5 References

[1] J. R. Yam, "Aportaciones al Modelado de Parques Eólicos para Estudios de Estabilidad Electromecánica" Centro de Investigación y Estudios Avanzados del I.P.N. (CINVESTAV), Unidad Guadalajara. Guadalajara Jalisco. June 2012.

[2] M. Nayebzadeh, A. R. Messina, "Advanced Concepts of Analyzing Static VAR Compensators to Damp Inter-Area Oscillation Modes" ETEP 9 (3) (1999) 159-165.

[3] P. Kundur, "Power System Stability and Control", McGraw-Hill, Inc. Ney York, 1994.

[4] P W. Sauer and M. A. Pai, "Power System Dynamics and Stability", Prentice Hall, 1998.

Chapter 6
Conclusions

6.1 General Conclusions

The work exposed in this thesis has focused primarily on the analysis and understanding of the modal quantities calculated with the modal voltage variations and modal power flow studies.

The analytical procedure proposed for modal voltage control areas permits, for an oscillation mode or combination of modes, to detect and group together buses showing coherent oscillation behavior into areas of voltage control. The analysis of reactive modal contribution allows the comprehension of the elements with more participation in the exchange of reactive power inside each area, whilst the study of the voltage magnitude variations suggests suitable locations for dynamic voltage support.

Study experience with power systems showed that not all buses can be grouped inside a modal voltage area whether for a low contribution the swing modes have on the bus voltage angle variations or for being located between two areas oscillating out of phase, and was also found that this can happen for buses between synchronous generators with different oscillation behavior.

The analysis tool for the voltage stability control presented in this document has been developed with a dynamic perspective that has not been widely addressed in the literature. Due to the linearization of the power system is only valid for small disturbances.

In the analysis of dominant loads the information from modal voltage phase angle and the modal active power is used to identify load buses with large influence over the system damping. The advantages of this approach are two-fold. First, loads having a larger impact on system behavior can be identified. Further, the nature of load contribution can be determined.

The results of practical application presented in this work clearly showed that for a load to be referred as dominant the contribution in modal active power as well the relative location for a mode/modes of concerns, modal voltage phase angle, are important.

The analogy of the active loads as forces can be extent, with proper considerations, for locating parallel devices focused on adding damping to electromechanical oscillations from a point of view of small signal behavior.

This work also focused on the development and discussion of a new methodology for computing the modal power flow from a section of the right eigenvector. The proposed technique is based in the equivalences between the solution for the modal voltage deviations developed in chapter 3 and the solution for the algebraic part of the DAE eigenvector. The proposed method was applied for the study of modal voltage areas and dominant loads.

The advantages of the new methodology for the analysis of oscillation modes of large power system are:

1. Allows the use of sparse methods for computing eigenvalues/vectors.

2. Avoids the calculation of the inverse of the modified admittance matrix for the computation of modal voltage deviations.

3. Maintains the structure of the system model.

A disadvantage is that the solution is only valid for time at $t=0$, not allowing the study in time of the effect of the electromechanical modes.

Other developments discussed in this research work include:

1. The study of the non-homogenous response as different approach for the formulation of the modal power oscillation flow.

2. Close loop representation of the augmented system model for the evaluation of the influence of feedback signals in the modal power flow.

3. Extensions to the basic algorithm to compute modal power flow from measured data based on least squares optimization were proposed with relations between the standard approach and the proposed methodology.

6.1 Suggestions for Future Work

1. The study of the non-linear behavior of the power system in the exchange of modal power with the use of 2nd or higher order equations for the modal oscillation power flow method, together with the normal form method.

2. The effect of reactive power load has on the system damping. As long as the study of loads where their dynamic behavior have a significant influence on the damping of the system, for active and reactive power loads.

3. The analysis of power systems from measured systems based on the concepts of modal power flow.

4. The modal power oscillation flow method indicates the participation that the elements already connected to the power system have in the exchange of modal active and reactive power for a mode or combination of modes of concern. It would be interesting to develop a variation of the method where the participation of a not connected element may be predicted.
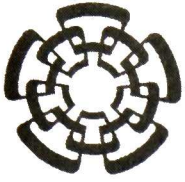
El Jurado designado por la   Unidad Guadalajara   del Centro de Investigación y de Estudios Avanzados del Instituto Politécnico Nacional aprobó la tesis

Métodos avanzados para el análisis de voltaje y flujo de potencia reactiva modal

Advanced methods for the analysis of modal voltage and reactive power flow

del (la) C.

Diego MIJANGOS PULIDO

el día 28 de Septiembre de 2012.

Dr. Arturo Román Messina
Investigador CINVESTAV 3C
CINVESTAV Unidad Guadalajara

Dr. José Javier Ruíz León
Investigador CINVESTAV 3B
CINVESTAV Unidad Guadalajara

Dr. Ramon Octavio Jimenez Betancourt
Profesor Investigador
Universidad de Colima